

Technical Preparation and Work Packages (WPs) during ILC Pre-lab

IDT-WG2

Contents

| | |
|---|----|
| Technical Preparation and Work Packages (WPs) during ILC Pre-lab | 1 |
| Outline : | 1 |
| Timeline (example of SRF and positron): | 3 |
| Area System 1: ML and SRF..... | 4 |
| Overview: | 4 |
| Area System ML-SRF: Work packages (WPs)..... | 5 |
| WP-1: Cavity Industrial-Production Readiness..... | 6 |
| Technical Preparations Plan:..... | 6 |
| Goals of the (9-cell) Cavity Technical Preparation:..... | 6 |
| List of items:: | 6 |
| Status and Prospects:..... | 7 |
| Figures related to WP-1:..... | 8 |
| WP-2: Cryomodule (CM) Global Transfer and Performance Assurance | 9 |
| Technical Preparation Plan: | 9 |
| Goals of the CM technical preparation: | 9 |
| List of items:: | 10 |
| Status and Prospects:..... | 11 |
| Figures related to WP-2:..... | 12 |
| WP-3: Crab Cavity System (for BDS Area System)..... | 13 |
| Technical Preparation Plan: | 13 |
| Goals of technical preparation:..... | 13 |
| List of items:: | 14 |
| Status and Prospects:..... | 14 |
| Figures related to this WP-3:..... | 15 |
| Area System 2: Electron Source | 16 |
| WP-4: Electron Source | 16 |
| Technical Preparation Plan: | 16 |
| Goals of the technical preparation (for Pre-Lab phase 2022-2025): | 16 |
| List of items:: | 17 |
| Status and Prospects..... | 17 |
| Items:..... | 19 |
| References: | 24 |
| Area System 3: Positron Source..... | 27 |
| Introduction: | 27 |
| References | 27 |
| Area System 3.1: Undulator Positron Source..... | 28 |

| | |
|---|----|
| Overview: | 28 |
| Technical preparation goals for the Pre-Lab phase (2022–2025):..... | 28 |
| Area System Undulator Positron Source: Work packages (WPs) | 28 |
| WP-5: Undulator Technology..... | 29 |
| Technical Preparation Plan: | 29 |
| List of items:: | 29 |
| Status and Prospects:..... | 29 |
| WP-6: Target Technology | 31 |
| Technical Preparation Plan: | 31 |
| Goals of the technical preparation (for Pre-Lab phase 2022-2025): | 31 |
| List of items:: | 31 |
| Status and Prospects:..... | 31 |
| WP-7: Magnetic Focusing System..... | 35 |
| Technical Preparation Plan: | 35 |
| Technical preparation goals for Pre-Lab phase (2022–2025):..... | 35 |
| List of items:: | 35 |
| Status and Prospects..... | 35 |
| References | 37 |
| Area System 3.2: Electron-Driven Positron Source | 38 |
| Overview: | 38 |
| Goals of the technical preparation: | 40 |
| Area System Electron-Driven Positron Source: Work packages (WPs)..... | 40 |
| References | 40 |
| WP-8: Target..... | 42 |
| Technical Preparation Plan: | 42 |
| Goals of the technical preparation (fore Pre-Lab phase 2022-2025) | 42 |
| List of items:: | 42 |
| Status and Prospects:..... | 42 |
| Summary table of tasks | 44 |
| References | 44 |
| WP-9: Flux Concentrator..... | 45 |
| Technical Preparation Plan: | 45 |
| Goals of the technical preparation (for Pre-Lab phase 2022-2025): | 45 |
| List of items:: | 45 |
| Status and Prospects:..... | 45 |
| Summary Table of tasks..... | 46 |
| References | 47 |
| WP-10: Capture Linac | 48 |

| | |
|--|----|
| Technical Preparation Plan: | 48 |
| Goals of the technical preparation (for Pre-Lab phase 2022-2025): | 49 |
| List of items:: | 49 |
| Status and Prospects | 49 |
| Summary Table of tasks..... | 50 |
| References | 50 |
| WP-11: Target Maintenance (common issue for undulator and e-driven sources)..... | 51 |
| Technical Preparation Plan | 51 |
| Goals of the technical preparation (for Pre-Lab phase (2022–2025): | 52 |
| List of items:: | 52 |
| Status and Prospects:..... | 52 |
| Summary Table of tasks..... | 52 |
| References | 53 |
| Area-System 4: Damping ring | 54 |
| Overview: | 54 |
| Area-System Damping ring: Work packages:..... | 54 |
| WP-12: System design of ILC damping ring | 55 |
| Technical Preparations Plan:..... | 55 |
| Goals of the technical preparation: | 55 |
| List of items: | 55 |
| Status and Prospects:..... | 56 |
| WP-13: Evaluation of collective effects in ILC damping ring | 59 |
| Technical Preparations Plan:..... | 59 |
| Goals of the technical preparation: | 59 |
| List of items:: | 59 |
| Status and Prospects:..... | 59 |
| WP-14: System design of ILC DR injection/extraction kickers | 62 |
| Technical Preparations Plan:..... | 62 |
| Goals of the technical preparation: | 62 |
| List of items:: | 62 |
| Status and Prospects:..... | 63 |
| Area-System 5: Beam Delivery System | 65 |
| Overview: | 65 |
| Area-System BDS: Work packages:..... | 65 |
| WP-15 : System design of ILC final focus beamline | 66 |
| Technical Preparation Plan: | 66 |
| Goals of the technical preparation: | 66 |
| List of items:: | 66 |

| | |
|---|----|
| Status and Prospects:..... | 66 |
| WP-16 : Final doublet design optimization | 69 |
| Technical Preparation Plan: | 69 |
| Goals of the technical preparation: | 69 |
| List of items:: | 69 |
| Status and Prospects:..... | 69 |
| Area System 6: Beam dump..... | 73 |
| Overview: | 73 |
| Area System Beam Dump: WPs: | 73 |
| WP-17: System design of the main beam dump | 74 |
| Technical Preparations Plan:..... | 74 |
| Goals of technical preparation:..... | 74 |
| List of items:: | 74 |
| Status and Prospects:..... | 75 |
| WP-18: System design of the photon dump for undulator positron source | 77 |
| Technical Preparation Plan: | 77 |
| Goals of technical preparation:..... | 77 |
| List of items:: | 77 |
| Status and Prospects:..... | 78 |
| Appendix | 80 |
| List of WPs | 80 |
| ILC parameters:..... | 83 |

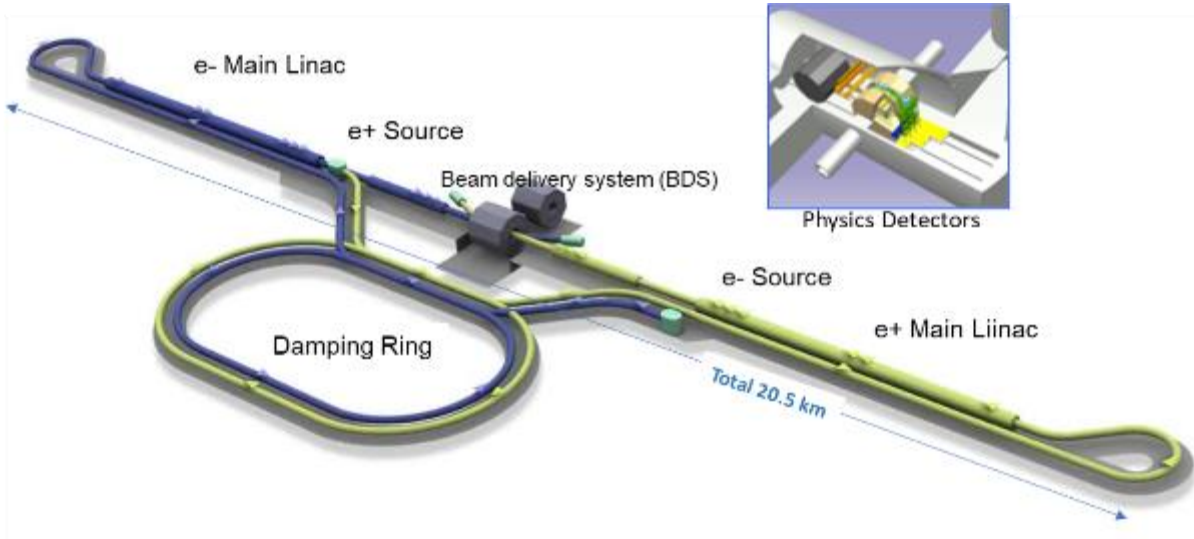
Technical Preparation and Work Packages (WPs) during ILC Pre-lab

IDT-WG2
(Ver.3,2021-Jan-26)

Outline :

The International Linear Collider (ILC) is an electron–positron collider with a total length of approximately 20 km. The ILC consists of the following components: (1) electron and positron sources, (2) damping rings (DRs) to reduce the emittance (a value corresponding to the spread of the beam) of the e-/e+ beams, (3) beam transportation from the damping rings to the main linear accelerators (RTML), (4) the main linear accelerators (MLs), including bunch compressors (to compress the beam bunch length) to accelerate the e-/e+ beams using superconducting RF technology, beam delivery, and a final focusing system (BDS) to focus and adjust the final beam to increase the luminosity, and (5) the beam interaction region for the machine and detector interface (MDI) where the detectors are installed. After passing through the interaction region, the beams go to the beam dumps (DUMP).

The technical preparation plan defines all activities necessary during the main preparation phase to prepare



for the construction phase of the ILC. The technical preparation plan will be conducted by ILC Pre-Lab. The plan assumes that most of the preparation tasks will involve international collaboration based on memoranda of understanding (MOUs) between laboratories/institutions. The technical preparation work packages (WPs) have been discussed and defined by IDT-WG2.

The WPs include:

- ML and SRF: Cavity and Cryomodule (CM) production readiness, which is based on the global cavity fabrication of $\sim 3 \times 40$ cavities and the required RF performance achievement with $\geq 90\%$ success

demonstrated with sufficient statistics by using part of them, and on the global CM fabrication of 3×2 CMs using 40% of the cavities fabricated.

- The global CM transfer program is conducted to simulate all the CM fabrication processes that satisfy high-pressure regulation, safe transport across oceans, and the qualification of the CM performance after shipping from Europe and the Americas to Japan across oceans. One of the two CMs in each region is used for this purpose.
- Positron source: The final design selection with either an undulator-driven or an electron-driven option and technology readiness to be demonstrated.
- DR and BDS: Readiness of nanobeam technology (ATF3 and related) based on DR and BDS subsystems to be demonstrated, particularly for fast kicker and feedback controls, and
- Beam dump: system design to be established, including beam window handling, cooling water circulation, and safety assurance.

A total of 18 (3 SRF, 8 Sources, 3 DR, 2 BDS and 2 Dumps) are proposed as shown in Table 1 and Figure 1. Each work package includes:

- Technical readiness evaluation (listed in each technical proposal)
- Engineering Design Report (EDR) documentation with cost estimate confirmation for the ILC construction

Table 1. List of WPs

| | | |
|------------------------------|----------------------|---------------------------------------|
| 1. ML&SRF: | | <i>41.7 MILCU*, 282 FTE-yr</i> |
| WP-1 | Cavity production | |
| WP-2 | Cryomodule transfer | |
| WP-3 | Crab cavity | |
| 2. Electron Source: | | <i>2.6 MILCU, 6 FTE-yr</i> |
| WP-4 | Electron source | |
| 3. Positron Source: | | |
| 3.1 Undulator scheme: | | <i>0.9 MILCU, 10 FTE-yr</i> |
| WP-5 | Undulator | |
| WP-6 | Rotating target | |
| WP-7 | Magnetic focusing | |
| 3.2 e-Driven scheme: | | <i>4.4 MILCU, 5 FTE-yr</i> |
| WP-8 | Rotating target | |
| WP-9 | Magnetic focusing | |
| WP-10 | Capture cavity | |
| WP-11 | Target replacement | |
| 4. DR | | <i>2.5 MILCU, 29 FTE-yr</i> |
| WP-12 | System design | |
| WP-13 | Collective effect | |
| WP-14 | Injection/extraction | |
| 5. BDS | | <i>2.2 MILCU, 14 FTE-yr</i> |
| WP-15 | Final focus | |
| WP-16 | Final doublet | |
| 6. Dump | | <i>3.2 MILCU, 12 FTE-yr</i> |
| WP-17 | Main dump | |
| WP-18 | Photon dump | |

* ILCU = 2012 US\$ estimate

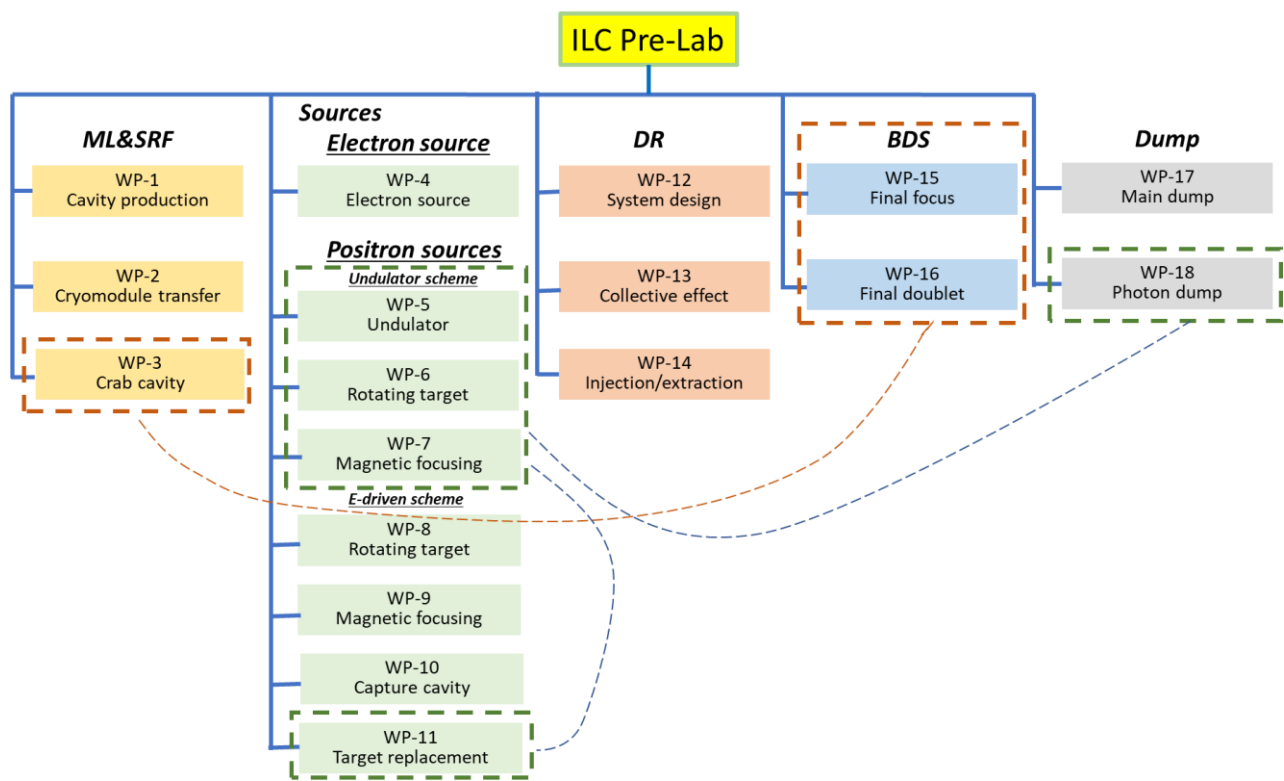


Figure 1: Summary of work packages.

Timeline (example of SRF and positron):

A four-year preparation period is assumed. In the case of the SRF and positron, the following schedule is considered.

1st year:

- Extend SRF cost reduction R&D, Start a pre-series SRF cavities production preparing for industrialization
- Continue positron survey, positron review

2nd year:

- Complete SRF cost-reduction R&D, and extend the work to assemble the cavities with cryomodule (CM)
- Positron review

3rd year:

- Demonstrate “Cryomodule Global transfer, aiming at HPG legal-process, shipment, and SRF QA test after transport
- Mature Lab. planning and preparation
- Establish positron scheme down-select, prototyping of critical items (such as positron target)

4th year:

- Evaluate CM performance after CM shipment, and prepare for Hub Lab. Functioning
- Progress prototyping of critical items (such as positron target)

Area System 1: ML and SRF

(Ver.3,2021-Jan-26)

Overview:

Approximately 9,000 superconducting RF cavities are produced and used for the assembly of approximately 900 SRF cryomodules (CMs), corresponding to about 25–30% of the total ILC construction cost. It should be noted that the production scales are a factor of at least 10 times larger than those of existing SRF accelerator projects. It is assumed that several regional Hub-Labs will be set up in order to share in the production of large numbers of CMs for the ILC. The CMs will be assembled and first tested in each hub laboratory in a planned fraction, and will then be transported to the ILC Laboratory, where the CM performances in some fraction will be checked, particularly more in the early production stage, before the CM installation into the ILC tunnel.

The Science Council of Japan (SCJ) and the Ministry of Education, Culture, Sport, Science and Technology (MEXT, ILC Advisory Panel) pointed out technical concerns about maintaining cavity quality during mass production and CM assembly. In response to these concerns, this technical preparation plan is proposed to demonstrate the SRF cavity and CM production readiness using cost-effective production methods on a scale of 1% of the full production, corresponding to about 120 cavities and 6 CMs during the ILC Pre-Lab phase in the global collaboration. It should be noted that these numbers of cavities and CMs may be adjusted, depending on regional cooperation/consortium formation with the regional responsibility and funding. The cavity performance will be evaluated to confirm their production success yields in each region, and the plug compatibility will be confirmed. One-third of the cavities will be produced in Japan, and a further one-third in each of the Americas and Europe regions. Of the 120 cavities, 48 were used for six CM assemblies, corresponding to 40%.

Other components such as couplers, tuners, and superconducting magnets are also expected to demonstrate production readiness with cost-effective methods, including their fabrication and performance. Overall testing after assembling these parts into the CM will be the last step for confirming the performance as an accelerator component unit. The Americas and Europe have already integrated significant experience in the cavity and CM production, including the formulation of countermeasures against performance degradation after cryomodule assembly as well as ground CM transport.

The production readiness of SRF crab cavities originally in the BDS sub-system are exceptionally included in the enlarged SRF category from a technical commonality viewpoint, and it is then included as part of the ML-SRF section.

Infrastructure associated with the series of items mentioned above will need to be newly prepared and/or improved with each regional responsibility and financial support, including facilities for cavity testing, surface treatment, conditioning of associate components, CM assembly, and testing.

The contents of this area system mentioned above need to be described in the EDR.

Note: Since 2017, R&Ds on Nb material and new Nb surface treatment methods have been conducted between Japan and the United States with the aim of further improving cavity performance with cost-effective approaches. Improving cavity performance is a theme that has always existed as the most basic motivation and will continue during and after the technical preparation period.

Area System ML-SRF: Work packages (WPs)

| <i>Work package</i> | <i>Items</i> |
|--|---|
| <p><u>WP- 1:</u> Cavity Industrial-Production Readiness</p> <p># production: 3 x 40 (16 of 40 go to CM assembly)</p> | Cavity production readiness, incl. cavities w/ He tank + magnetic shield for cavity, high-pressure-gas regulation, surface-preparation/heat treatment (HT)/Clean-room work, partly including the 2nd pass, vertical test (VT) |
| | Plug compatibility, Nb material, and recipe for surface treatment to be reconfirmed/decided |
| | Cavity Production Success yield to be confirmed (before He tank jacketing) |
| | Tuner baseline design to be established |
| | <u>Note:</u> Infrastructure for surface treatment, HT, VT, pre-tuning, etc. (with each regional responsibility) |
| <p><u>WP-2:</u> Cryomodule (CM) Global Transfer and Performance Assurance</p> <p># production: 3 x 2</p> | Coupler production readiness, including preparation/RF processing (# Couplers, 3 × 20) |
| | <u>Note:</u> Infrastructure for coupler conditioning: klystron, baking furnace, and associated environment (with each regional responsibility) |
| | Tuner production readiness, including reliability verification (# Tuners, 3 × 20) |
| | Superconducting Magnet (SCM: Q+D combined) production readiness (# SCMs, 3 × 3 (1 prototype + 2)) |
| | CM production readiness incl. high-pressure-gas, vacuum vessel (VV), cold-mass, and assembly (cavity-string, coupler, tuner, SCM etc.) |
| | CM test including degradation mitigation (in 2-CM joint work, etc.) at assembly site before ready for CM transportation |
| | CM Transportation cage and shock damper to be established |
| | Ground transportation practice, using mockup-CM |
| | Ground transportation test, using production-CM longer than Eu-XFEL |
| | Global transport of CM by sea shipment (requiring longer container) |
| | Performance assurance test after CM global transport (at KEK) |
| | Returning transport of CM back to home country (by sea shipment) |
| | <u>Note:</u> Hub-lab Infrastructure for the CM production, assembly, and test (with each regional responsibility) |
| <p><u>WP-3:</u> Crab Cavity (CC) for BDS</p> <p>#CC production: 4 # CC-CM production: 1</p> | Decision of installation location with cryogenics/RF location accelerator tunnel |
| | Design and development of prototype cavity/coupler/tune/CM including beam extraction line |
| | Cavity production, including cavities w/ He tank + mag. shield for CM, high-pressure gas regulation, EP/HT/Clean work, including VT |
| | Coupler production including preparation/RF processing readiness (excluding klystron, baking furnace, clean room) |
| | Tuner production readiness |
| | CM production including High-pressure-gas formality, vacuum vessel, cold-mass, and assembly (cavity-string, coupler/tuner, SCM, etc.) |
| | CM test including harmonized operation with two cavities |
| | CC-CM transport cage and shock damper |
| | CC-CM transport tests |
| | Infrastructure for CC and CM development and test (with each regional responsibility.) |

WP-1: Cavity Industrial-Production Readiness

(Ver.2,2020-Jan-26)

Technical Preparations Plan:

WP-1 aims to prepare for the mass production of cavities. Specifically, 120 (3 regions produce 40) cavities are produced using a cost-effective method, and surface treatment (EP and heat treatment) is performed to obtain a higher performance than the conventional cavities, and the cavity performance and success yield are evaluated. 48 ($3 \times 2 \times 8$) out of the 120 cavities are used for the production of six (three regions produce two each) CMs. The goal of cavity performance is as shown in “Goals of the technical preparation” on the next page. The required budget is as shown in “List of items:.” Here, the cost of cavity production includes the He tank, the magnetic shield, the surface treatment, the high-pressure-gas safety act, and the budget required for the second (and subsequent) vertical tests. Prior to the production of cavities, a basic consensus needs to be arrived at regarding plug compatibility, cost-effective cavity production, and surface treatment methods/recipes. It is also necessary to re-establish the tuner design for cost-effective production as well as good performance and long-term stability/reliability. No specific budget (value for production) is assumed for the plug compatibility, the success yield, and the tuner design that is to be established. There is also the possibility of the need for infrastructure development, such as electron beam welding (EBW) machines, vertical cryostats, surface treatment facilities, vacuum furnaces for heat treatment, pre-tuning machines, etc. The required budget is expected to be provided with each regional responsibility, separated from the global WP budget. On the last page of WP-1, there are some figures that show global cooperation and the number of cavities/couplers (/CMs) produced in each region, items about the plug compatibility, and the surface treatment recipe to be re-established.

Goals of the (9-cell) Cavity Technical Preparation:

| <i>Parameters</i> | <i>Unit</i> | <i>Design</i> |
|---|-------------|---|
| Baseline: Cavity gradient, E, at Q value (Q_0) (Cost-Reduction R&D goal: E at Q value) | MV/m | 35 at $Q \geq 0.8 E10$, 31.5 ($\pm 20\%$) at $Q \geq 1E10$ (38.5 at $Q \geq 1.6E10$, 35 at $Q \geq 2E10$) |
| Cavity production yield | % | 90 |

List of items:.

| <i>Items</i> | <i>Quantity</i> |
|--|-----------------|
| Cavity production, partly including cavities w/ He tank + magnetic shield for CM, high-pressure gas regulation, EP/HT/Clean-room work, partly 2nd pass, incl. VT, pre-tuning | 3×40 |
| Plug compatibility, surface treatment, Nb material spec. to be reconfirmed/established | — |
| Cavity production success yield | — |
| Tuner baseline design to be decided | — |
| Infrastructure for EP, HT, VT, pre-tuning, etc. (with regional responsibility) | — |

Status and Prospects:

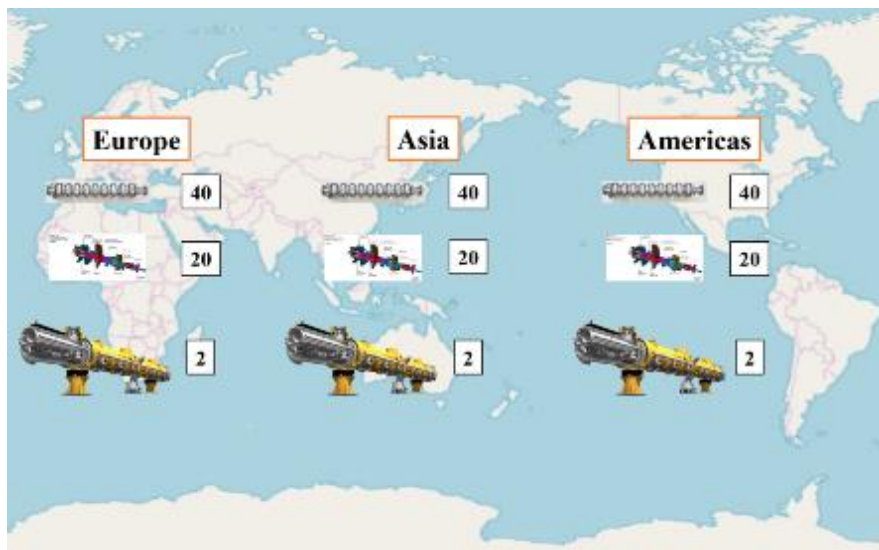
The beam commissioning for the STF-2 accelerator was successfully realized in March 2019 at KEK's Superconducting RF Test Facility (STF). The maximum beam energy achieved was 280 MeV, and the average accelerating gradient evaluated with the beam energy was 33.1 MV/m, exceeding the ILC operational specification/requirement of 31.5 MV/m. DESY and FNAL have already demonstrated CM operation, satisfying the requirements of the ILC.

At KEK's Cavity Fabrication Facility (CFF), single-cell, 3-cell, and 9-cell cavities have been fabricated partly in cooperation with local companies since 2012. CFF is equipped with an EBW machine, a chemical polishing (CP) system, and a mechanical pressing machine. Efforts are being made to achieve cavity fabrication conforming to Japanese high-pressure gas regulations.

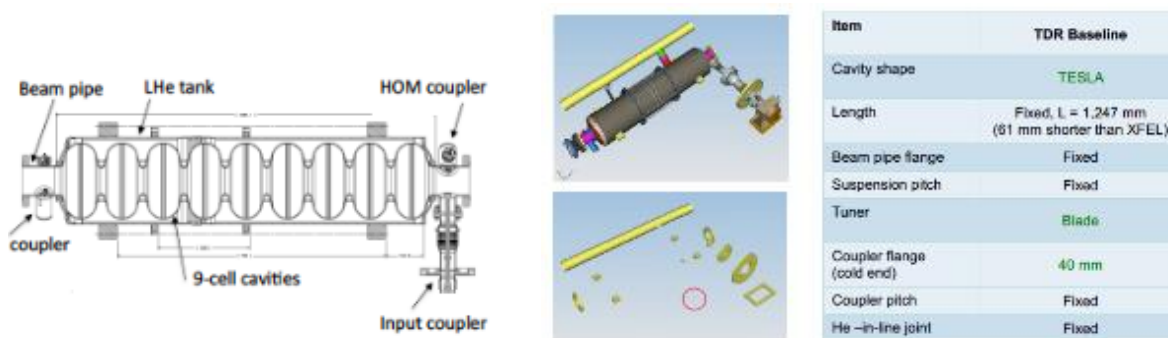
Since 2017, the US and Japan have collaborated on cost-reduction R&D projects. There are two ways to reduce the cost of cavities. One is reducing the cost of the niobium material, and the other is to improve the cavity performance, enabling savings to be realized with respect to the required number of cavities. Research on improving the cavity performance has been extended with worldwide collaboration, including new surface treatments such as "nitrogen-infusion" and "two-stage baking."

Technology for industrial cavity production has matured and has been demonstrated through the successful production of ~ 800 cavities (housed in ~ 100 CMs) for the European XFEL, and through another successful production with a similar level at LCLS-II in the US, which is currently under construction.

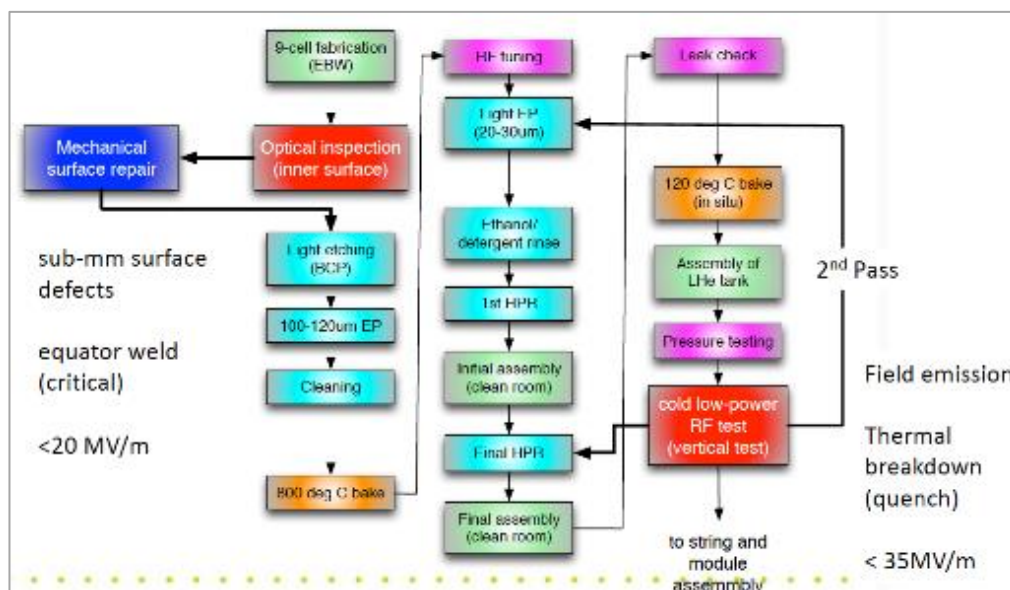
Figures related to WP-1:



Global sharing Plan in Technical Preparation for ML-SRF cavities, couplers/tuners, and cryomodules.



ILC-TDR, ML-SRF cavity, cross-section and envelope plug-compatibility.



ILC-TDR, ML SRF cavity surface process concept.

WP-2: Cryomodule (CM) Global Transfer and Performance Assurance

(Ver.3,2021-Jan-26)

Technical Preparation Plan:

During the technical preparation period, 6 (3×2) CMs will be produced (Type B with a superconducting magnet at center is preferred) in three regions, namely Asia, the Americas, and Europe, and the first test is to confirm performance at each institute before the global transfer. For CM production, the 48 cavities satisfying the “Cavity Industrial-Production Readiness” (WP-1) will be used.

The production readiness of associated components such as couplers, tuners, and superconducting magnets is also important: they are required to be sustainable and reliable for long-term operation and need to be ready for future SRF cavity performance upgrades. The sustainability of superconducting magnets under SRF dark current irradiation and heating initiated by high-gradient SRF linac operation needs to be established.

The ILC-type CM has never been shipped by sea, and the “CM Global Transfer Program” will realize the first sea shipment to confirm the overall SRF technology readiness for the ILC. One CM each from the Americas and Europe will be transported to Japan by sea. The second test will be performed at KEK to examine/verify the required performance to be satisfied. The goals of the technical preparation are shown on the next page. Then, the CM will return to its home country for further investigation, if necessary.

It is also necessary to prepare a dedicated cage, shock damper, and container for the transportation stage. In previous projects, i.e., Euro XFEL and LCLS-II, it was confirmed that the cavity performance remained acceptable after CM ground transportation. However, the ILC CM Global Transfer program will be the first case to confirm the performance after sea transportation. All CMs produced during the technical preparation period are expected to comply with the high-pressure gas regulation. Then, they will be ready for SRF industrial production in the ILC construction after the technical preparation period.

The program includes the preparation of infrastructure and utilities required for the cavity and CM production and testing, if necessary, in each region’s responsibility. On the last page of WP-2, there are some figures that show the concept of CM transport from each region.

Goals of the CM technical preparation:

| <i>Parameters</i> | <i>Unit</i> | <i>Design</i> |
|--|-------------|--------------------------------------|
| Cavity-string field gradient after CM assembly, E, at Q value (Q_0) Note: 10% lower E than that of the 9-cell cavity specification | MV/m | 31.5 ($\pm 20\%$) at $Q \geq 1E10$ |

List of items::

| <i>Items</i> | <i>Quantity</i> |
|--|-----------------|
| Coupler production incl. preparation/RF processing readiness | 3 × 20 |
| Infrastructure for coupler conditioning and performance test: klystron, baking furnace, clean room, etc. (with each regional responsibility) | – |
| Tuner production readiness | 3 × 20 |
| SCM (Q-D combined) production readiness | 3 × 3 |
| CM production including high-pressure-gas, vv, cold-mass, and assembly (cavity-string, coupler/tuner, SCM, etc.) | 3 × 2 |
| CM test and degradation mitigation (in 2-CM joint work) at production site | 3 × 2 |
| CM Transportation cage and shock damper | 3 × 1 |
| Mockup-CM ground transportation practice | 3 × 1 |
| Real-CM ground transportation test | 3 × 1 |
| Global CM transfer (sea shipment, longer than CM at E-XFEL, to be checked) | 2 × 1 |
| Performance assurance test after global CM transfer | 1 × 2 |
| Returning transport to home country again (by sea shipment) | 1 × 2 |
| Hub-lab Infrastructure for the CM assembly, and test (with each regional responsibility) | – |

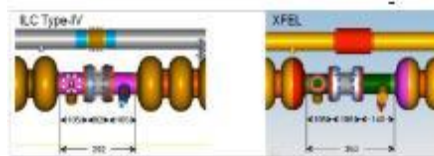
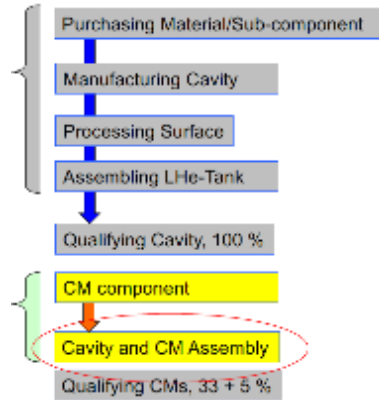
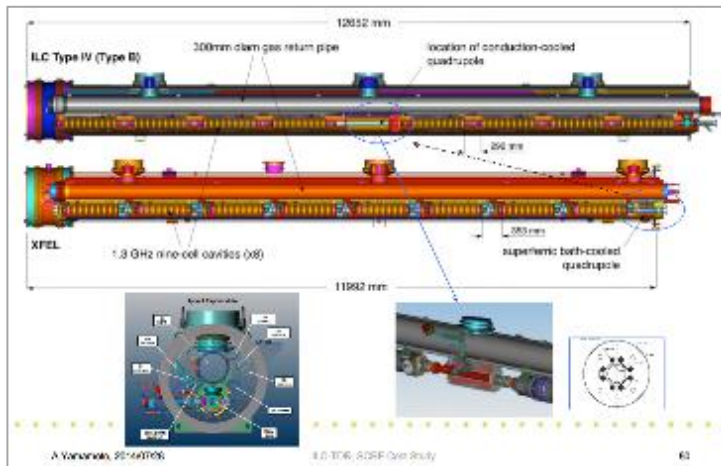
Status and Prospects:

Beam commissioning with an SRF linear accelerator using a series of CMs was successfully realized in March 2019 at the KEK's Superconducting RF Test Facility (STF-2). The maximum beam energy achieved was 280 MeV, and the average accelerating gradient estimated from the beam energy was 33.1 MV/m, exceeding the ILC specification of 31.5 MV/m. DESY and FNAL have already demonstrated CM operation exceeding the requirements of the ILC.

With respect to CMs, cavities and other components that are manufactured in three different regions (Asia, Europe, and the Americas) with a common interface design have been brought together and assembled into a CM at the KEK STF as an international cooperation program that is called S1-Global. The CM performance was successfully demonstrated with a common interface design for the ILC.

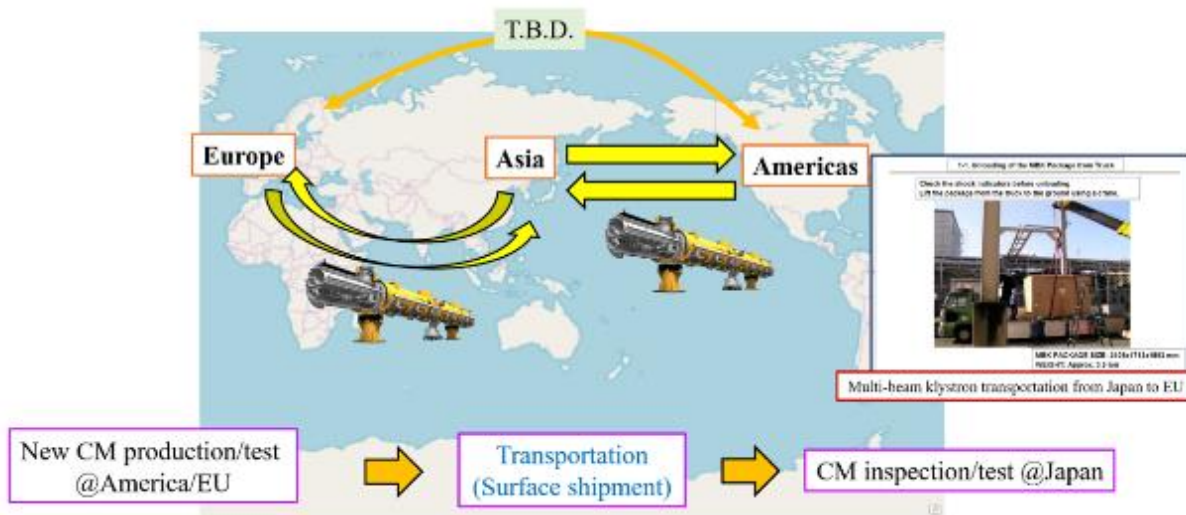
Technology for the CM assembly and SRF accelerator system has matured. The European XFEL accelerator system has been in operation since 2017, a similar accelerator currently under construction for LCLS-II in the US. In both cases, after the CM assembly, the ground transportation of the CMs gained experience during the construction phase and the performance was successfully confirmed before the installation into the accelerator tunnels, with no major transportation-related issues. However, the marine/ship transport of CMs between two different regions across oceans is yet to be demonstrated. This is an important program to be realized as a part of crucial technical preparation in the ILC Pre-Lab phase.

Figures related to WP-2:



(Note: ILC CM length (12,652 m) is longer than that of Euro XFEL/LCLS-II (~ 11,992)).

ILC-ML, Cryomodule (Type-B, with SCM) X-sections and assembly with split-table SCM placed at center.



Plan for the ILC-ML, Cryomodule Global Transfer Program.

WP-3: Crab Cavity System (for BDS Area System)

(Ver.3,2021-Jan-26)

Technical Preparation Plan:

There are two technical issues with Crab Cavity (CC) preparation. First, it will need to be installed in a narrow space 14 m from the ILC collision point, and secondly, two sets of CCs for the electron beam and the positron beam must be operated synchronously. It is expected that the experiences with respect to the design of the CC for the HL-LHC at CERN and the LLRF control system based on the S-band (2856 MHz) operation will assist these technical concerns to be addressed.

The CC technical preparation plan in the ILC Pre-Lab phase aims to produce and test a prototype CM (pCM) system containing two cavities. Because the ILC is required to perform the synchronized operation of two sets of cavities for the electron and the positron beams, it is necessary to demonstrate the synchronized operation with two sets of cavities in one pCM. At the beginning of the technical preparation period, it is necessary to first establish the location of the CC to be installed, including the availability of the cryogenics and RF distribution systems.

Next, the cavity, power coupler, tuner, and pCM will be designed and developed. If it is installed at a location 14 m from the collision point, the beamline beam-pipe for counter-beam extraction will also need to pass through the pCM. After producing these components and testing each component individually, the pCM containing the two cavities is assembled. Then, in the final year of the technical preparation period, a synchronized operation with two crab cavities will be performed to complete the technical demonstration of the CC system. For the series of items mentioned above, the infrastructure will be newly introduced and improved, if necessary, with regional responsibility. With respect to the CC system, a collaboration is expected to be formed and the preparation to be advanced mainly abroad (i.e., not based in Japan).

The “Goals of the technical preparation” and “List of items” are shown on the next page. On the last page of WP-3, there are some figures pertaining to the top view of the near interaction point, the effect of luminosity degradation without CC, and the CC design in the Technical Design Report (TDR).

Goals of technical preparation:

| <i>Parameters</i> | <i>Unit</i> | <i>Design</i> |
|---|-------------|------------------------------------|
| Crab kick voltage at beam energy of 125 GeV | MV | 0.615 @ 3.9 GHz 1.845 @ 1.3 GHz |
| Uncorrelated phase jitter at 125 GeV (rms) | fs | 49 |

List of items::

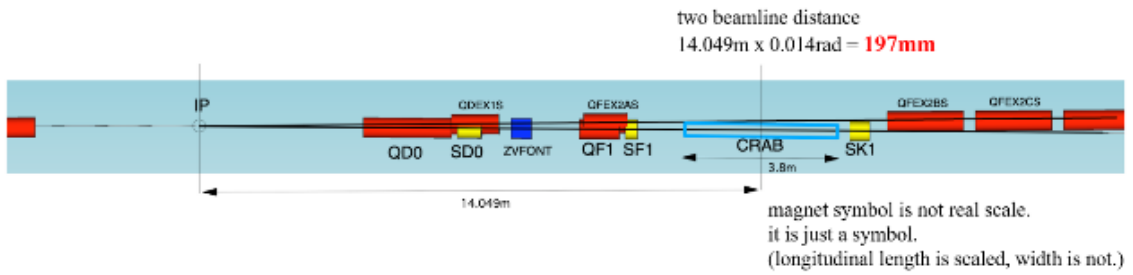
| <i>Items</i> | <i>Quantity (T.B.D.)</i> |
|---|------------------------------|
| Decision of installation location with cryogenics/RF location in the accelerator tunnel | – |
| Design and development of prototype cavity/coupler/tuner/CM including beam extraction line | – |
| Cavity production, including cavities w/ He tank + mag. shield for CM, high-pressure gas regulation, EP/HT/Clean work, including VT | 4 |
| Coupler production including preparation/RF processing readiness (excluding klystron, baking furnace, clean room) | 4 |
| Tuner production readiness | 4 |
| CM production including High-pressure-gas formality, vacuum vessel, cold-mass, and assembly (cavity-string, coupler/tuner, SCM, etc.) | 1 |
| CM test including harmonized operation with two cavities | 1 |
| CC-CM transport cage and shock damper | 1 |
| CC-CM transport tests | 1 |
| Infrastructure for CC and CM development and test (with each regional responsibility.) | – |

Status and Prospects:

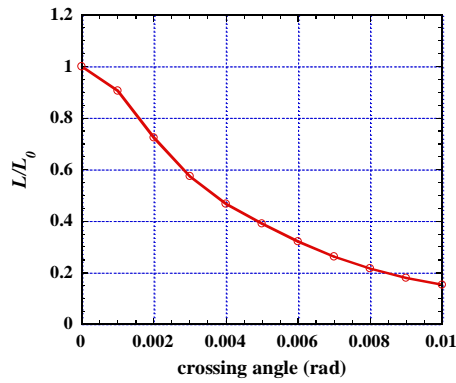
KEKB-Factory was the first collider to introduce a CC system, and it was successfully operated from 2007 to 2010. This success proved for the first time worldwide that the luminosity could be increased by using the CC system. After the KEKB-Factory progress, the HL-LHC CC prototype has been developed through cooperation between CERN/Europe and Americas, and cavities with different shapes (so-called DQW and RFD) have been developed with a common CM design to fit into the narrow space of the HL-LHC beamline. These experiences will also be very useful for the ILC CC design and development.

The development of the ILC CC was carried out mainly in Europe and the Americas during the ILC-GDE phase period. Unfortunately, it was not realized to fabricate a prototype CM in this period, and then no systematic test was realized for the synchronized operation with two cavities. Therefore, the CC technical preparation plan needs to reach a synchronized operation. The CC CM needs to be compact and to enable to accommodate the beam-pipe for another beam line in the same cryostat, while satisfying the high-pressure-gas regulation also during the four-year ILC Pre-Lab phase. It is important to establish a global collaboration that is mainly organized with participations from Europe and/or the Americas.

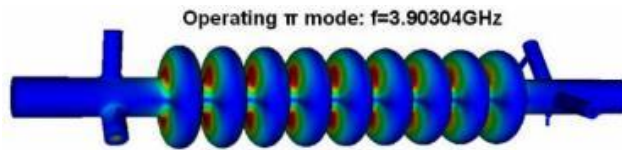
Figures related to this WP-3:



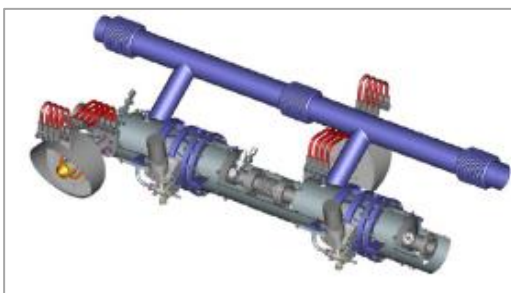
Top view near the interaction point to install crab cavity (CC)



Luminosity degradation by crossing angle (7 mrad in the case of ILC)



Design of 3.9-GHz 9-cell CC presented in TDR.



(a)



(b)

- (a) Two 3.9 GHz packages in CM for Euro-XFEL injector as a reference (C, Maiano et al., SRF2015, MOPB076), and
 (b) 3.9 GHz CM for Euro-XFEL as a reference (cited from ILC Technical Design Report (TDR))

Area System 2: Electron Source

(Ver.2,2021-Jan-26)

WP-4: Electron Source

Technical Preparation Plan:

The baseline design of the polarized electron source, includes the drive laser, a 200 kV DC high voltage photogun, GaAs/GaAsP photocathodes which provide polarization >85%, and the design requirements of the electron injector. This review of Pre-Lab technical preparations is based upon beam specifications in the 2013 TDR (see below). While there are no foreseeable “show-stoppers” leading to the construction of the ILC polarized electron source, there remain unfinished critical technical tasks from the GDE period which include completing a prototype drive laser, and then using it to test the high bunch charge, high peak current conditions from a strained superlattice GaAs/GaAsP photocathode from the high voltage gun. Additionally, since the GDE there have been meaningful technological improvements in lasers, high voltage guns and photocathodes which should be incorporated to the baseline design and incorporated, as opportunities for reliability, performance or cost improvement. The contents of this area system mentioned above need to be described in the EDR (Engineering Design Report).

This section defines one WP:

| | | |
|------|-----------------|--------------------------|
| WP-4 | Electron Source | Drive laser system |
| | | HV Photogun |
| | | GaAs/GaAsP Photocathodes |

Goals of the technical preparation (for Pre-Lab phase 2022-2025):

1. Reevaluate the drive laser design and cost, build a prototype to demonstrate the beam pattern,
2. Design a higher voltage gun 350 kV with greater reliability/headroom, and build it,
3. Evaluate if higher gun voltage and shorter laser pulse length relaxes harmonic bunching,
4. Produce GaAs/GaAsP photocathodes with P>90%, QE>1%, work with vendor to commercialize

The parameters described in the TDR are still valid as shown in the table below:

| Parameters | Symbol | Unit | Design |
|---------------------------------------|------------|------|--------------------|
| Electrons per bunch (at gun exit) | $N_{_}$ | | 3×10^{10} |
| Electrons per bunch (at DR injection) | $N_{_}$ | | 2×10^{10} |
| Number of bunches | n_b | | 1312 |
| Bunch repetition rate | f_b | MHz | 1.8 MHz |
| Bunch train repetition rate | f_{rep} | Hz | 5 (10) Hz |
| FW Bunch length at source | Δt | ns | 1 ns |
| Peak current in bunch at source | I | A | 3.2 A |

| | | | |
|----------------------------------|--------------|---------|--------------|
| Energy stability | σ_E/E | % (rms) | < 5 |
| Polarization | P_e | % | > 80 |
| Photocathode quantum efficiency | QE | % | 0.5 |
| Drive laser wavelength (tunable) | λ | nm | 790 \pm 20 |
| Single bunch laser energy | u_b | μ J | 5 |

List of items::

| <i>Items</i> | <i>Tasks</i> |
|--------------------------|--|
| Drive laser system | Design and provide a prototype drive laser with ILC bunch train |
| HV Photogun | Design and build a photogun operating at 350 kV without field emission and static vacuum <2x10 ⁻¹² Torr |
| GaAs/GaAsP Photocathodes | Commercialize strained superlattice GaAs / GaAsP photocathodes with P>90% and QE>1% |

Status and Prospects

Drive Laser

A new drive laser must be developed for the ILC polarized injector. SLAC previously owned this task however, their polarized source group no longer exists, staff have retired or moved on to other projects. During the GDE period SLAC built a prototype to demonstrate the required ILC pulse pattern, based on an external high power cavity, however the tested scheme was not fully successful. The drive laser was meant to be moved to JLab to demonstrate the electron beam pattern from a HV gun, but ultimately this task was not completed before the GDE period ended.

The original ILC drive laser is complicated and costly (>1M\$). Given that laser technology has continued to improve since the GDE it is worthwhile to reevaluate the design and cost. Notably, gain switched fiber lasers now produce ~MHz rep rate, high peak power pulses, are extremely reliable and have become quite affordable. In addition, it would be worthwhile to explore a) narrowing the wavelength tunability for highly predictable GaAs/GaAsP photocathodes, and b) shortening the optical pulse to 100's of picoseconds to relax the harmonic bunching requirements for energy spread.

The basic specifications of drive laser are listed in Table 1, assuming a 5 nC bunch charge from a GaAs/GaAsP with QE>0.5%. To achieve these specifications, we propose a practical laser architecture involving multi-stage amplification, non-linear frequency conversion, and optical parametric amplification, as shown in Figure 1. There are four wavelengths present in the system, 1560 nm, 780 nm, 1030 nm, and 515 nm. The 515 nm laser pulses serve as the pump pulses to the 780 nm seed pulses in the optical parametric amplifier (OPA).

The 780 nm pulses start with a 1.8 MHz/1 ns/1560 nm low power fiber seed laser, which can be built or commercially available. Following fiber pre-amplifiers and a power-amplifier, the energy of each micro-pulse reaches 2.5 uJ with 5 W average power. The 1560 nm laser wavelength is then converted to 780 nm with a second-harmonic generator (SHG), usually yielding 40% efficiency, and leading to 1 uJ pulse energy.

The OPA pump laser has the same technical scheme except that the seed wavelength is 1030 nm. This seed beam is split into 2 separate beams, each of which goes through an independent chain of fiber pre-amplifiers and a power-amplifier to booster the pulse energy to 50 uJ and the average power to 100 W. After SHGs, the two pump beams provide about 50 uJ total pulse energy in 515 nm beam.

A Pockels cell will be used to generate the pulse trains in each beam as defined by the number of pulses which is 1321, and the repetition rate which is 5 Hz. This will also dramatically reduce the average power of the three beams before they reach the OPA. When the OPA is optimized, the 1 uJ/780 nm seed pulse is expected to be amplified to over 10uJ, which leaves a comfortable headroom for sending 5 uJ to the photocathode through optical transport and helicity control unit.

It shall be mentioned, the laser schematic provided here can accommodate flexible laser parameters different from what are listed here. For example, it is possible to change the pulse length, repetition rate, etc. In addition, both transverse and longitudinal beam shaping may be added if necessary to satisfy special requirements by the electron bunches.

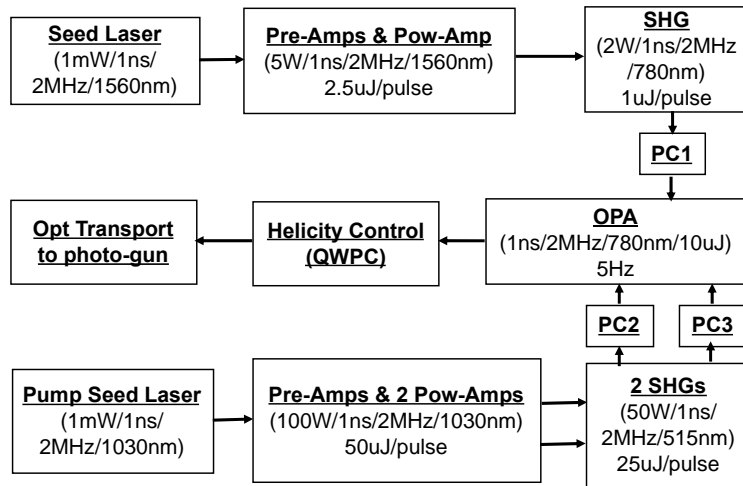


Figure 1. Laser system schematic. PC, Pockels cell. SHG, second harmonic generator. OPA, optical parametric amplifier. QWPC, quarter wave Pockels cell.

Table 1. Basic specifications of proposed drive laser.

| Parameter | Unit | Specification |
|-------------------------|--------------------------|---------------|
| Laser wavelength | nm | 750~780 |
| Pulse length (Gaussian) | ns | 1 |
| Pulse shape | Gaussian or as specified | |
| Pulse energy | uJ | >5 |
| Pulse rep rate | MHz | 1.8 |
| Pulse train length | us | 729 |

| | | |
|--------------------------------|----------|----------|
| Pulse train rep rate | Hz | 5 |
| Number of pulses/pulse train | # | 1312 |
| Laser beam size | Gaussian | 1 to 5mm |
| Laser pulse energy instability | % (rms) | ~3% |
| Timing jitter | ps (rms) | ~5 |
| Pulse contrast | dB | 60 |

Items:

- Seed lasers at 1030 nm and 1560 nm
- Fiber laser amplifiers at 1030 nm and 1560 nm
- Wavelength converters for 780 nm and 515 nm
- Pulse train generator
- Optical parametric amplifier(s)
- Helicity control unit
- Optical transport
- Longitudinal and / or transverse shaping systems (if needed)

DC High Voltage Photo-gun

A high voltage photo-gun meeting or exceeding the specifications of the 90-120 kV SLC gun was required during the GDE, with increased voltage, reduced vacuum and no field emission. JLab built two ILC prototype guns, each constructed using a compact inverted insulator and with a vacuum load-lock that supports relatively quick photocathode replacement [Gr-11].

By adopting an inverted geometry HV feedthrough design based on commercial X-Ray tubes that significantly reduces the HV chamber size and surface area. The inverted HV feedthrough also eliminates the long metallic stalk found in large bore cylindrical insulators, significantly reducing the electrode surface area and thus minimizing risk of field emission and eliminating risk of punch-through induced vacuum break.

The photo-gun employs a cathode electrode manufactured from large grain niobium that was demonstrated to reach higher voltages and field strengths compared to stainless steel electrodes that were prepared using traditional diamond-paste polishing. High voltage processing in the presence of inert gas (He and Kr) was demonstrated to significantly improve the performance of stainless steel and niobium cathode electrodes, eliminating field emission (< 10 pA) at voltages to 225 kV and field strengths > 18 MV/m [Ba-14].

The vacuum chambers and many internal components were baked at 400 C prior to final construction which served to reduce the outgassing rate by a factor of ~ 20 and resulted in the lowest observed static vacuum of all the Jefferson Lab photo-guns to date. The pressure registered by a Leybold extractor gauge was 2e-12 Torr (nitrogen equivalent), which is very close to the x-ray limit of the gauge. This photo-gun has undergone

extensive testing, demonstrating reliable beam delivery from strained-superlattice GaAs/GaAsP photocathodes at average current up to 4 mA.

A second load-locked photo-gun with an inverted insulator was constructed for CEBAF [Ad-10]. It employs a stainless steel cathode electrode biased at 130 kV. It has operated reliably since ~2010 free of field emission, delivering more than 200 uA average beam current for month-long periods without interruption and with electron beam polarization > 85%.

These observations motivated JLab to design a higher voltage photo-gun, still based on inverted ceramic HV feedthrough. By designing a triple point junction shield, and working with the French Ceramics company SCT, JLab developed a 300kV photo-gun with a larger inverted HV feedthrough compatible with X-ray commercial cables and plugs [He16]. This photo-gun was commissioned and delivered over 1000 hours of un-polarized 300 keV beam using multi-alkali photocathodes, albeit with nA of field emission despite being conditioned to 350kV [He19]. A similar photo-gun based on this design has been built at BNL for the EIC polarized source, with electrodes designed for managing space charge in ns-long pulses [Wa-20]. Since the GDE even higher voltage unpolarized guns 350-500 kV for various projects been built and tested at JLab [Wa-20a], JAEA/KEK [Ni-19,Na-10] and Cornell [Ma-14], however, this higher voltage technology has yet to be implemented in a polarized gun where zero field emission is essential.

During Pre-Lab reconsideration to increase the operating voltage of the ILC *polarized* photo-gun also offers the possibility to relax the sub-harmonic bunching requirements on optical pulse length (that is, maybe a laser pulse than 1 ns is feasible and improves injection), with the added benefit of reducing photocathode ion back bombardment QE degradation, as the ionization cross section decreases with electron beam energy. The ILC source requirements utilizing shorter (<1 ns) pulses may be met with a photo-gun design using custom HV inverted feedthrough compatible with commercial cable/plug capable of 500 kV without breakdown during HV conditioning, and reliable operation at 350kV without detectable field emission and ~10-12 Torr vacuum level (see Table 2).

The HV chamber design must meet multiple criteria: a) sufficient voltage and geometry for the ILC, b) the smallest possible volume and surface area to achieve extreme high vacuum conditions for long photocathode QE lifetime, and c) keeping the maximum gradient near 10 MV/m at the desired operating voltage. The design work includes

- beam dynamics simulations of short, high peak current bunches to define initial longitudinal and transverse laser pulse shape,
- electrostatic design to maximize gradient at the photocathode while limiting gradient on the electrode < 10 MV/m at 350kV,
- shaping the triple point junction shield to linearize the potential along the HV inverted feedthrough, and a custom HV inverted feedthrough (This feedthrough does not exist. MPF Inc in SC has expressed interest in SBIR R&D. Note, there are no US companies that make inverted HV feedthroughs for DC photo-guns (BNL and JLab use small and medium inverted HV feedthroughs, and recently ASU and Cornell are begun using small inverted HV feedthroughs for cryo-cooled electrodes for UED sources).
- designing a biased anode to limit ionized beam from entering cathode-anode gap

- cathode-anode gap vacuum and ion-bombardment modeling to limit photocathode damage

Table 2. Proposed ILC gun operating parameters.

| Parameters | Unit | Design |
|---|------|----------------------|
| Operating voltage without measurable field emission | kV | 350 |
| Expected conditioning voltage | kV | 450 |
| Maximum gradient at operating voltage | MV/m | 10 |
| Static vacuum at operating voltage | Torr | $<1 \times 10^{-12}$ |

GaAs/GaAsP Superlattice Photocathodes

Since the first demonstration of polarized electron beam from GaAs in 1976 [Ma-92] accelerator programs have come to rely heavily on GaAs based photocathodes. There is a long rich history, with breakthroughs and lessons learned that lead to the strained superlattice GaAs/GaAsP photocathodes like those used at JLab today, which provide near 90% polarization and possess ~1% QE. Maruyama *et al.*, working with samples grown at the University of California Berkeley were the first to break the 50% theoretical limit of bulk GaAs, by growing InGaAs on GaAs. The lattice mismatch between the two compounds introduces the desired strain to break the valence band energy level degeneracy, with splitting large enough to achieve polarization 70% but with very small yield, or quantum efficiency (QE). Soon after, similar demonstrations were reported by groups at Nagoya University in Japan [Na-91], and St. Petersburg Technical University in Russia [Ma-91]. Accelerators around the world were quick to install these so-called “strained-layer” photocathodes, with reports of beam polarization approaching 80% but with QE only of the order 0.1%.

The single, relatively-thick, strained-layer photocathode suffered from the give and take of polarization versus QE. Higher QE could be obtained using a thicker strained-layer but at the expense of polarization. There was a limit to how thick the top strained layer could be –too thick and the strain would relax, with polarization returning to the typically low value of bulk GaAs. The problem of strain relaxation was overcome by growing superlattice photocathodes composed of thin-layer pairs of lattice-mismatched material. The combination of many thin-strained layers yielded both high polarization and high QE. The same institutions that pioneered single strained layer photocathodes were also the ones to pioneer strained superlattice photocathodes – SLAC, Nagoya University and St. Petersburg Technical University [Na-98, Ma-04, Ma-08, Na-09].

But it wasn’t until researchers at SLAC teamed with commercial vendors via the SBIR/STTR program that reliable sources of high polarization photocathode material became commercially available: first with SPIRE/Bandwidth Semiconductor [Sp-01] to grow single strained layer photocathodes, and then with SVT Associates [Sv-01] to develop the strained-superlattice photocathode which now represents the benchmark for

success. Both of these photocathodes are based on GaAs grown on GaAsP. Examples of polarization and QE plots from both photocathode types are shown below in Figure 2 [Ba-05]. Besides exhibiting higher polarization and QE, the strained-superlattice photocathode is preferable because peak polarization can be obtained at 780 nm which is accessible with inexpensive telecommunications lasers.

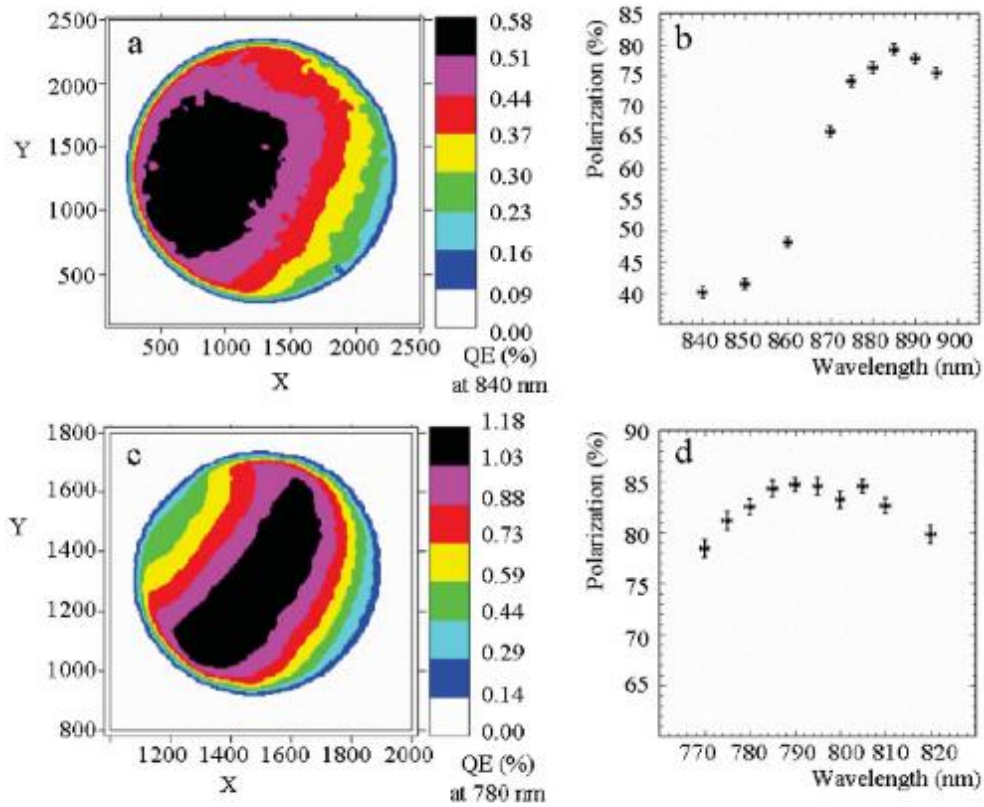


Fig. 2. Quantum efficiency and polarization versus wavelength for commercial photocathodes: (top) Single-strained layer GaAs/GaAsP photocathode fabricated by SPIRE/Bandwidth Semiconductor, (bottom) strained-superlattice GaAs/GaAsP photocathode fabricated by SVT Associates.

Another noteworthy achievement resulting from the commercial R&D program is the demonstration of high polarization and significantly higher QE obtained by growing the “standard” strained-superlattice photocathode atop a distributed Bragg reflector (DBR) [11]. Light penetrating the surface of the photocathode can be trapped within a storage cavity etalon formed by the DBR and front surface of the photocathode (see Figure 3), enhancing light absorption and resulting in 6x increase in photocathode QE. This photocathode – with six times the QE of the standard strained-superlattice photocathode (Figure 4) would relax the requirements for the drive laser and offer greater operating lifetime.

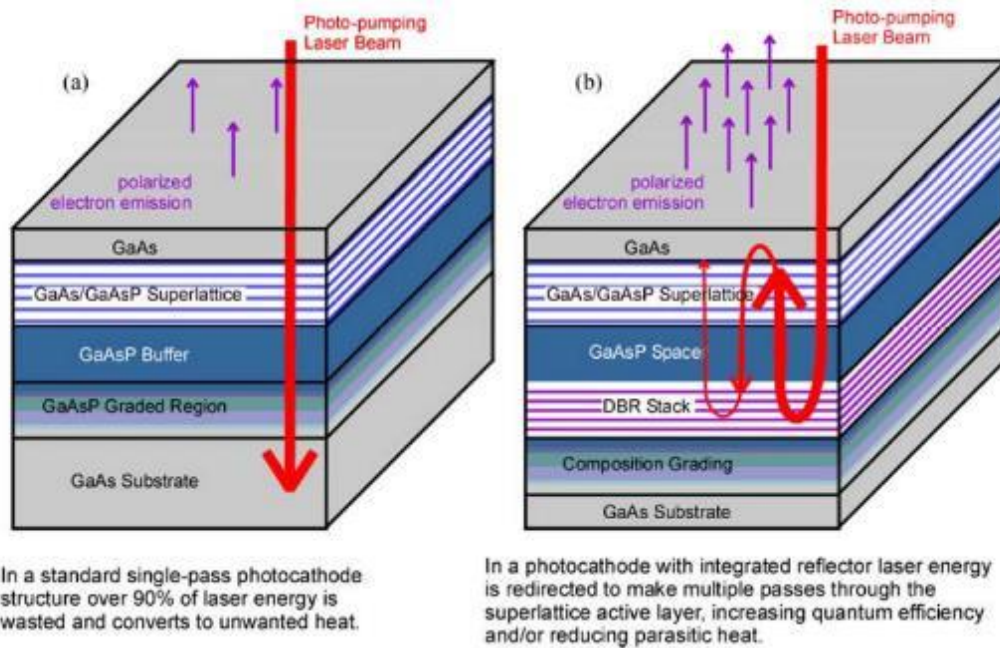


Fig. 3. Illustrations of standard strained-superlattice GaAs/GaAsP photocathode (left) and the standard strained-superlattice GaAs/GaAsP photocathode grown atop a distributed Bragg reflector (DBR). An optical storage cavity is formed by the DBR and front surface of the photocathode resulting in significantly more light absorption and higher QE. These photocathodes were manufactured by SVT Associates.

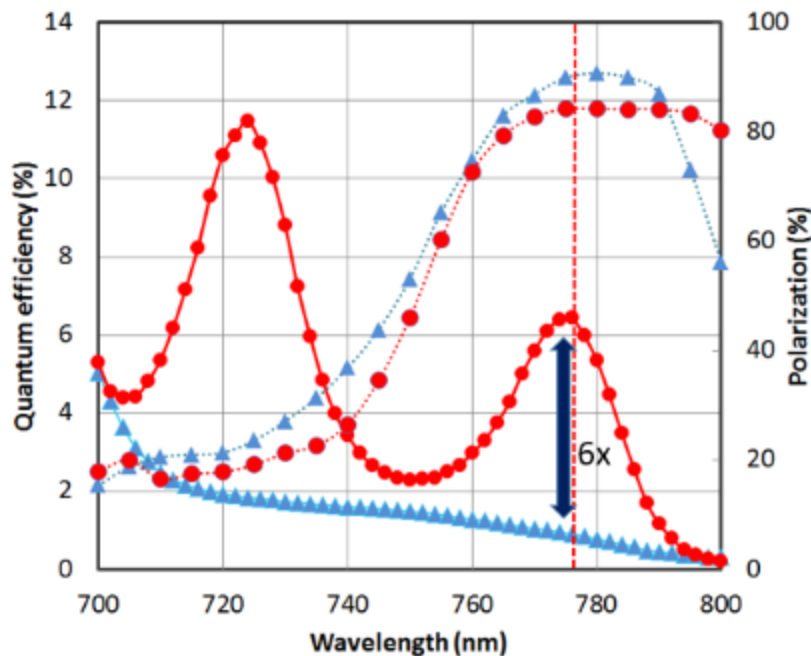


Fig. 4. Photocathode QE and polarization, comparing the standard strained-superlattice GaAs/GaAsP and the similar photocathode grown atop a distributed Bragg reflector providing 6 times the QE at the wavelength of peak polarization. Photocathodes manufactured by SVT Associates.

Unfortunately, without a routine demand for photocathodes, the company SVT Associates no longer sells them. The safety and equipment hazards working with flammable phosphorous, as well as the small market for photocathodes, is generally unfavorable to a commercial vendor without a financial commitment. It would likely take a commitment of ~2 M\$ and 2 FTE to restore this commercial capability in the US.

The alternative to the commercial approach is for the national laboratories to ‘team up’ with a university to develop a reliable approach, or one that is viable to eventually commercialize. Two companies produced high polarization photocathodes in the US. SPIRE/Bandwidth Semiconductor employed MOCVD (metal organic chemical vapor deposition) to fabricate 100 nm thick single strained layer GaAs/GaAsP photocathodes, and SVT Associates employed MBE (molecular beam epitaxy) to fabricate the GaAs/GaAsP strained superlattice photocathodes. In both cases, this required a national lab or university working with the commercial vendor to characterize the samples, using Mott scattering polarimeters and tunable light sources, to characterize the polarization and QE, respectively. Finally, the capability to test photocathode materials in a test gun and beam line is essential.

Experts claim good photocathodes can be fabricated using either method, but it is often stated that MBE provides the required precise control of the strained superlattice photocathode, where layers are only 3 to 4 nm thick. However, some other studies have shown that the quality of the MOCVD grown photocathodes might be better due to the fact that that carrier build-up near photocathode surface in the MOCVD device is more efficient compared to the MBE device [13].

An alternative to both is Chemical Beam Epitaxy (CBE). Rather than directly use the solid or gaseous phase of phosphorous, the CBE process uses precursor gases rather than pure chemical sources as in MBE, reducing the significant hazards associated with solid phosphorus or phosphine gas sources. The precursors are chosen such that they deposit the desired semiconductor element in the structure then are pumped away, leaving a strained superlattice semiconductor structure as in MBE. Compared to MOCVD, the pressures in CBE are much lower, and thus, CBE does not have some of the drawbacks of MOCVD arising from the stagnant gas boundary layer at the growth surface.

Given that polarized photocathodes are on the horizon of accelerator laboratories world-wide, it may be that a globally funded R&D program is the best strategy to address this issue.

References:

[Ad-10] P. A. Adderley, J. Clark, J. Grames, J. Hansknecht, K. Surler-Law, D. Machie, M. Poelker, M. L. Stutzman, and R. Suleiman, “*Load-locked dc high voltage GaAs photogun with an inverted-geometry ceramic insulator*”, *Phys. Rev. ST Accel. Beams* 13, 010101 (2010).

[Ba-05] M. Baylac, *et al.*, “*Effects of atomic hydrogen and deuterium exposure on high polarization GaAs photocathodes*”, *Phys. Rev. ST Accel. Beams*, vol. 8, pp. 123501-1–123501-11, December 2005.

[Ba-14] M. BastaniNejad *et al.*, *Nucl. Instrum. Methods Phys. Res. Sect. A* 762, 135 (2014).

[Gr-11] J.M. Grames, P.A. Adderley, J. Clark, J. Hansknecht, M. Poelker, M.L. Stutzman, R. Suleiman, K. Surler-Law, M. BastaniNejad, J.L. McCarter, CEBAF 200 kV Inverted Electron

Gun, Proc. PAC11, New York, NY, 2011.

[He-16] C. Hernandez-Garcia, M. Poelker, and J. Hansknecht, “*High voltage studies of inverted-geometry ceramic insulators for a 350 kV dc polarized electron gun*”, IEEE Trans. Dielectrics Electrical Insul. **23**, 418 (2016).

[He-19] C. Hernandez-Garcia, et al., Phys. Rev. Accel. And Beams **22**, 113401 (2019).

[Li-16] Wei Liu, Yiqiao Chen, Wentao Lu, Aaron Moy, Matt Poelker, Marcy Stutzman, and Shukui Zhang, “*Record-level quantum efficiency from a high polarization strained GaAs/GaAsP superlattice photocathode with distributed Bragg reflector*”, Appl. Phys. Lett. **109**, 252104 (2016).

[Ma-04] T. Maruyama, D.-A. Luh, A. Brachmann, J.E. Clendenin, E.L. Garwin, S. Harvey, J. Jian, R.E. Kirby, C. Y. Prescott, R. Prepost, and A.M. Moy, “*Systematic study of polarized electron emission from GaAs/GaAsP superlattice photocathodes*”, Appl. Phys. Lett. **85**, 2640 (2004).

[Ma-08] Yu. A. Mamaev, L. G. Gerchikov, Yu. Y. Yashin, D. A. Vasiliev, V.V. Kuzmichev, V.M. Ustinov, A.E. Zhukov, and V.S. Mikhrin, “*Optimized photocathode for spin-polarized electron sources*”, Appl. Phys. Lett. **93**, 81114 (2008).

[Ma-14] J. Maxson, I. Bazarov, B. Dunham, J. Dobbins, X. Liu, and K. Smolenski, “*Design, conditioning, and performance of a high voltage, high brightness dc photoelectron gun with variable gap*”, Review of Scientific Instruments **85**, 093306 (2014); <https://doi.org/10.1063/1.4895641>.

[Ma-91] Yu. A. Mamaev, Y. & Yashin, Y. & Subashiev, A. & Galaktionov, M. & Yavich, B. & Kovalenkov, Oleg & Vinokurov, D. & Reichert, E. & Plutzer, S. & Drescher, P. & Schemies, M. “*Spin-polarized electrons from the surfaces of GaAsP strained films*”, 10.1109/IVMC.1996.601918.

[Ma-92] T. Maruyama et al, “*Electron-spin polarization in photoemission from strained GaAs grown on GaAs_{1-x}P_x*”, Phys. Rev. B, **46**, 4261 (1992).

[Na-91] T. Nakanishi, et al., “*Large enhancement of spin polarization observed by photoelectrons from a strained GaAs layer*”, Physics Lett. A, **158**, 345-349, 1991.

[Na-98] T. Nakanishi, et al., “*Highly polarized electrons from superlattice photocathodes*”, in AIP Conf. Proc., vol. **421**, 300-310 (1998).

[Na-09] Nishitani, M. Tabuchi, Y. Takeda, Y. Suzuki, K. Motoki and T. Meguro, “*Superlattice photocathode with high brightness and long NEA-surface lifetime*”, AIP Conf. Proc., vol 1149, 2009, pp 1047-1051.

[Na-10] R. Nagai, R. Hajima, N. Nishimori, T. Muto, M. Yamamoto, Y. Honda, T. Miyajima, H. Iijima, M. Kuriki, M. Kuwahara, S. Okumi, and T. Nakanishi “*High-voltage testing of a 500-kV dc photocathode electron gun*”, Rev. Sci. Instrum. **81**, 033304 (2010); <https://doi.org/10.1063/1.3354980>.

[Ni-19] N. Nishimori, R. Nagai, R. Hajima, M. Yamamoto, Y. Honda, T. Miyajima, and T. Uchiyama, “*Operational experience of a 500 kV photoemission gun*” Phys. Rev. Accel. Beams **22**, 053402 – Published 14 May 2019.

[Sp-01] SPIRE Semiconductor, L.L.C., 25 Sagamore Park Drive, Hudson, NH 03051, <http://www.spirecorp.com/spire-bandwidth-semiconductor/index.php>.

[Sv-01] SVT Associates, Inc., 7620 Executive Drive, Eden Prairie, MN 55344, <http://www.svta.com>.

[Wa-20] E. Wang, private communication.

[Wa-20a] Y. Wang, M. A. Mamun, P. Adderley, B. Bullard, J. Grames, J. Hansknecht, C. Hernandez-Garcia, R. Kazimi, G. A. Krafft, G. Palacios-Serrano, M. Poelker, M. L. Stutzman, R. Suleiman, M. Tiefenback, S. Wijethunga, J. Yoskowitz, and S. Zhang, "*Thermal emittance and lifetime of alkali-antimonide photocathodes grown on GaAs and molybdenum substrates evaluated in a -300 kV dc photogun*", Phys. Rev. Accel. Beams **23**, 103401, Published 7 October 2020.

Area System 3: Positron Source

(Ver.2,2021-Jan-06)

Introduction:

Two different positron sources are simultaneously being studied currently: the undulator scheme (baseline) and the electron-driven scheme (backup). The former is described in detail in the ILC TDR (Vol 3-II, Chapter 5). The undulator scheme can provide a polarized positron beam; however, it is a new technology. Therefore, a backup scheme has also been studied for safety as briefly described in the TDR (Vol 3-I 4.3.11.1). As of May 2018, the status of the two schemes has been summarized in [1]. One of these two schemes must be selected by an appropriate deadline as the positron source for the project start. The two schemes require significantly different civil engineering designs for the tunnel and utility, which demand considerable cost and time. Hence, the positron scheme for the project start must be selected sufficiently early. According to the timeline of the Pre-Lab that is presently considered, an internal review is planned in the middle of the third year of Pre-Lab. Thus, the scheme must be selected early in this respect as well. In contrast, more time is necessary to achieve the required technology with 100% certainty. As a compromise, we plan to make the decision at the first half of the third year of the Pre-Lab period. According to the presently accepted schedule for Pre-Lab this corresponds to September 2024. (Note that the Pre-Lab start at the beginning of Japanese fiscal year 2022, i.e., April 2022.) The procedure for making the decision is to be discussed in the ILC Pre-Lab, not in the IDT.

In the following sections, some R&D items are assigned “priority” (or “Goal by Sep. 2024”). This means that such items must produce results by the above deadline, whereas work on items that are not assigned “priority” can continue during the remaining years of the Pre-Lab period.

If the corresponding scheme is not selected, the R&D of these items may not be performed in the Pre-Lab but may be subject to future upgrades, depending on their contents.

The two schemes both require a remote target replacement technology. The technologies contain many common aspects such that only one of them is listed in the following (in the e-driven positron source section).

The contents of this area system mentioned above need to be described in the EDR.

References

- 1) Positron Working Group Report, May 23, 2018,
<http://edmsdirect.desy.de/item/D00000001165115>

Area System 3.1: Undulator Positron Source

(Ver.3,2021-Jan-26)

Overview:

The baseline design of the positron no longer has impediments to its further progress, however, a few final design choices and engineering works have yet to be completed. Since the ILC positron working group report [1] was made in 2018, substantial progress had been achieved in the following areas: successful experimental tests of thermal target stress, the detailed design of radiative target cooling, and the design of an alternative solid optical matching device (OMD) (pulsed solenoid) for securing yield with respect to the currently anticipated quarter wave transformer (QWT). Within the Pre-Lab period, laboratory tests of the rotating target wheel and a detailed design of the magnetic bearing, including a laboratory mock-up test, are envisaged.

Other minor open problems, such as optimized undulator parameters for the 250-GeV phase, are to be finalized within the IDT phase.

Technical preparation goals for the Pre-Lab phase (2022–2025):

Three areas have been identified for development in the Pre-Lab period

- A) WP-5: Undulator
- B) WP-6: Target
- C) WP-7: Magnetic Focusing System

Other fields, such as acceleration to the damping ring, also require development; however, they are not essential because the design presented in the TDR is mostly sufficient.

The current status of the undulator scheme is summarized in the 2018 positron working group report [1]; for further details, see [2].

Area System Undulator Positron Source: Work packages (WPs)

| <i>Work package</i> | <i>Items</i> |
|---------------------------------------|--|
| WP- 5: Undulator | Simulation (field,errors, alignment) |
| WP- 6: Rotating target | Design finalization, partial laboratory test, mock-up design |
| | Magnetic bearings: performance, specification, test |
| WP- 7: Magnetic focusing system | Full wheel validation, mock-up |
| | Design selection (FC, QWT, pulsed solenoid, plasma lens), with yield calculation |
| | OMD with fully assembled wheel |

WP-5: Undulator Technology

(Ver.3,2021-Jan-26)

Technical Preparation Plan:

The TDR adopted a superconducting helical undulator with an 11.5 mm pitch, a maximum K parameter of 0.92 (a maximum field of 0.86 T), and a beam aperture diameter of 5.85 mm. One undulator is 1.75 m long (field length), and two undulators are stored in a cryostat at an operating temperature of 4.2 K. The total net length presented in the TDR was 147 m; however, it was increased to 231 m (132 undulators) when the center-of-mass energy at the project start was reduced from 500 to 250 GeV.

A pair of undulators was fabricated and tested at the Rutherford Appleton Laboratory (RAL) and at Cornell University (TDR 3-I, p.128); the pair exhibited sufficient magnetic field strength. Thus, in the entire undulator scheme, the undulator technology itself is relatively well established, even though a few simulation problems remain. Moreover, it may be possible to reoptimize the undulator parameters. These are the subjects of this WP.

Goals of the technical preparation (for Pre-Lab phase 2022-2025)

The technical preparation items for the target technology are as follows.

- * Simulation of heating by the photons
- * Simulation with field errors and misalignment
- * Optimization study of undulator parameters (pitch, K, aperture)

List of items:

| <i>Items</i> | <i>Priority</i> |
|--------------------------------------|-----------------|
| Simulation (field errors, alignment) | |

Status and Prospects:

Undulators at the European XFEL: Three long undulator systems are stably and routinely operating in the European XFEL; these are two planar undulator systems, each approximately 200 m long, and a shorter, planar undulator system that is approximately 120 m long. The shot-to-shot beam alignment requirement is extremely tight for the FELs to lase, and sophisticated feedback systems ensure that this requirement is routinely satisfied. All other X-ray FELs (LCLS, SwissFEL, FERMI@Elettra, SACLA, and PAL XFEL) similarly operate with extremely long undulator systems and tight electron beam alignment control. A prototype ILC undulator module was successfully fabricated and tested at the STFC RAL.

Remaining simulation works

- (1) Detailed simulation studies focused on protection of the undulator walls from photons via the use of masks (to keep the energy deposition at less than 1 W/m). The masks (made of Cu material) have an aperture radius of 2.2 mm and are placed behind the quadrupoles. The total energy deposition in the masks reaches 300 W at the end of the undulatory section. These studies are expected to be completed within

the IDT phase; further details will be provided in [3].

(2) Detailed simulation studies, including field errors and misalignment of the undulators and the orbit correction algorithm. These studies can also be completed within the IDT phase; further details are given in [3].

(3) Further undulator optimization for the ILC 250 GeV stage.

It is anticipated that the possibilities of a lower K value ($K \leq 0.92$) and a smaller undulator aperture (≤ 5.85 mm) at the full undulator length of 231 m will be studied in the IDT phase. In addition the possibility of a shorter pitch undulator may be investigated. This is expected to increase the energy of the first harmonics; hence, the pair production efficiency increases, resulting in yield enhancement or a decrease in the active undulator length. Both intense simulation and engineering studies are planned for the final optimization.

The current positron baseline design offers a positron beam polarization of approximately 30% and is required to achieve the physics goals that are already at the ILC 250 GeV stage (without positron polarization, systematic uncertainties cannot be controlled; for more details, see [4]). The inclusion of variations in undulator parameters (K and λ variations derived from the undulator prototype) can result in a maximum polarization reduction to 27%. Ongoing studies have demonstrated that this effect is mitigated by a more uniform K and λ setup along the undulator modules [3].

The feasibility of the final design approaching a yield of 1.5 e^+/e^- even with a 125 GeV drive beam is the goal within the Pre-Lab phase. The operation of the undulator at higher energies is straightforward; it enhances the yield and even facilitates the operation. With respect to the luminosity upgrade, no constraints are expected.

WP-6: Target Technology

(Ver.3,2021-Jan-26)

Technical Preparation Plan:

TDR adopted a target made of a titanium alloy (Ti6Al4V) of 14mm thick (0.4 radiation length). It is mounted at the rim of a wheel with a diameter of 1 m and rotating at 2000 rpm (100 m/s at the rim). This wheel is placed in a vacuum of $\sim 10^{-6}$ Pa. In the current ILC250 design, the target thickness is reduced to 7 mm without any yield loss. The heat deposited by the beam is approximately 2 kW.

The main problem encountered in previous studies was cooling. The TDR adopted a water-cooling system, with magnetic fluid as the vacuum seal. However, the R&D on this system was discontinued because of vacuum leakage through the seal. Since then, a target with the radiation cooling mechanism has been investigated. To date, principal engineering studies have been conducted, but detailed engineering and manufacturing studies have never been performed. This work package is focused on the target model, from design finalization to fabrication of a full model.

Radiation cooling is a promising new concept for the ILC positron target. Nevertheless, there are already several prototype examples in former experiments, where radiation cooling has been used. For instance the graphite target at CNGS (CERN), immersed in stationary He gas, was cooled mainly by radiation complemented by natural convection as well as experiments at FRIB-US, J-PARC and RAL-UK have studied or used radiation cooled targets

Goals of the technical preparation (for Pre-Lab phase 2022-2025):

The technical preparation items for the target technology are as follows.

- Design finalization of the rotating wheel with radiative cooling design and laboratory test of a stationary sector model. This is labeled as “priority” item.
- Magnetic bearings, feasibility study
- Fabrication of full model
-

List of items::

| <i>Items</i> | |
|---|----------|
| Design finalization, partial laboratory test, mock-up design* | priority |
| Magnetic bearings: performance, specification, test | |
| Full wheel validation, mock-up | |

* high priority to be completed by Sep.2024

Status and Prospects:

a) Target Material Tests

Experimental tests were performed with the electron beam of the microtron in Mainz (MAMI) to simulate the expected cyclic load during the ILC operation. The results of the irradiation tests at MAMI, the comprehensive material analyses (surface and structure) via laser scanning and synchrotron diffraction methods and the comparison with detailed simulation studies using ANSYS revealed that the expected load in the ILC

positron target is less than the material capacity; more details are available in [5]. The experiment demonstrated that the chosen Ti alloy material is well suited for the ILC operation. Nevertheless, further target tests at MAMI using alternative target materials SF61 (Ti with 5.9% Al, 2.7% Sn, 4%Zr, 0.45% Mo, 0.35% Si, 0.22% Y) and Tungsten) are expected in 2020 and will be finalized within the IDT phase.

Institutes currently involved in this:

DESY

Hamburg University

Helmholtz-Zentrum Geesthacht

Mainz University

b) Cooling by thermal radiation

Shown in Fig. 1 is the design for radiation cooling of the rotated wheel. No technical show stoppers are expected and the engineering design has been further revisited for optimization reasons only.

The deposited power in the target is 2kW (nominal luminosity) and heat radiates from the spinning target in vacuum to a stationary water-cooled cooler. The cooling efficiency depends on the temperature, radiating surface, and surface emissivity and is determined by the Ti alloy's thermal conductivity, which is low (approximately 0.06–0.15 K/cm/s). A monolithic Ti target/radiator unit is assumed; hence, a thermal interface with different materials is not required. The heat accumulates in the rim near the beam path. With the nominal load (1312 bunches/pulse), the peak temperature in the Ti6Al4V target wheel reaches ~500 °C; the maximum average temperature along the beam path in the target is approximately 460 °C. The experimental target tests at MAMI, which simulated the cyclic impact at the ILC (as mentioned previously), have demonstrated that the target can sustain the load. Further optimization of the device is anticipated. For instance, extending the wheel radius to approximately 55–60 cm with the beam impact at 50 cm could result in substantial reductions. In principle, increasing the Ti thickness from 0.7 to 1.5 cm outside the beam impact area is equivalent to a substantial increase in thermal conductivity. Further detailed simulations are planned within the IDT period. For the luminosity upgrade, mounting a special radiator (e.g., graphite or copper) to the rim of the target is expected.

For the IDT and the first year of the Pre-Lab phase, it is planned to set-up an experimental mock-up test is planned to check the cooling efficiency with a small sector of the wheel in vacuum. Owing to the T^4 dependence, $dT/T = 1/4 dE_m/E_m$ (where E_m is the emissivity); hence, the impact of emissivity change is not remarkable. Nevertheless, a mock-up test is planned to check the average temperatures and to confirm that the cooling approach works as expected, considering the emissivity and special cooling surface design.

c) Rotating target

Detailed ANSYS simulations are to be performed to verify the dynamic effects, stress waves, and vibration modes of the wheel, using the specifications for the final drive and bearing of the rotating target designed by engineers within the Pre-Lab phase.

d) Magnetic bearings

Radiation cooling allows the use of magnetic bearings. Magnetic bearings are vacuum compatible and can be operated over a long time at high rotational speeds without maintenance. Magnetic bearings are widely used and are standard components. They can easily be adapted to our needs by the industry (e.g., SKF worldwide

and Jülich Kernforschungszentrum (FZJ)). For the Pre-Lab phase, a feasibility study and prototyping with the respective supplier are envisaged. The feasibility test is planned in a vacuum with a subunit, consisting of a realistic axis, weight and preferable with the correct moment of inertia, accomplishing the expectations about vibrations and required velocity control. Magnetic bearings are used in pumps, energy storage devices with extreme loads and a rotation speed even 6000 rpm. Such magnetic bearings are used for Fermi choppers in neutron spallation sources. ESS in Lund-Sweden and Jülich Kernforschungszentrum (FZJ) are specialized on this topic.

Institutes currently involved in this:

DESY

Hamburg University

Juelich Kernforschungszentru, FZJ-Germany (for magnetic bearings)

UK

Principal Layout: Ti-Wheel with a Diameter of 1.0 m, rotating at 100 m/s, 2000 rpm.

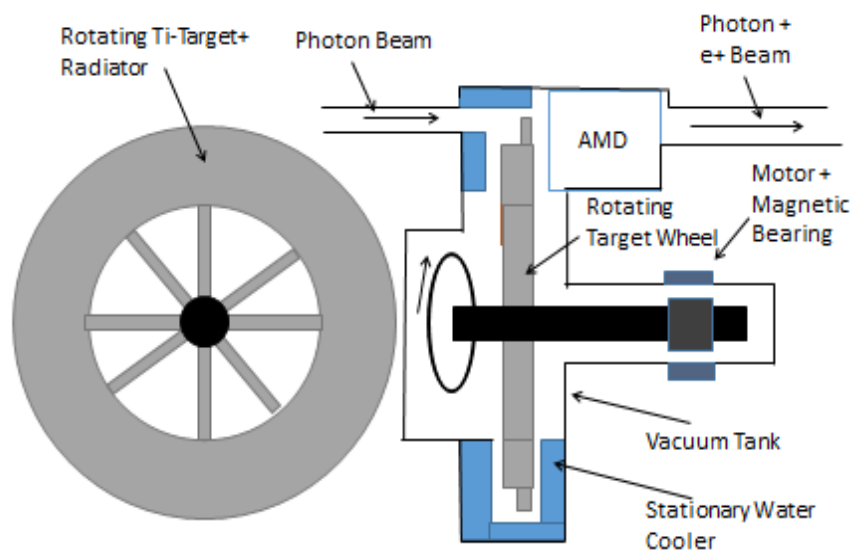
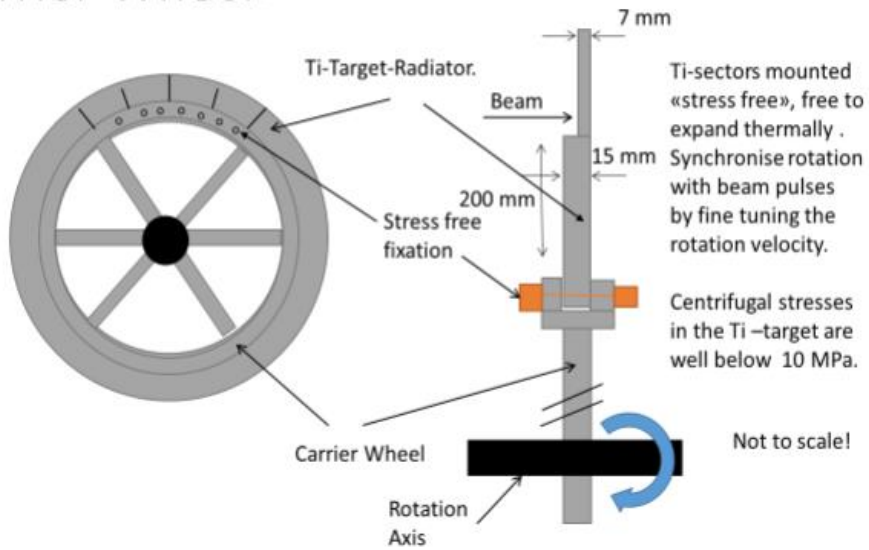


Fig. 1-1 Layout sketch of the rotating wheel including main components: cooling system, magnetic bearing, OMD

Ti-Target Sector Modules, mounted onto a «Carrier Wheel»



5

Fig. 1-2 Ti-Target Sector Modules OMD

WP-7: Magnetic Focusing System

(Ver.2,2021-Jan-26)

Technical Preparation Plan:

The positrons created at the target must be immediately focused after the target. In the TDR, a flux concentrator with a 3.2 T peak field as the OMD was adopted; it was expected to have a field flat-top of approximately 1 ms. However, it was subsequently found that the time dependence of the field is inevitable for such a long pulse due to the skin depth effect.

In the latest design the QWT (Quarter Wave Transformer) with the peak field of approximately 1 T is adopted as the OMD. However, it does not seem to provide sufficient positron yield. The choice of the OMD is essential for the positron source of the undulator scheme.

The possible OMD candidates are as follows:

- (a). pulsed solenoid
- (b). plasma lens
- (c). QWT with increased field
- (d). flux concentrator

First, a choice from among these candidates must be made realistically by considering the engineering involved and the full simulation of the positron yield.

Technical preparation goals for Pre-Lab phase (2022–2025):

The technical preparation items for the magnetic focusing system (OMD) are the following:

- Final design choice among the possible focusing devices with yield calculation
- Construction of the prototype of OMD and the rotating wheel
-

List of items::

| <i>Items</i> | <i>priority</i> |
|---|-----------------|
| Design selection (FC, QWT, pulsed solenoid, plasma lens), with yield calculation* | priority |
| OMD with fully assembled wheel | |

* high priority to be completed by Sep.2024

Status and Prospects

The OMD candidates are described as follows.

a) Pulsed solenoid

As shown in Fig. 2 and Fig. 3, the use of a pulsed solenoid as the OMD can produce a sufficiently high magnetic field in the capture section to provide a yield of $e^+/e^-=1.5$ at a peak magnetic field of approximately 3 T. The main engineering problems were studied, and no showstoppers were found. The interference of the pulsed solenoid with the fast-rotating Ti-wheel has been estimated. On average, less than 200 W is expected to be deposited in the wheel. More detailed simulations are also ongoing. Within the IDT phase, these simulations are expected to be accomplished via yield calculations, including the computation of possible field deformations

caused by the fast-rotating target wheel.

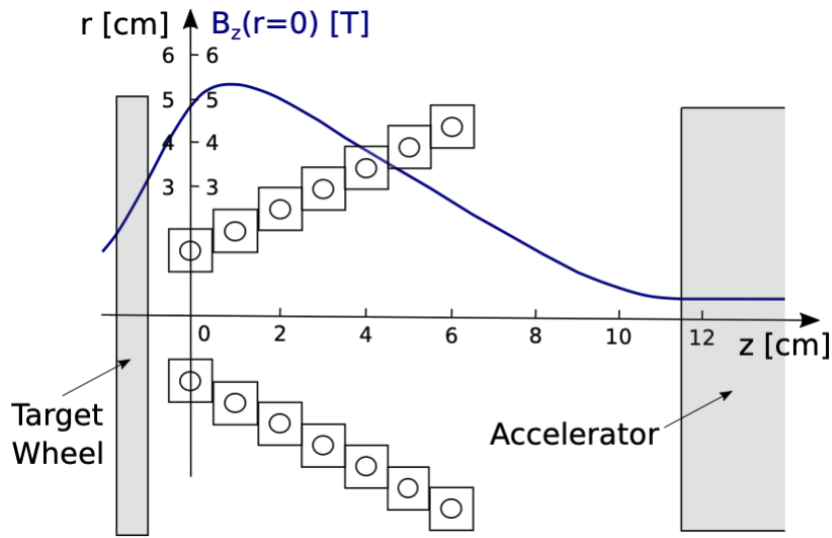


Fig. 2 OMD: Pulsed solenoid and generated B-field.

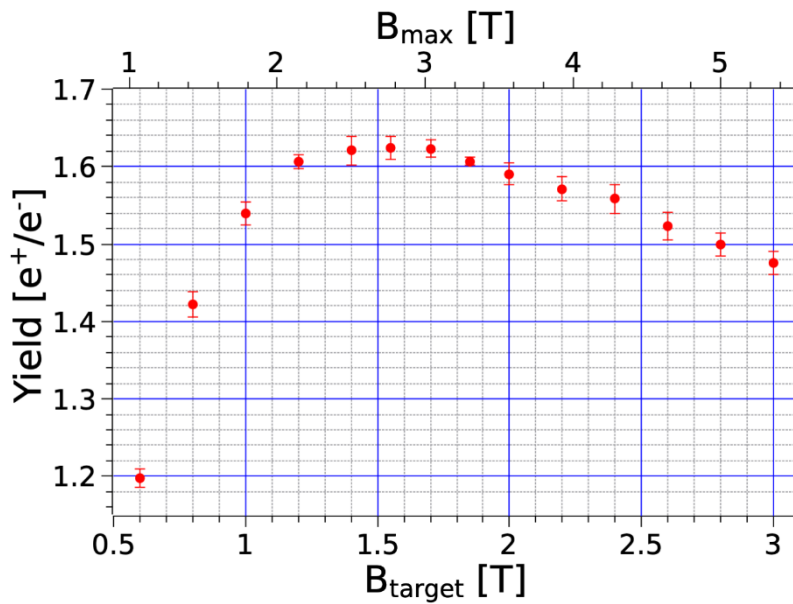


Fig. 3 Expected e^+ yield depending on the B-Field at the target exit

b) Plasma lens

New studies exploit the current progress made in plasma technologies and employ a 3000 A plasma lens as the OMD for the ILC e^+ source. The simulations predict yields that are approximately two times higher than that of the QWT; more details can be found in [7]. This emerging technology involves new sectors in the community to provide possible novel contributions in the field. Grant applications with respect to prototype experiments for such plasma lenses have been submitted. Depending on the approval, the prototype experiments have to be performed within the Pre-Lab phase; an alternative OMD is envisaged at a later stage.

c) QWT

The QWT considered thus far (ANL) provides a matching device with zero magnetic field at the target and a maximum magnetic field of 1 T. However, the expected yield with the current set-up seems not to be sufficient (yield below 1). No engineering study has been performed.

d) Flux concentrator

The TDR design adopted a flux concentrator with a peak field exceeding 3 T. However, it is subsequently found that the field within a beam pulse length of ~ 1 ms is time dependent owing to the skin depth at low frequencies. Nonetheless, it may still be possible to develop a better flux concentrator.

The highest priority for the OMD is the pulsed solenoid. Within the IDT phase and the first year of the Pre-Lab period, a detailed simulation is expected to yield the specification required for the engineering design planned for the Pre-Lab phase.

Institutes currently involved in this:

ANL

CERN

DESY

FNAL

Karlsruhe Institute of Technology

LBNL

Mainz University

University of Frankfurt

University of Hamburg

SLAC

References

[1] Positron Working Group Report, May 23, 2018,

<http://edmsdirect.desy.de/item/D00000001165115>

[2] S. Riemann et. al., 2002.10919 [physics:acc-ph].

[3] K. Alharbi, et al., 2001.08024 [physics:acc-ph]

[4] K. Fujii et al., 1801.02840 [hep-ph], PhD Thesis, R. Karl, Hamburg University, 2019,

J. Beyer et al., 2002.02777 [hep-ex])

[5] F. Dietrich et al., 1902.07744 [physics:acc-ph], A. Ushakov et al.,

IPAC2017 (TUPAB002), and T. Lengler, Ba Thesis, Hamburg University, 2020.

[6] I. Bailey et. al, EUROTeV-Report-2008-028-1, EPAC08 (MOPP069)

[7] M. Formela et al., 2003.03138 [physics:acc-ph]

Area System 3.2: Electron-Driven Positron Source

(Ver.3,2021-Jan-26)

Overview:

The positron source is one of the ILC sub-systems regarding which SCJ and the ILC Advisory Panel of MEXT expressed their concern. This reflects the situation that neither an electron-driven (e-driven) nor an undulator positron source is developed with sufficient technical maturity to start the construction at that moment. Developing an ILC positron source with sufficient technical feasibility and maturity is our goal in the IDT for the Pre-Lab period. In contrast to the undulator source, the e-driven positron source is considered to be “closer to reality”; for the TDR, the system is considered a technical backup [2]. For the ILC, establishing an e-driven ILC positron source as a technical backup is extremely important from the point of view of risk control.

A schematic of the e-driven source is presented in Fig. 1. It consists of a 3.0 GeV electron driver, a W-Re rotating target, followed by a flux concentrator (adiabatic matching device (AMD)), a capture linac placed in a solenoid, a booster, and an ECS. An e-driven source for the ILC was proposed as an alternative to linear colliders [3]. At that time, the pulse structure is identical to that of a superconducting accelerator (1 ms) and requires an

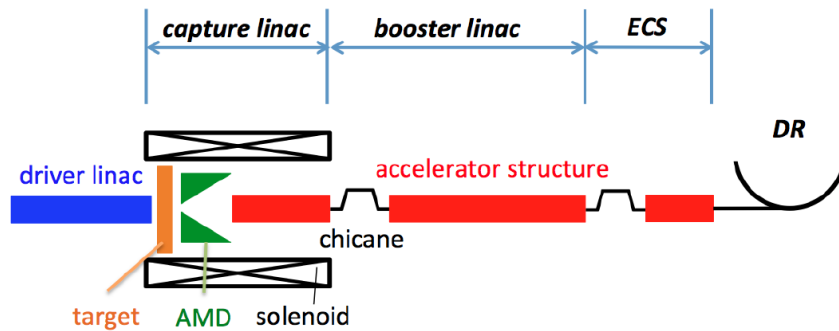


Fig. 1: Schematic of the e-driven ILC positron source. Positrons generated in target are captured by capture linac. After removing electrons by chicane, positrons are boosted up to 5 GeV and injected to the DR via the ECS.

extremely high rotation speed (tangential speed: 400 m/s) on the target. This technical problem was solved by T. Omori [4] by changing the pulse structure, as shown in Fig. 2; consequently, the tangential speed was reduced to 5 m/s. The first technical design was performed by Y. Seimiya [5] with L-band and S-band accelerators; however, the beam loading effect in the capture linac was not fully included. The first complete technical design was performed by H. Nagoshi [6], fully considering the beam loading effect and its compensation. Even though the e-driven source is based on established or closed to existing technology, there are several technical problems that hinder the completion of the engineering design of the e-driven positron source for the ILC. This is because the operation regime is not fully compatible with those used in preceding projects, such as the SLC; therefore, it has to be improved in terms of technical maturity. One of the most distinct differences is the pulse format. In the ILC, the positron is generated in a multi-bunch format in which 33 bunches with a 6.15 ns spacing form a

mini-train, as shown in Fig. 2; two mini-trains with an 80 ns train gap compose one pulse. Twenty pulses were repeated at 300 Hz over a period of 60 ms. The positrons in these 20 pulses fully occupy the DR bucket, corresponding to one pulse of the ILC main linac. Because the positron is handled in this format, the beam current becomes 0.78 A in the system. Our final task is to generate positrons in this format with excellent uniformity (i.e., the same bunch charge).

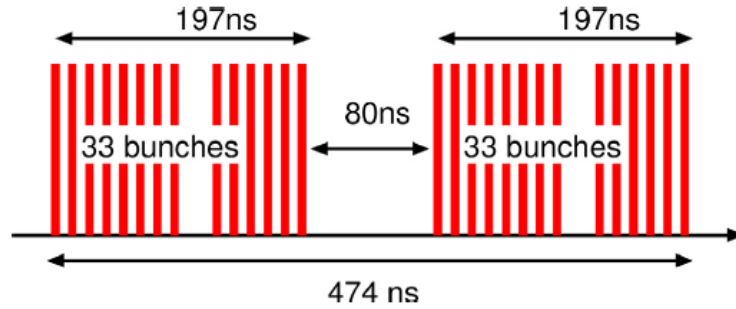


Fig.2: Pulse format of E-Driven ILC positron source. 33 bunches with 6.15 ns spacing form a mini-train. Two mini-trains with 80 ns train gap compose one pulse.

There are other three critical problems that have to be resolved to achieve this final task. The first is the handling and removal of the average power of 18.8 kW from the target. To resolve this, dispersing this power over a water-cooled slowly rotating target wheel is proposed. The most critical measure of the target load is PEDD (peak energy deposition density). Its unit is J/g. Based on experience with the SLC positron source, 35 J/g [7] is presumed to be operable with a sufficient safety margin. A higher PEDD may be operable according to the test experiment at SLAC [8]; however, we are inclined to assume that 35 J/g is the threshold for the safe operation of the target. Hence, the PEDD for an e-driven ILC positron source should be equal to or less than 35 J/g.

The second is the development of a flux concentrator (FC) as an adiabatic matching device (AMD). The AMD is an important device for the efficient capture of positrons by reducing the transverse momentum. The technical design of the FC has already undergone several modifications [9], and a single turn FC with an aperture of 16 mm has been found to be feasible. The positron yield was confirmed through a simulation with this FC, and the performance was sufficient to generate the required positron [6]. To complete the engineering design of the FC system, the reliability of the system (FC conductor, power source, and transmission line) should be confirmed. The third problem is the maintenance of the positron production target considering that 18.8 kW of power [6] is deposited in the target. We should consider the radiation safety problem of the target system from two perspectives: the radiation dose during the operation and the residual radiation after the operation. Protection from radiation during the operation of components outside of the target station is straightforward; an adequate shield thickness should surround the target. Boronized concrete with a thickness of 2 m is sufficient to confine radiation [10]. Another problem is target maintenance. The entire target area (i.e., not only the target itself but also the FC, accelerating cavity, solenoid, etc.) is highly activated during the operation; consequently, maintenance after cooling is not realistic. We have to replace the highly activated target every two years because

of radiation damage to the target material, and it is necessary to develop a “workable” target maintenance system from the point of view of radiation safety.

There are many problems that have to be resolved in the IDT in the course of the Pre-Lab period apart from these issues; however, they are not critical for the system. Hence, in this document, the focus is on these four problems.

Goals of the technical preparation:

The goal of the IDT and Pre-Lab period is establishing the engineering design of the e-driven ILC positron source such that it is capable of generating 4.8 nC/bunch (150% of the 3.2 nC/bunch design value) in DR acceptance. Moreover, the system should stably operate with high reliability and availability, which should be established through the stable operation of the prototype modules or other equivalent investigations during the Pre-Lab period. The critical components are as follows:

- A) Positron production target
- B) Flux concentrator as adiabatic matching device
- C) Capture linac
- D) Target maintenance system

All components and subsystems should be highly reliable in preparation for the ILC construction. These four problems are separated into 13 tasks. For each task, the goals by the end of the first year of Pre-Lab (Sep. 2024) and at the end of Pre-Lab (Mar. 2026) are defined. Owing to these studies, the Engineering Design Report (EDR) for the ILC positron source is well founded.

Area System Electron-Driven Positron Source: Work packages (WPs)

| <i>Work package</i> | <i>Items</i> |
|------------------------------------|--|
| WP- 8: Rotating target | Target stress calculation with FEM |
| | Vacuum seal |
| | Target module prototyping |
| WP- 9: Magnetic focusing system | Flux concentrator conductor |
| | Transmission line |
| | Flux concentrator system prototyping |
| WP- 10: Capture cavity, linac | APS cavity for the capture linac |
| | Capture linac beam loading compensation and tuning method. |
| | Capture linac operation and commissioning |
| | Power unit prototyping |
| | Solenoid prototyping |
| WP-11: Target Maintenance | Capture linac prototyping |
| | Target Maintenance (common issue for undulator and e-driven sources) |

References

[1] Report of Linear Collider Accelerator Review Committee, March 2017 (in Japanese).
 [2] Technical Design Report, KEK Report 2013-1, 2013.
 [3] Accelerator Technology Option Report, 2004; <https://www.slac.stanford.edu/xorg/accelops/>
 [4] T. Omori, T. Takahashi, et al., A conventional positron source for International Linear Collider,

Nucl. Instrum. Methods A672 (2012) 52.

[5] Y. Seimiya et al., Positron capture simulation for the ILC electron-driven positron source, Prog. Theory. Exp. Phys. (2015) 103G01.

[6] H. Nagoshi et al., A design of an electron driven positron source for the international linear collider, Nucl. Instrum. Methods A953(2020)163134.

[7] Report on the next linear collider, The NLC Collaboration, SLAC-R-571, 2001.

[8] S. Ecklund, Positron target materials tests, SLAC-CN-128, 1981.

[9] T. Kamitani, P. Matyshkin, et al., Zero-th order design of flux concentrator for ILC conventional positron source, KEK Preprint 2015–65 (2016).

[10] M. Kuriki et al., Facility design for the positron production target station of ILC e-driven positron source, Proc. of Annual meeting of PASJ, FRPP56, 2020.

WP-8: Target

(Ver.3,2021-Jan-26)

Technical Preparation Plan:

A conceptual drawing of the cross section of the target is presented in Fig. 3. A detailed description can be found in [1]. A W-Re rim with a diameter of 0.5 m and a thickness of 16 mm is rotated in vacuum with a tangential speed of 5 m/s (225 rpm). The W-Re rim is attached to a copper disk with water channels for cooling. The copper disk is fixed to a rotating shaft with water channels. A detailed design of the rotating shaft is presented in Fig. 4. The rotating shaft is supported by a couple of mechanical bearings, and the vacuum is sealed by ferrofluid. The ferrofluid seal is an organic solvent with fine iron powder that fills the gap between the rotating shaft and unit body to create the seal; it is held in place by a permanent magnet. The motor, bearing, and rotatory joint for the water inlet are exposed to air.

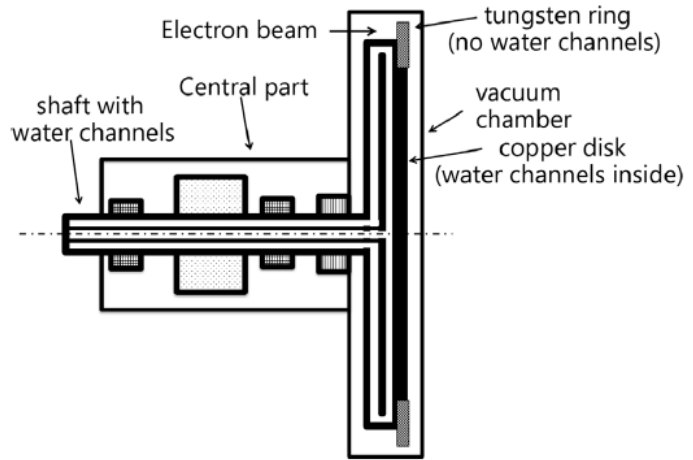


Fig. 3: Schematic of the target cross section. [1]

Goals of the technical preparation (fore Pre-Lab phase 2022-2025)

The technical preparation items for the target are as follows.

- More accurate calculation of the target stress and fatigue effect to improve the design
- The required high vacuum (in the order of $e-6$ Pa at the accelerator) should be maintained for a long time.
- Stable target prototype operation; the test operation of the target prototype is set to start in the Spring of 2021.

List of items::

| <i>Items</i> |
|------------------------------------|
| Target stress calculation with FEM |
| Vacuum seal |
| Target module prototyping |

Status and Prospects:

The beam target stress was investigated using finite element method (FEM) simulation. The result reveals that the instantaneous effects (stress) on the ILC target are comparable to those on the SLC target. The fatigue effect is substantially less for the ILC than for the SLC because the target size is considerably larger for the ILC than for the SLC. A test experiment at SLAC demonstrated that the damage threshold was 70 J/g. Moreover, the SLC

target was operated for more than three years with a 35 J/g positron source and a safety margin factor of two without experiencing severe problems; for the KEKB, the positron source was 29 J/g. The ILC design is 33.6 J/g, and this quantity has a sufficient safety margin based on the experiences at SLAC and KEKB. To improve the safety margin, a more detailed simulation is useful. For example, a temporal variation of the stress amplitude should be conducted to evaluate the fatigue effect more accurately, even if the fatigue effect is expected to be considerably less for the ILC than for the SLC. Generally, the destruction process is complicated, and a careful investigation, including consultation with experts, is preferable.

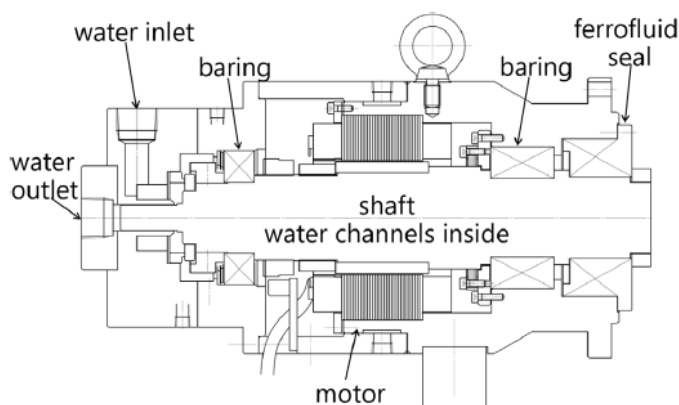


Fig. 4: Design of the central shaft of the target. [1]

A rotor shaft with a ferrofluid seal is fabricated as a prototype for the target module, as shown in Fig. 4. The right side of the module was connected to a vacuum chamber to examine the vacuum seal performance of the unit. The unit was continuously operated with rotation. Spikes in the vacuum pressure (sudden pressure increment) were frequently observed initially; however, over time, the spike frequency decreased. Finally, a pressure intensity of $5e-7$ Pa, with a rotation of 225 rpm, was stably achieved. The outgas rate of

the test module was estimated to be $5.0e-8$ Pa·m³/s, and the pressure at the first accelerating structure was expected to range from $4e-9$ to $\sim 7e-9$ Pa with an estimated conductance [7]; this value is considerably less than requirement of $1e-6$ Pa [2].

Radiation damage is a problem, especially for the ferrofluid seal because the solvent is organic oil. Several irradiation tests were performed with a ⁶⁰Co gamma ray source, and no problems were observed for the oil after 4.7 MGy (corresponding to six years of ILC operation) and up to a rotation of 600 rpm. In addition to the fluid, the entire module, including the bearing, motors, and mechanical joints, was irradiated with 0.6 MGy at the motor (corresponding to two years of ILC operation). The irradiated module was used for the experiment with rotation; no detrimental effect was observed.

As mentioned, all the problems for the target have already been solved, and the target can be designed with sufficient technical reliability. To improve system reliability further, a study of the target stress and further investigations must be continued. The test operation of the rotating target using a disk that is mechanically equivalent (i.e., in terms of mass and moment) to the target disk is expected until Mar. 2027 to guarantee the experimental reliability of the system. A small experiment in a laboratory to measure the thermal conductivity between W-Re and Cu and between Cu and water boundary is very useful for confirmation

Rigaku Co. has a rich experience of the rotating target with ferro-fluid seal for X-ray source. The test experiment and FEM analysis of the target stress have been carried out as a collaboration with Rigaku Co. and we continue the collaboration.

Summary table of tasks

| Items | Current status | Goal by Sep. 2024 | Goal by Mar. 2026 |
|--|---|---|--|
| Target stress calculation using the FEM | Calculation using the FEM completed; instantaneous heat load and stress less than those in SLC; fatigue effect considerably less than that in SLC | None | More accurate calculation preferred for design improvement |
| Vacuum seal | Seal module operated with rotation in vacuum for three years without severe problems; pressure spikes but no rise in base pressure | None | Prolongation of high vacuum ($e-6$ Pa order at accelerator) for extended period |
| Target module prototyping | Radiation damage test corresponding to three years of ILC operation for the ferrofluid; corresponding to one year for module | Operation test with target equivalent load to start by Spring of 2021 | Confirm stable operation of the target prototype |

References

- [1] H. Nagoshi et al., A design of an electron driven positron source for the international linear collider, Nulc. Instrum. Methods A953(2020)163134.
- [2] Technical Design Report, KEK Report 2013-1, 2013.

WP-9: Flux Concentrator

(Ver.3,2021-Jan-26)

Technical Preparation Plan:

The cross section of the FC conductor is shown in Fig. 5. This is a two-conductor flux concentrator made of copper. The primary conductor is a spiral coil, as shown at the bottom of the figure; it generates a B field along the axis. The other component is the secondary conductor. The cross section of the upper and bottom parts of this secondary conductor are conductive, but the central part is a gap. The eddy current in the secondary conductor, which is induced by the primary B field, flows and generates a B field in the conical space. The target is placed outside of the smallest aperture where the B field is strongest; detailed information is available in [1],[2]. A 5 T field is induced along the axis. The diameter of the beam hole is 16 mm. The device provides several advantages over that used in the SLC (one-spiral FC conductor): it has mechanical strength, good symmetry along the longitudinal axis, and less transverse field.

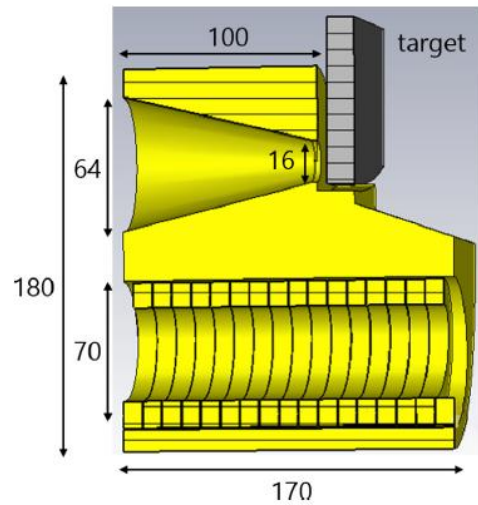


Fig. 5 Flux Concentrator Design.

Goals of the technical preparation (for Pre-Lab phase 2022-2025):

The technical preparation items for FC are as follows.

- The electrical, thermal, and mechanical properties of the FC conductor should be verified through simulations
- Transmission line design
- Power source design
- FC system (FC conductor, transmission line, and power source) prototyping and test operation are useful for confirming system reliability.

List of items::

| <i>Items</i> |
|--------------------------------------|
| Flux concentrator conductor |
| Transmission line |
| Flux concentrator system prototyping |

Status and Prospects:

In the Pre-Lab period, the prototyping of the FC system and test operation with the power source are useful for confirming system reliability; however, this is not always necessary. This is because the same type of FC, the VEPP5 collider, which has a higher field (10 T) is already in operation at BINP, Russia [3]. Table 1 summarizes the comparison between the ILC FC and VEPP5 FC. For the VEPP5 FC, the B field is higher, but the average power is higher for the ILC FC owing to the high repetition. The dynamic force in the FC can be compared to the product of the current and B field. This is considerably higher for the VEPP5 FC; therefore, mechanical stress is considerably lower for the ILC FC than for the VEPP5 FC. According to these considerations, the experience with the VEPP5 FC is applicable to the ILC FC, thereby indicating the high reliability of the ILC FC.

Table 1. Parameter comparison between FC for the ILC and BINP.

| Parameter | ILC | VEPP5 | Unit |
|-----------------------------|------|-------|------|
| Maximum B field | 5.0 | 10 | T |
| Current on the cone surface | 25 | 120 | kA |
| Dynamic Force | 125 | 1200 | kA·T |
| Pulse energy | 140 | 90 | J |
| Average power | 13.7 | 4 | kW |

The transmission line and power source should anyway be designed for the preparation of the EDR. Prototyping of the transmission line and power source is also useful for confirming reliability.

The FC heat loads are expected to be 14 and 4 kW by Ohmic loss and beam loss, respectively [2]. This heat should be removed from the FC by the water channel; hence, the problem in the thermal design of the FC has to be resolved. Recently, we have collaborated with some companies (Kondo equipment Co. and Metal Tech. Laboratory) in Kitakami, Iwate. Through this collaboration, the thermal design of the FC is to be undertaken. The electrical, thermal, and mechanical stability should be confirmed through an FEM simulation. The heat load caused by beam loss is concentrated on the smallest aperture. Special attention is required for the high heat concentration, which should be examined in the thermal design.

Summary Table of tasks

| Items | Current status | Goal by Sep. 2024 | Goal by Mar. 2026 |
|------------------------------------|--|--|--|
| Flux concentrator conductor | Conductor, including electrical property, designed | Complete thermal design; prototype not always necessary because of equivalent FC operational in BINP | Confirm stable operation of electrical, thermal, and mechanical properties; prototype fabrication advantageous |
| Transmission line | Design transmission line to match FC conductor; fabricate module | None | Confirm performance through FEM simulation; prototype fabrication |

| | | | |
|--------------------------------------|---|------|--|
| | | | advantageous |
| Flux concentrator prototyping | Fabricate FC system, including the power source and transmission line | None | Confirm stable operation; prototype advantageous but not always necessary because of equivalent FC operational in BINP |

References

- [1] H. Nagoshi et al., A design of an electron driven positron source for the international linear collider, *Nucl. Instrum. Methods A*953(2020)163134.
- [2] T. Kamitani, P. Matyshkin, et al., Zero-th order design of flux concentrator for ILC conventional positron source, KEK Preprint 2015-65 (2016).
- [3] F.A. Emanov et al., “Feeding BINP Colliders by the New VEPP-5 Injection Complex” *in proc. RuPAC-2016*, WEXMH01 (2016).

WP-10: Capture Linac

(Ver.3,2021-Jan-26)

Technical Preparation Plan:

The capture linac consists of an L-band alternate periodic structure (APS) cavity. The entire linac is surrounded by 0.5 T solenoid magnets. The simulation by Superfish is shown in Fig. 6. It operates at a frequency of 1.3 GHz and has 11 accelerating cells and 10 idle cells. The length of the accelerating part is 1.265 m. The shunt impedance and Q_0 value are estimated to be 53 MW/m and 25 000, respectively. The foremost reason for its structural form is its wide aperture ($2a = 60$ mm), which affords better RF stability than the pi-mode standing wave cavity. The basic

RF parameters were obtained, and the simulation of the positron generation was performed with these parameters; however, the full RF design of the structure, including the coupler and end cell, was not performed. The operational condition of the capture linac is unique. Because we employed the deceleration capture method developed by Kamitani [1], the positron was initially placed at the deceleration phase and then slipped down to the acceleration phase. The RF phase of the positron moves along the linac. The beam loading is then dynamically changed over the linac, especially in the upstream part. This dynamic aspect, which is enhanced by the electrons, perturbs the linac operation and may cause instability. A study of the beam loading by assuming

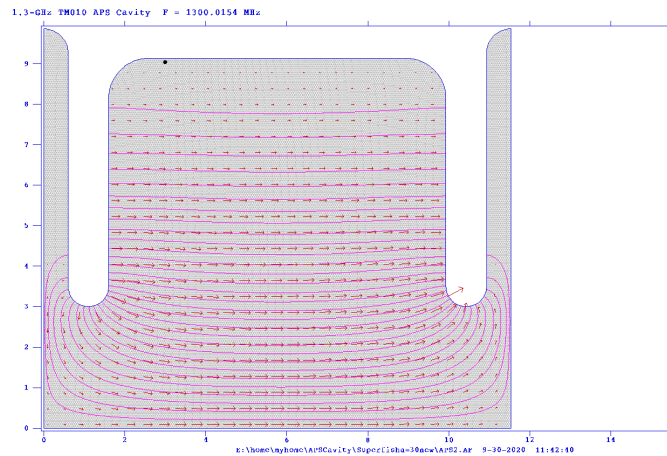


Fig. 6: Field map of APS cavity calculated by

the APS structure to be a single cavity [2] reveals that its effect on the positron capture can be controlled by amplitude modulation in the RF such that it becomes negligible.

The APS cavity is not a new device; an L-band APS cavity with a frequency of 1428 MHz and 37 cells is operational in SACLA, XFEL facility [3]. It operates stably with a 9.5 MV/m acceleration field and 5 μ s pulse width. The field flatness exceeded 99%. Our structure has 21 cells, which are shorter than those in SACLA. The field with beam loading is approximately 10 MV/m, which is similar to that in SACLA. The pulse width is 1.5 μ s, which is shorter than that in SACLA. However, it is not necessary for the APS cavity in the e-driven system to exceed the performance of



Fig. 7: K300 modulator by Scandinova Co. for L-band APS cavity.

the APS cavity in SACLA. From this point of view, there is no reason to develop a test module; however, an operation test through a module is preferred to confirm the high reliability of the system.

A modulator designed by Scandinova Co. based on a solid-state power unit [4] is shown in Fig. 7. As a klystron, it requires a 50 MW power supply with a 2 μ s pulse width. Although there is no commercially available klystron that satisfies these requirements, an S-band klystron that has better performance exists. Fabricating an L-band klystron by scaling the S-band klystron is preferred to guarantee certainty.

Goals of the technical preparation (for Pre-Lab phase 2022-2025):

The technical preparation items for the target technology are as follows.

- RF design of APS cavity
- Establish beam loading compensation and linac tuning method
- Power unit design and prototyping (L-band klystron + modulator)
- Solenoid magnet design
- Test operation of APS cavity with developed power source

List of items::

| <i>Items</i> |
|--|
| APS cavity for the capture linac |
| Capture linac beam loading compensation and tuning method. |
| Capture linac operation and commissioning |
| Power unit prototyping |
| Solenoid prototyping |
| Capture linac prototyping |

Status and Prospects

The completion of the full RF design is one of the required tasks. Concurrently, the thermal design should proceed as collaborative work with Kondo Equipment Co. and Metal Tech. Laboratory (whose experience in the thermal design of RF cavities for KEKB is rich), J-PARC, X-band LC, etc. The heat load by beam loss, especially for the first and second accelerators located downstream of the target, exceeds that of the RF (10 kW). The impact on the RF property through heat deformation is expected to be controllable; however, it is preferable to study the effect quantitatively using the real geometry of the structure and cooling channel.

Comprehending the beam loading effect and its compensation is the foremost problem for the capture linac. As mentioned, the beam loading dynamically changes along the linac owing to the phase slip of the positron. In addition, the electron movement differs because of the opposite charge. The field in a cavity is determined by the sum of the input RF and beam loading field by electrons and positrons. We intend to develop a cavity model to simulate the cavity field in this situation. Coupling among cells in a cavity should also be considered, and a PIC (Particle-in-Cells) simulation of its effect has to be performed for cross-checking. Based on the model, the tuning scenario of the linac is investigated.

Even though the technology of the APS cavity is well established, the fabrication of the prototype of one RF module (APS cavity and power source) is extremely useful to verify the reliability of the linac. The modulator

and klystron should be designed and fabricated, and the stable operation of the RF module should be confirmed.

Summary Table of tasks

| Items | Current status | Goal by Sep. 2024 | Goal by Mar. 2026 |
|--|--|---|--|
| APS cavity for capture linac | Cavity RF design ongoing | Complete RF and thermal design | RF design; fabricate prototype for test unit |
| Capture linac beam loading compensation and tuning method | Study of beam loading compensation and tuning method ongoing | Complete first study of beam loading compensation and tuning method | Independently confirm uniform acceleration via simulations |
| Power unit prototyping | Design completed | None | Confirm operation by test unit |
| Solenoid prototyping | No special design for e-driving; reference: solenoid in KEKB positron source | None | Prototyping and test operation advantageous |
| Capture linac prototyping | None | None | Stable operation of test unit |

References

[1] T. Kamitani and L. Rinolfi, Positron production for CLIC, CLIC-Note 465 (2001)

[2] H. Nagoshi et al., A design of an electron driven positron source for the international linear collider, *Nucl. Instrum. Methods A* 953(2020)163134.

[3] T. Ishikawa, et al., A compact X-ray free-electron laser emitting in the sub-ångström region, *Nature Photon* 6, 540–544 (2012).

[4] Scandinova Co. <https://scandinovasystems.com/>

WP-11: Target Maintenance (common issue for undulator and e-driven sources)

(Ver.3,2021-Jan-26)

Technical Preparation Plan

Positron production targets cause a number of problems for radiation safety. One is radiation during the operation; another is the activation of the target and environment. To isolate the radiation from the target, the target module is surrounded by a 2 m thick boronized concrete shield, as shown in Fig. 8. The red rectangle is the target module. The upper area is the service tunnel, where various electronics modules are placed. The radiation in the upstream direction (left side in Fig. 8) is also confined within the 2 m concrete. The electron-driven linac is placed upstream, and a similar shield is placed downstream of the capture linac. The lower cavern in Fig. 8 is the storage area of the target. After 100 h of cooling operation, a 10 Sv/h

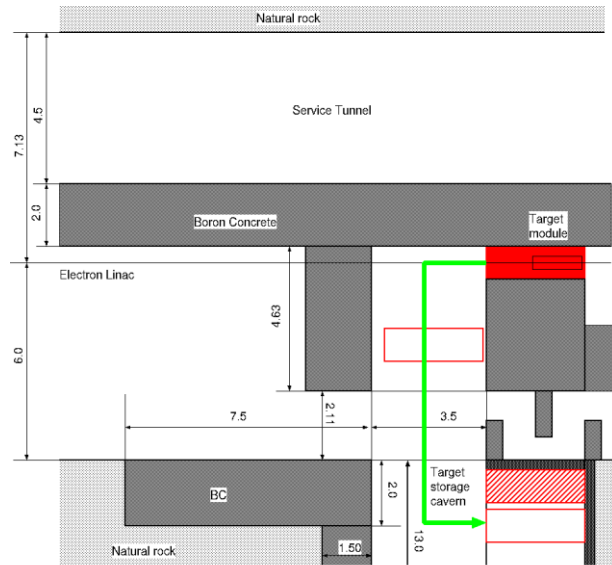


Fig. 8: Floor layout of the target section: the central red rectangle is the target module; the shaded gray area is boronized concrete shield; the lower cavern is the target storage area.

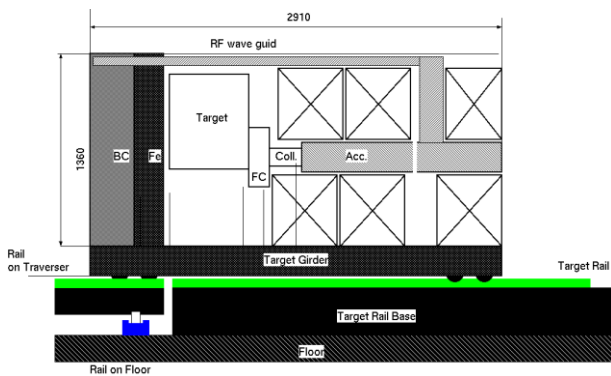


Fig. 9: Side cross-sectional view of target module on rails for easy transportation: front side (upstream of beam), 30 cm boronized concrete shield and 20 cm Fe shield placed for protection.

dose is expected on the target surface. To protect the target from this intense radioactivity, it is assembled as a shielded module, as shown in Fig. 9. The target module is assembled with the FC module, first accelerator, solenoid magnet, and shields. The module is mounted on a wagon that moves along rails in the beam-line direction. By placing these shields, the radiation dose in front of the target module is reduced to 50 $\mu\text{Sv/h}$; personnel can work in this area. Many of the joint connections for the RF, electric power, water, control, etc. are assembled on the front panel of the module, and these joints can be safely disconnected without any remote robotic work; this is a fail-safe system. The target is moved along the upstream direction (left direction in Fig. 8 or Fig. 9). A special wagon (called a traverser) is placed in the transverse aisle (up-down direction in Fig. 8). The target module is transferred from the target mount to the traverser. The rails are aligned on the same level as those on the target mount, as shown in Fig. 9, and the traverser moves along the rails with a small force. After the target module is mounted on the

traverser, the traverser moves in the transverse direction toward the beam line (up–down in Fig. 8) and transports the target module to the target storage area. The target module is then moved to one of the storage areas in a similar manner. In the storage area, the target module is surrounded by a 20 cm iron shield (rear), 5 cm iron shield (left and right sides), and 30 cm boronized concrete with a 20 cm iron shield (front). The radiation dose in the cavern aisle is 50 $\mu\text{Sv/h}$ or less.

There is no radiation shield on the backside (opposite side where personnel can work) when the module is transported by the traverser; nevertheless, the concrete around the target acts as a shield. The side aisle (chicane) leading downstream to the capture linac is closed during transport. If a strict policy for safety is required, the aisle can be completely closed.

Goals of the technical preparation (for Pre-Lab phase (2022–2025)):

The technical preparation items for target maintenance are as follows.

- Complete the technical design
- Fabricate a mock-up to confirm the function
- Develop a fail-safe system

List of items::

| <i>Items</i> |
|---|
| System design and fabrication of mock-up module |

Status and Prospects:

As explained, a conceptual target maintenance procedure with safety considerations has already been formulated; a more detailed explanation can be found in [1]. To improve the maturity of the system, we have to develop technical and engineering designs. For example, a vacuum joint that can be remotely disconnected is necessary. This joint should be used between the first and second accelerators, where the radiation activity is extremely high. One candidate is an inflatable joint, which is used in the J-PARC neutron target area. This joint, including a failsafe system, has to be carefully considered. A mock-up of the system is also extremely advantageous to verify the function of each component and reveal potential problems in the system.

Target maintenance considerably depends on the management of the target module; for example, the installation and extraction of modules to and from the accelerator tunnel. Module management should be determined with the CFS and radiation safety groups.

Summary Table of tasks

| Items | Current status | Goal by Sep. 2024 | Goal by Mar 2026 |
|---------------------------------------|------------------------------|----------------------------|---|
| System design and mock-up fabrication | Conceptual design is ongoing | Complete conceptual design | Complete technical design; mock-up fabricated to confirm function |

References

[1] M. Kuriki, et al., Facility design for the positron production target station of ILC e-driven positron source, *Proc. of Annual meeting of PASJ*, FRPP56, 2020.

Area-System 4: Damping ring

(Ver.1,2020-Dec-29)

Overview:

Damping rings (DRs) are circular accelerators that are placed after the electron and positron sources with the goal of creating high-quality electron and positron beams for the ILC. The dynamic aperture of the circular accelerator is affected by the multipole errors of the magnets, especially for the fringe fields of the bending magnets. The present baseline beam optics for the ILC DR is updated to have a smaller horizontal emittance than that of the ILC TDR in 2017. we will have to carry out the system design of the updated DR optics by considering the multipole errors of the actually designed magnets of the ILC DR during the ILC Pre-Lab period for the ILC EDR.

The ILC DR possesses many collective effects that may affect the beam quality in the DRs. These include impedance-driven instabilities, intrabeam scattering, space-charge effects, electron cloud effects in the positron ring, and ion effects in the electron ring. The largest sources of emittance dilution were found to be the electron cloud (EC) instability in the positron DR and the fast ion instability (FII) in the electron DR. However, because the effects on the old TDR optics were evaluated, but, not for current updated DR optics, we will have to investigate the collective effects on current updated DR optics.

The circumference of the DRs is approximately 3.2 km, and corresponds to approximately 1/90 of the beam pulse length at the electron and positron sources and at the main linac. A fast kicker system compresses and decompresses the beam pulse during injection and extraction, respectively. The system design of the ILC DR injection-extraction system will have to be carried out during the system development at KEK-ATF, including the assurance of the long-term reliability of the injection-extraction system during the ILC Pre-Lab period. Furthermore, because the injection system for the electron-driven positron source is different from other ILC injection and extraction kickers, we will have to develop the injection kicker, when we will adopt the electron-driven positron source for the ILC positron source.

The contents of this area system mentioned above need to be described in the EDR (Engineering Design Report).

Area-System Damping ring: Work packages:

| <i>Work package</i> | <i>Items</i> |
|--|---|
| WP- 12: System design of ILC damping ring | Optics optimization, simulation of the dynamic aperture with magnet model |
| | Magnet design : Normal conducting magnet |
| | Magnet design : Permanent magnet |
| | Prototyping of permanent magnet |
| WP- 13: Evaluation of the collective effect in the ILC damping ring | Simulation : Electron cloud instability |
| | Simulation : Ion-trapping instability |
| | Simulation : Fast ion instability (FII) |
| | System design : Fast FB for FII |
| | Beam test : Fast FB for FII |
| WP- 14: System design of ILC DR injection/extraction kickers | Fast kicker: System design of DR and LTR/RTL optics optimization |
| | Fast kicker: Hardware preparation of FID pulsar |
| | Fast kicker: System design & prototyping of induction kicker |
| | Fast kicker: Long-term stability test at ATF |
| | E-driven kicker: System design,including induction kicker development |

WP-12: System design of ILC damping ring

(Ver.2,2021-Jan-26)

Technical Preparations Plan:

The basic design of the ILC DR is shown in the document of the Linear Collider Collaboration (LCC); “The International Linear Collider Machine Staging Report 2017”. The horizontal emittance is 4.0mm, while achieving a dynamic aperture of 0.07m. The dynamic aperture was evaluated by assuming the hardedge ideal magnets, however, the dynamic aperture of the circular accelerator is affected by the multipole errors of the magnets, especially for the fringe fields of the bending magnets. Therefore, magnet design is required for the DR magnets. Then, we will optimize the DR beam optics by considering the multipole errors of the actually designed magnets of the ILC DR.

In addition, we investigate the potential for introducing a permanent magnet (PM) in the arc section of the DR. A major advantage of PMs is the reduced operating costs relative to electromagnets; related to this we can also cite lower emissions (even when factoring in those due to mining PM materials), reduced infrastructure (no large power supplies or water pipes) and lower vibrations (no flowing water). The disadvantages can be summarized as follows: PMs are fixed-field, sensitive to small changes in temperature, and susceptible to radiation damage. It is necessary to investigate the magnetic field uniformity, stability, and radiation damage by prototyping several field-adjustable PMs during the ILC Pre-Lab period. Then, we will decide whether to use them for ILC DR.

Goals of the technical preparation:

System design of the beam optics for the ILC DR. The DR specifications are as follows.

| <i>Parameters</i> | <i>Symbol</i> | <i>Unit</i> | <i>Design</i> |
|-------------------------|---------------------------------------|---------------------------|--------------------------|
| Normalized emittance | $\gamma\epsilon_x / \gamma\epsilon_y$ | $\mu\text{m} / \text{nm}$ | 4.0 / 20 at N=2E10 |
| Dynamic aperture | $\gamma(A_x + A_y)$ | M | 0.07 (action variable) |
| Longitudinal acceptance | $\Delta\delta \times \Delta z$ | $\% \times \text{mm}$ | $\pm 0.75 \times \pm 33$ |

List of items:

| <i>Items</i> |
|---|
| Optics optimization, simulation of the dynamic aperture with magnet model |
| Magnet design : Normal conducting magnet |
| Magnet design : Permanent magnet (PM) |
| Prototyping of PM |

Status and Prospects:

The ILC DR must provide a low emittance beam as well as a large dynamic aperture to achieve a large acceptance for the positron beam. A DR with a horizontal emittance of 5.5mm was designed while achieving a large dynamic aperture of 0.07m (action variable) in the ILC TDR published in 2013. Subsequently, DR optics with a lower horizontal emittance was proposed and approved by the LCC in 2017 with the aim of achieving higher luminosity in the ILC250. The LCC document “The International Linear Collider Machine Staging Report 2017” shows the basic design of a DR with a horizontal emittance of 4.0mm, while achieving the same dynamic aperture of 0.07m as the TDR design. The dynamic aperture was evaluated by assuming the hardedge ideal magnets; however, the dynamic aperture of the circular accelerator is affected by the multipole errors of the magnets, especially for the fringe fields of the bending magnets.

PM devices have been used in accelerator facilities for many years. Their primary function is as insertion devices (undulators and wigglers) on synchrotron light sources. The two most prevalent materials used are $\text{Sm}_2\text{Co}_{17}$ and $\text{Nd}_2\text{Fe}_{14}\text{B}$. The latter has a higher remanent field (meaning it can produce a stronger magnetic field) but a smaller intrinsic coercivity (meaning it is more easily demagnetized by an external field or by radiation). Recent developments include the use of PrFeB and cryogenic PM undulators, both of which aim to enhance the on-axis field. In recent years, many light sources worldwide have embarked upon programs of upgrades, reducing their beam emittance and enhancing their output brightness. The disadvantages of PMs can be summarized as follows: PMs are fixed-field, sensitive to small changes in temperature, and susceptible to radiation damage. However, several groups have produced highly adjustable PM designs using mechanical adjustment. Furthermore, excellent temperature stability can be achieved, even for NdFeB , by adding small amounts of FeNi alloy which has a temperature coefficient with the opposite sign. In terms of radiation damage, synchrotron light sources have employed PM-based insertion devices for many years without significant radiation damage. Maintaining the PMs out of the plane of the circulating beam may be the most important factor in reducing this risk. Some examples of light source facilities that utilizing PMs extensively are:

- ESRF (France): PM longitudinal gradient (LG) dipoles, 128 magnets each consisting of five fixed-field modules, stepping up in the field. Diamond Light Source (UK) has a similar design for its planned upgrade.
- ZEPTO tunable dipole: fixed steel pole with horizontally-moving PM.
- SPring-8 tunable dipole prototype, using a vertically-moving outer plate.
- Sirius (LNLS, Brazil): ‘Superbend’ dipole/quadrupoles, mechanical adjustment gives $\pm 4\%$.
- CBETA (USA): fixed-field Halbach combined function magnets providing dipole and quadrupole fields.
- ZEPTO quadrupoles: fixed steel poles with vertically-moving PMs in outer yoke.
- QUAPEVA quadrupole at COXINEL: Halbach array with rotating PM cylinders in outer yoke.

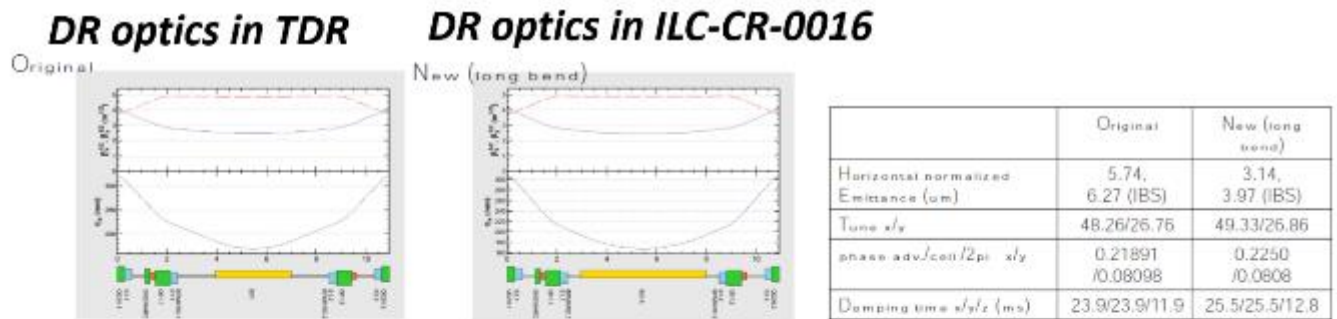
We consider whether the PMs will be used in the arc section of the ILC DR. The current considered baseline devices of the PMs are the Sirius type for the bending magnets, the ZEPTO type for the quadrupole magnets and the ZEPTO type for sextupole magnets. However, because there are no prototypes of the ZEPTO type of sextupole magnet, we will have to make prototypes for the PM. For other baseline PMs, we do not have to make prototypes only for ILC-optimized magnets, but we should design to be optimized for the ILC. Furthermore, we also consider the use of the CBETA type of bending magnets, and the QUAPEVA type of

quadrupole magnets as optional devices for ILC. Using these optional PMs would be more compact and cheaper. However, we should evaluate the field qualities for optional magnets (field uniformity and movement of the magnetic center, when the magnetic field strength is changed, and the effect of radiation damage etc.).

Finally, prototyping of the PMs is planned for the following magnets:

- CBETA type bending magnet (i.e. 90cm long with 30 cm segments)
- QUAPEVA type quadrupole magnet
- ZEPTO type sextupole magnet

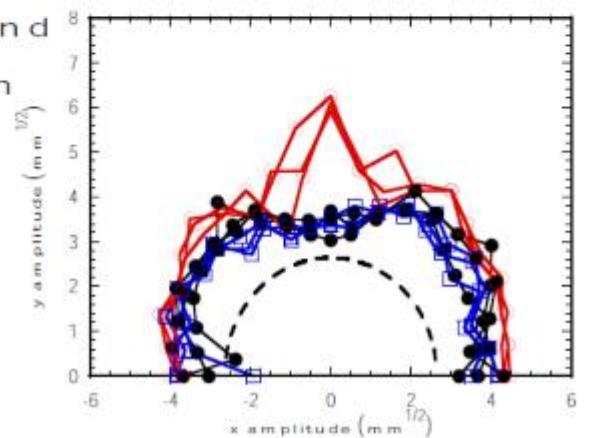
The prototyping for the PM will be iterated twice each (a total of six prototype magnets) during the ILC Pre-Lab period, and the PM design is determined based on the results of the prototype test. The prototype PMs will also be useful for process making of the PM installation, the test of the radiation damage and the field control by the temperature variation.



Dynamic aperture: long bend Misalignment + correction

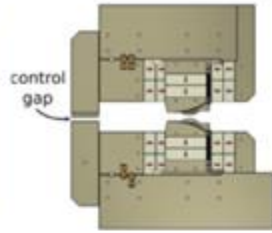
New arc cell: long (5 m) bend.
tune/cell: x.225 y.0808
Tune: x49.33 y26.86

Quadrupole & sextupole offset: 50 μm
 Quadrupole roll: 100 μrad
 BPM offset: 100 μm
 BPM roll: 10 mrad
 COD & Dispersion correction.





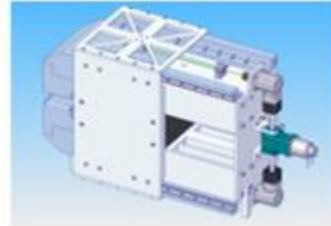
ESRF
Fixed field



Sirius
Small
adjustment
(~3%)



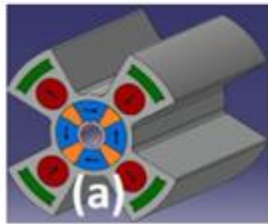
CBETA
Fixed field



ZEPTO
Variable field (factor 2)



CBETA
Fixed field



QUAPEVA (Soleil)
Factor of 2 tuning



ZEPTO-Q1
High strength
Factor of 4



ZEPTO-Q2
Lower strength
Very large adjustment range

WP-13: Evaluation of collective effects in ILC damping ring

(Ver.2,2021-Jan-26)

Technical Preparations Plan:

DR optics with a lower horizontal emittance was proposed and approved by the LCC in 2017 with the aim of achieving higher luminosity in the ILC250. Therefore, it is necessary to investigate the collective effects of the present updated DR optics. The largest sources of emittance dilution were found to be the EC instability in the positron DR and the FII in the electron DR. The effect of the ion-trapping instability should also be evaluated by simulations.

MEXT's ILC Advisory Panel expressed technical concerns about the need for a high-resolution fast feedback system. SuperKEKB has a circumference that is close to that of the ILC DR and a feedback system similar to ILC250. System development of the high-resolution fast feedback system for the ILC will be performed based on the experience of the system operation and upgrade development at SuperKEKB. In addition, when there is a need for experience in FII suppression under conditions that exceed the performance of SuperKEKB in evaluation by simulations, etc., additional beam tests should be performed to suppress the FII at other accelerators..

Goals of the technical preparation:

Evaluation of the collective effect correction in the ILC DR. The beam stabilities in the DR after correction are reduced to be following parameters:

| <i>Parameters</i> | <i>Unit</i> | <i>Design</i> |
|---------------------------|-------------|--------------------|
| Bunch population | | 2E10 |
| Number of bunches in DR | Bunches | 1312 / 2625 |
| Beam position fluctuation | | $\leq 0.2\sigma_y$ |

List of items::

| <i>Items</i> |
|---------------------------------------|
| Simulation : EC instability |
| Simulation : Ion-trapping instability |
| Simulation : FII |
| System design of fast FB for FII |
| Beam test of fast FB for FII |

Status and Prospects:

The many collective effects that may affect the beam quality in the DRs were examined in the ILC TDR. These include impedance-driven instabilities, intrabeam scattering, space-charge effects, EC effects in the positron DR and ion effects in the electron DR. The largest sources of emittance dilution were found to be the EC instability in the positron DR and the FII in the electron DR. In contrast to the more familiar ion-trapping effect,

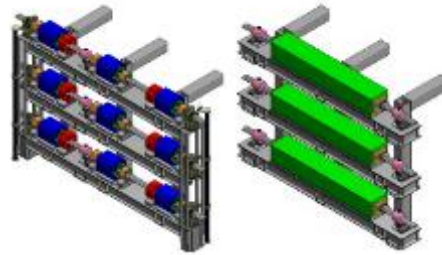
where ions oscillate stably for long periods in the potential well of the stored beam, FII is associated with ions that are created in the beam path by interaction with the circulating beam during a single turn. Ions created at the head of the bunch train move slowly, and remain in the beam path, influencing the motion of subsequent bunches. The resultant ion-induced beam instabilities and tune shifts are critical issues owing to the ultra-low vertical emittance. The FII create emittance growth, betatron tune shifts, and coherent bunch-by-bunch instabilities. A low base vacuum pressure at the 1×10^{-7} Pa level is essential to reduce the number of ions formed. To mitigate bunch motion, bunch-by-bunch feedback systems with a damping time of 0.1 ms are also employed. The DR optics design with a lower horizontal emittance was approved by the LCC in 2017, and the horizontal emittance was reduced from 5.5mm to 4.0mm.

In 2014, SuperKEKB started machine commissioning, and many experiences were obtained for the collective effects. The circumference of the SuperKEKB is comparable to the ILC DR. For the EC of the positron ring, the vacuum chamber designs for the ILC DR and the SuperKEKB low energy ring (LER) are almost the same, except for the chamber diameter (50 mm for the ILC DR, and 90 mm for SuperKEKB). At the first stage commissioning of the SuperKEKB, the beam size growth in the LER (positron ring) was observed by the EC. However, the beam size growth by the EC was cured after the bellows chambers were covered with permanent magnets.

The cloud density of the ILC DR was evaluated to be a factor of about three below the expected single bunch instability threshold in the ILC TDR evaluation for the baseline configuration. However, there is a need for twice the number of bunches to be stored in the DR for high-luminosity upgrade. The doubling of the current in the rings is of particular concern for the positron DR owing to the effects of the EC. In the ILC TDR design, allowance was made for the installation of a 2nd positron DR in the same tunnel in the event that the EC mitigations that have been recommended are insufficient to achieve the required performance for this configuration. Based on our experience with EC at SuperKEKB, we will have to investigate the impact of the newly updated ILC DR to examine whether the 2nd positron DR is really needed during the luminosity upgrade. For the FII of the electron ring, the same concept of the fast FB system was adopted for the SuperKEKB high energy ring (HER) to suppress the coherent bunch-by-bunch instabilities. The design horizontal and vertical emittances for the SuperKEKB HER are roughly one order larger than those for the ILC electron DR, but the design stored beam current of SuperKEKB is 6-7 times higher than that for the ILC DR. The growth times of the coherent bunch-by-bunch instabilities due to FII for the ILC electron DR and those for the SuperKEKB HER are comparable, although the SuperKEKB HER is in the commissioning stage, and the beam current has not yet reached the design value. We expect that they will store a higher beam current operation at the SuperKEKB HER. The reproduction of FII in the SuperKEKB HER by performing simulations is useful for the evaluation of FII in the ILC electron DR.

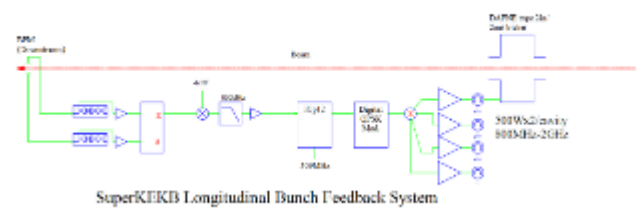
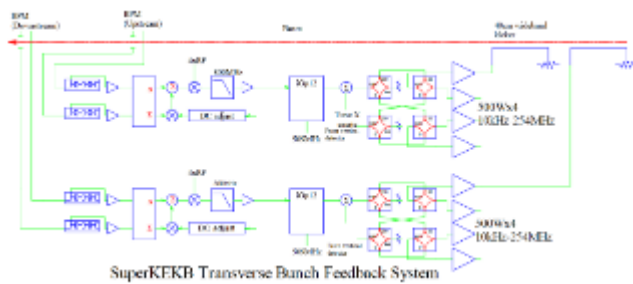
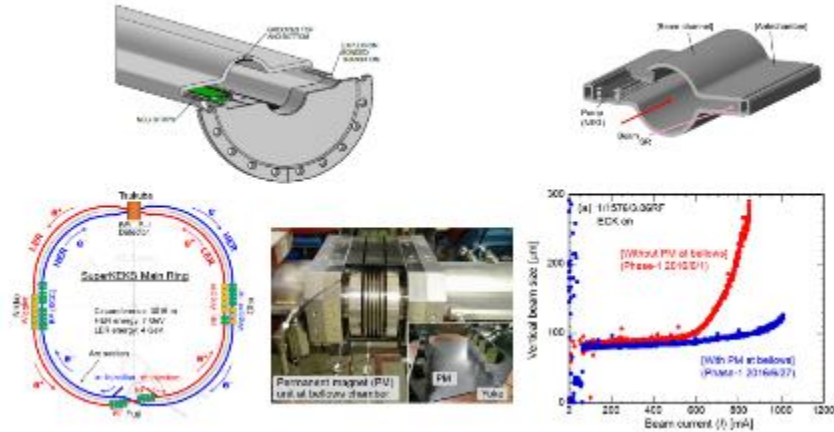
In SuperKEKB, the fast FB is used to suppress coherent bunch-by-bunch instabilities due to FII. The dynamic range of the SuperKEKB fast FB was updated from 8 bits to 12 bits to extend their dynamic range. Because the experience of suppressing FII in the SuperKEKB HER using fast FB is helpful for understanding the suppression of the instability in ILC electron DR, we hope that this experience will provide useful information to ILC. In addition, when there is a need for experience in FII suppression under conditions that exceed the performance

of SuperKEKB in evaluation by the simulation, etc., additional beam tests are needed to suppress the FII at other accelerators. When we test FII suppression with other accelerators, it is necessary to prepare the FB system used in SuperKEKB or the FB system that exceeds its performance, and scientists are also required to perform the performance evaluation. Furthermore, in general, since the beam orbit oscillations can be created by cultural noise, working pumps and cryogenic system vibrations etc., we should consider development of the orbit FB to stabilize the beam orbit oscillations in ILC DR down to the required level.



Typical beam pipe design in the arc section of the ILC DR

Typical beam pipe for SuperKEKB arc section



WP-14: System design of ILC DR injection/extraction kickers

(Ver.2,2021-Jan-26)

Technical Preparations Plan:

Fast kicker magnets and fast-pulsed power sources have been developed, and multiple kicker systems have already been operated under beam operation at the Accelerator Test Facility (ATF) at KEK. However, considering the current dynamic aperture of the present design of the ILC DR, the electrode gap of the stripline kicker must be expanded to 50 mm. Then, when using a pulsar tested at the ATF, it is necessary to make minor modifications to the beam optics in the straight section of the ILC DR. Furthermore, when the straight section of the ILC DR is modified, it is necessary to modify the injection and extraction lines for the DR as well.

The remaining task for the ILC kicker system, as reported by MEXT's ILC Advisory Panel is to ensure the stability and reliability over long-term operation. A long-term stability test of the fast kicker system will be performed at the ATF. The kicker pulsar used for the long-term test is basically the FID pulsar used in the ATF, but the power that can be supplied by the FID pulsar is limited and there is no margin when applying it to the ILC. We would like to develop a power source that is considered to be capable of realizing higher voltage simultaneously.

Furthermore, because the injection system for the electron-driven positron source is different from other ILC injection and extraction kickers, the injection kicker will need to be developed, when we adopt the electron-driven positron source for the ILC positron source.

Goals of the technical preparation:

System design of the beam injection and extraction for the ILC DR, based on the existing hardware. The specifications of the DR beam injection/extraction are as the follows.

| <i>Parameters</i> | <i>Unit</i> | <i>Design</i> |
|-------------------------|-------------|------------------------|
| Number of bunches in DR | Bunches | 1312 / 2625 (optional) |
| Repetition rate | Hz | 5 |

List of items::

| <i>Items</i> |
|--|
| Fast kicker: System design of DR and LTR/RTL optics optimization |
| Fast kicker: Hardware preparation of FID pulsar |
| Fast kicker: System design & prototyping of induction kicker |
| Fast kicker: Long-term stability test at ATF |
| E-driven kicker: System design, include induction kicker development |

Status and Prospects:

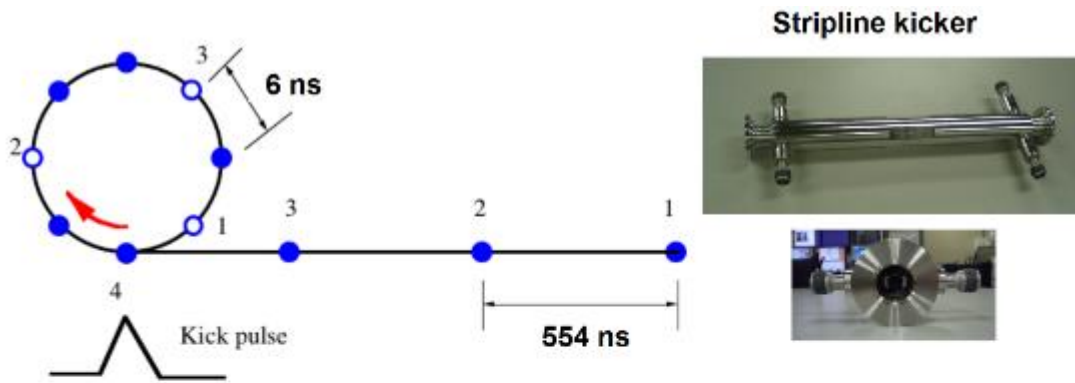
The electron beam or positron beam is converted into a low emittance beam while circulating the DR. In the ILC, a bunch train of 1312 bunches with a bunch interval of 554 ns is generated by the electron or positron source, and is stored in the DR. These bunches must be stored in the DR by compressing the bunch interval down to 6 ns, which enables a smaller 3.2 km ring compared to that of the uncompressed one. After the bunches become low emittance, they are extracted bunch by bunch from the DR by recovering the bunch interval of 554 ns. These requirements will be changed for the luminosity upgrade option of ILC, that is, a beam consists of 2625 bunches with an interval of 332 ns, and the bunch interval in DR becomes 3 ns. The injection and extraction kickers require high repetition frequencies of 2 MHz, as well as very fast rise/fall times of the kick field of 6 ns and 3 ns for the nominal and luminosity upgrade option, respectively. These parameters cannot be realized by using an ordinary kicker system, which consists of a pulse magnet and a pulse power supply with a thyratron switch. A system using multiple units of stripline kicker and fast high-voltage pulsars is the most promising candidates to realize the parameters.

One of the key technologies of the kicker is a high-voltage pulsar to drive the stripline. The pulsar requires over a peak voltage of 5 kV, a 1 ns rise/fall time, a 2 MHz burst pulse with a 1 ms duration, and operation at 5 Hz to realize the ILC parameters. A semiconductor device called a drift step recovery diode (DSRD) has a very fast switching speed and high repetition rate, and the pulsar using DRDS switches (fabricated by FID Technology, Ltd.) meets these parameters. The beam kick test using a single unit of stripline kicker and DSRD pulsar was carried out in the ATF DR.

Successful beam extraction was demonstrated in the beam operation from the ATF DR to the ATF2 beamline. For this experiment, two units of stripline kickers were installed, temporarily replacing the conventional extraction kicker, which has been placed offline. Two pairs of 10 kV pulsars were used to drive the striplines. The stripline kicker produced a 3 mrad kick angle for a 1.3 GeV beam. Owing to geometrical restrictions, the pulse bump orbit and the auxiliary septum magnet were used with the stripline kicker. This 10KV pulsar succeeded in extracting the beam, but could not generate the burst pulse of 1312 bunches required by the ILC. A long-term stability test of the fast kicker system will be performed at the ATF. The kicker pulsar used for the long-term test is basically the FID pulsar used in the 1st ATF test (5 kV pulsar), which can generate a burst pulse of 1312 bunches. Because the voltage of 5kV is not sufficient for the actual beam extraction from the ATF DR, a long-term test will be performed at the ATF extraction line.

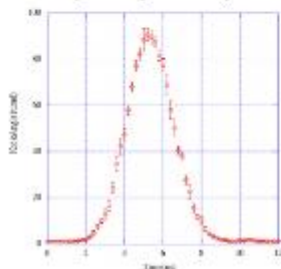
In addition, CERN has been developing an induction-type kicker pulsar for CLIC. By applying this technology, it is expected that a kicker pulsar with a voltage higher than the FID pulsar will be realized. It is hoped that the ILC Pre-Lab period will be able to proceed with the development of an induction type kicker pulsar and perform beam tests using the developed pulsar at the ATF.

Unlike the kicker used in other ILC kickers, an injection kicker for the electron-driven positron source is required to operate at a rise/fall time of 70 ns, the flat-top of 470 ns, and a repetition rate of 300 Hz. Because the induction-type kicker pulsar may meet this requirement, there is also the need to develop it as an injection kicker for the electron-driven positron source.



Beam extraction test from ATF DR (10kV pulsar)

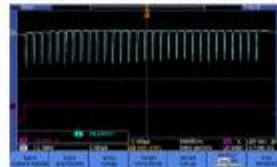
Beam test in ATF DR (5kV pulsar)



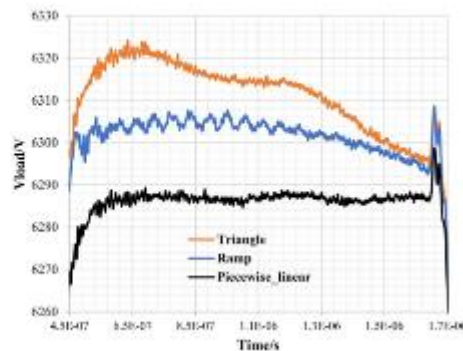
DR bunches(3train, 10bunches, 5.6ns bunch spacing)



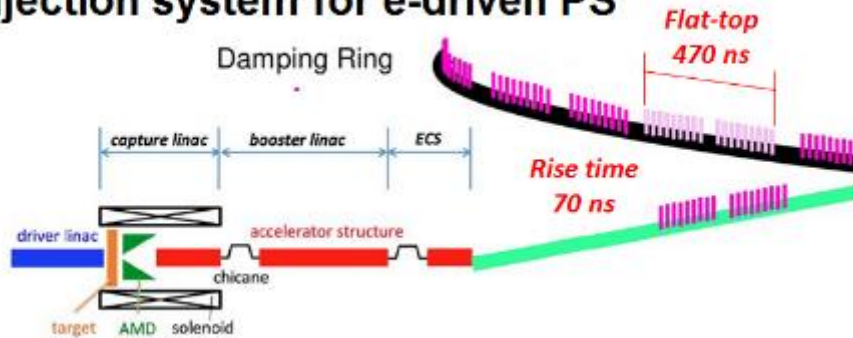
Extracted bunches(308ns bunch spacing, 30 bunches)



Induction kicker pulsar for CLIC DR



Injection system for e-driven PS



Area-System 5: Beam Delivery System

(Ver.1,2020-Dec-29)

Overview:

The ILC beam delivery system (BDS) is responsible for transporting the electron and positron beams from the exit of the main linac (ML), focusing them to the sizes required to satisfy the ILC luminosity goals, causing them to collide, and then transporting the spent beams to the main beam dumps.

The final focus (FF) system is one of the main systems of the BDS. The main purpose of the FF system is to squeeze the electron and positron beams until nanometer level at the interaction point (IP) keeping at the same time a control of the position at the order of nanometer. The ATF2 beamline was designed and constructed by an international collaboration as a facility to validate the design of the ILC FF system. The tuning of the beam to achieve the nanometer beam size level as well as the feedback system to control the position at the IP have been carried out as part of this collaboration. In particular a prototype feedback system for the ILC has been verified to satisfy all ILC requirements, such as time delay, beam position monitor resolution, drive amplifier power, and beam correction dynamic range. A complete validation of the ILC FFS will be continued during the Pre-Lab period in the framework of the ATF international collaboration.

The present ILC design includes a single IP with a 14 mrad beam crossing angle. The 14 mrad geometry provides space for separate extraction lines and requires crab cavities to rotate the bunches horizontally for head-on collisions. There are two detectors in a common interaction region (IR) hall that alternately occupy a single collision point, in a so-called “push-pull” configuration. This approach, which is considerably more exigent for detector assembly and operation than a configuration with two separate interaction regions, has been chosen for budget reasons. The superconducting FD magnet and cryostat package for the ILC were designed by BNL, and the technology for the superconducting FD magnets was demonstrated by a series of short prototype multi-pole coils at the ILC TDR stage. To assess the choice of the most appropriate technology a detailed FD system based on the ILC TDR will be necessary in the ILC pre-Lab period. Furthermore, since the FD package has an impact on the ILC physics detectors, the system design will have to be implemented in coordination with the ILC physics detector groups.

The contents of this area system mentioned above need to be described in the EDR (Engineering Design Report).

Area-System BDS: Work packages:

| | |
|--|--|
| <u>WP-15:</u> System design of ILC final focus beamline | ILC-FFS system design: Hardware optimization |
| | ILC-FFS system design: Realistic beam line driven / IP design |
| | ILC-FFS beam tests: Long-Term stability |
| | ILC-FFS beam tests: High-order aberrations |
| | ILC-FFS beam tests: R&D complementary studies |
| <u>WP-16:</u> Final doublet design optimization | Re-optimization of TDR FF design considering new coil winding technology and IR design advances. |
| | Assemble QD0 prototype, connect to Service Cryostat and undertake warm/cold vibration stability measurements with a sensitivity of a few nanometers. |

WP-15 : System design of ILC final focus beamline

(Ver.2,2021-Jan-26)

Technical Preparation Plan:

The beam size at the ATF2 focal point is designed to be 37 nm, which is technically equivalent to a 7 nm beam size for ILC250. A vertical electron beam size of 41 nm, which essentially satisfies the ATF2 design goal, has been produced at ATF2, with a bunch population of approximately 10% of the nominal value of 10^{10} electrons and with a reduced aberration optics. Recent studies indicate that the vertical beam size growth with the beam intensity owing the effects of wakefields. Furthermore, SCJ expressed technical concerns about the technology of the control and feedback systems and the long-term stability of the beam focus and position for the ATF2 beam experiment.

To overcome these apprehensions, the main objective of this plan is to pursue the necessary R&D to maximize the luminosity potential of ILC. In particular, the ILC final focus system (FFS) design must be assessed from the point of view of beam dynamics, choice of technology and hardware, and long-term stability operation issues. To implement this program based on the outstanding and unique results achieved by the ATF/ATF2 collaboration, an **ATF3 collaboration** is underway with the ATF2 partners and with new possible partners worldwide. The results are expected to provide important information necessary for the system design of the ILC FF beamline.

Goals of the technical preparation:

System design of beam optics and hardware for the ILC FF beamline, based on the established technologies is necessary. The specification of the ILC FF beamline is designed using the following parameters.

| <i>Parameters</i> | <i>Unit</i> | <i>Design</i> |
|---------------------------|-------------|----------------------|
| Beam Energy | GeV | 125 |
| Bunch population | | 2E10 |
| IP beam size (H/V) | mm / nm | 0.515 / 7.66 |
| IP position stabilization | | $\leq 0.2\sigma_y^*$ |

List of items:

| <i>Tasks</i> |
|---|
| ILC-FFS system design: Hardware optimization |
| ILC-FFS system design: Realistic beam line driven / IP design |
| ILC-FFS beam tests: Long-Term stability |
| ILC-FFS beam tests: High-order aberrations |
| ILC-FFS beam tests: R&D complementary studies |

Status and Prospects:

The FF system is one of the most exigent systems in the ILC. Its function is to provide nanobeam sizes (0.5

$\mu\text{m}/7.7\text{ nm}$) and stabilization at the nanometer level ($< 20\%$ of the IP beam size) to achieve the design luminosity of $10^{34}\text{ cm}^{-2}\text{s}^{-1}$ at 2×10^{10} bunch intensity. To achieve the design luminosity of $10^{34}\text{ cm}^{-2}\text{s}^{-1}$, the ILC requires nanometer-sized electron and positron beams colliding at the IP. To demagnify the beams to the required spot sizes, a novel local chromaticity correction-based FF system was proposed and considered for the baseline ILC designs.

The ATF2 FF system was designed as an energy-scaled version of the ILC FFS, with two main aims: (1) to demonstrate the effectiveness of the local chromaticity correction scheme for achieving an IP vertical beam size as small as 37 nm, and (2) to demonstrate the feasibility of beam orbit stabilization at the nanometer level. The effectiveness of the local chromaticity correction scheme was successfully demonstrated, and the potential or direct beam orbit stabilization at the nanometer level was also demonstrated. To date, an electron vertical beam size as small as 41 nm, essentially satisfying the ATF2 design goal, and stabilization with feedback latency of 133 ns (366 designed) have been achieved.

These are unique and outstanding results; however, the vertical beam size has been demonstrated only a bunch population of approximately 10% of the nominal value of 10^{10} electrons. The extremely large β involved and the presence of non-linear elements make it sensitive to imperfections, such as wakefields, magnet misalignments and jitter. Recent studies indicate that the vertical beam size growth with the beam intensity is generated by wakefield effects. The high content of wakefield sources in ATF2 could be explained by the fact that most of the vacuum chambers are re-used or replicated; hence, there is no dedicated vacuum chamber design. In contrast, to mitigate the impact of aberrations, optics with reduced aberration, i.e., the so-called $10\beta_x^*\times\beta_y^*$ optics with an IP horizontal β function that is 10 times larger than the original design, has been employed in recent operations.

It is recognized that the ATF/ATF2 achievements have already verified the minimum technical feasibility of the ILC FF system. However, to maximize the luminosity potential of the ILC, a further investigation of the effects of the intensity dependence on the IP spot size and optical aberrations especially with smaller β_x^* is crucial. To implement this program and based on the outstanding and unique results achieved by the ATF/ATF2 collaboration, an ATF3 collaboration is underway with the ATF2 partners and with new possible partners worldwide.

To resolve the aforementioned technical issues and establish the design of the ILC FF system beam optics as well as the associated hardware, the ATF3 collaboration to be implemented in the following technical preparation tasks and associated hardware preparations during the ILC Pre-Lab period.

ATF3 ILC-FFS assessment system design

- ✓ Hardware optimization: vacuum chambers, magnets, IP-BSM laser, CBPMs, IP-BPMs
- ✓ Realistic (wakefields, jitter, and magnet error) S2E “beam-dynamics-driven” design and IP optimization

ATF3 ILC-FFS oriented beam tests

- ✓ Long-term stability: nominal ($10\beta_x^*\times\beta_y^*$) routine operation assessment, vibration monitoring, intra-train feedback, intensity dependence and beam-based mitigation techniques (orbit and wakefields)
- ✓ High-order aberrations: design optics ($\beta_x^*\times\beta_y^*$), ultra-low β_y^* (octupoles, long L*)

- ✓ Other ILC R&D complementary studies: ILC collimation issues, ILC type CPBMs, new instrumentation, etc.

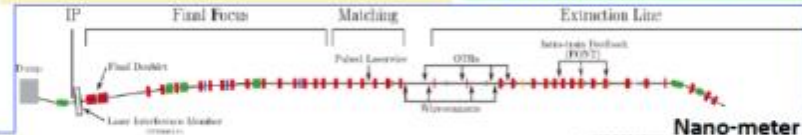
ATF2 goals and achievements

Goal 1: Establish the ILC final focus method with same optics and comparable beamline tolerances

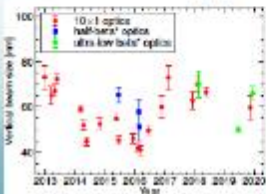
- ATF2 Goal : 37 nm \rightarrow ILC 7.7 nm (ILC250)
- Achieved **41 nm** (2016)

Goal 2: Develop a few nm position stabilization for the ILC collision

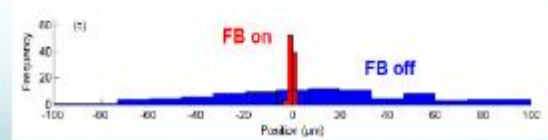
- **FB latency 133 nsec achieved** (target: < 366 nsec)
- **position jitter at IP: 106 \rightarrow 41 nm** (2018) (limited by the BPM resolution)



Nanometer beam sizes at IP

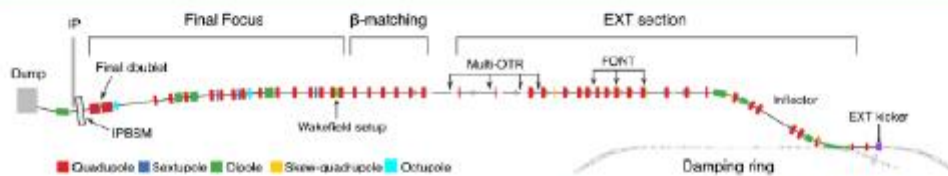


Small beam sizes were obtained with beam intensities of $0.5-1.5 \cdot 10^9 e^-/\text{bunch}$ (10^{10} design value) and reduced aberration optics ($10\beta_x^* \times \beta_y^*$)

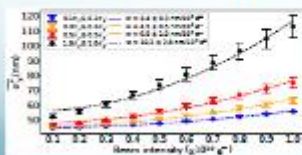


ILC FFS - ATF3 objective and collaboration:

Based on the achievements of the ATF2, ATF3 plan is to pursue the necessary R&D to **maximize the luminosity potential of ILC**. In particular the assessment of the ILC FFS system design from the point of view of the beam dynamics aspects and the technological/hardware choices and the **long-term stability operation issues**.

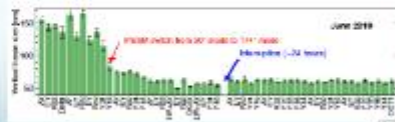


Long Term stability



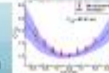
Intensity dependence studies

High-order aberrations



Ultra-low β^* studies

Energy bandwidth



Instrumentation R&D



Collimator



Waveguide BPM

Incoherent Diffraction Cherenkov Radiation Monitor

WP-16 : Final doublet design optimization

(Ver.2,2021-Jan-26)

Technical Preparation Plan:

The superconducting coil winding technology has advanced since the TDR was finalized, and later projects have proposed and/or implemented new IR design options. Subsequent to the TDR we recognize that for the 250 GeV CM operation, a significant opportunity exists to raise the luminosity and improve the final doublet (FD) layout to benefit both the experiment and accelerator operation. We will have to reevaluate and reoptimize the FD design by considering these new developments in the ILC Pre-Lab period.

In the TDR baseline, the first QD0 cryostat assembly is supported by and moves with the detector. The 1.9 K superfluid helium supply for QD0 and the interface to external magnet power leads are via the Service Cryostat. The Service Cryostat connects to QD0 via a long He-II cryogenic line that must pass through a labyrinth in the end Pacman radiation shielding to avoid having a direct path for beam line radiation to the presumptively occupied experimental detector hall. The vertical beam fluctuation to QD0 must be stable in the order of 50 nm, to stay within the capture range of the intra-train collision feedback. This requirement is well beyond the experience with existing accelerators and has been considered in the choice of the 1.9 K superfluid He-II cooling for QD0. Therefore, we will have to evaluate the QD0 vibration via the Service Cryostat for the system design of the FD system during the ILC Pre-Lab period.

Goals of the technical preparation:

The goal of the present work is to ensure that the 250 GeV ILC FD EDR design yields the best possible luminosity for the experiments and achieves the most cost-effective smooth accelerator operation by accounting for the new magnet winding technology and IR magnet design concepts that are developed after the original ILC TDR is finalized.

List of items:

| <i>Items</i> |
|--|
| Re-optimization of TDR FD design considering new coil winding technology and IR design advances. |
| Assemble QD0 prototype, connect to Service Cryostat and undertake warm/cold vibration stability measurements with a sensitivity of a few nanometers. |

Status and Prospects:

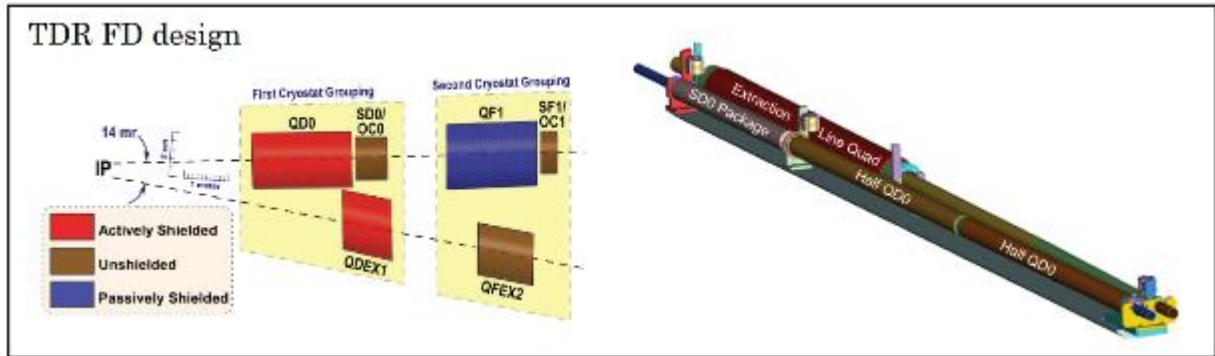
There are four superconducting quadrupole magnets around the ILC IR. QF1 and QD0 are located along the incoming beamline, and QDEX1 and QFEX2 are the superconducting magnets for the extraction beamline. The QD0 and QDEX1 magnets are housed in the QD0 cryostat, whereas QF1 and QFEX2 are housed in the QF1 cryostat, separated only by warm components and vacuum valves. Two sets of the QD0 cryostats are arranged into two physics detectors to facilitate “push-pull” at a shared IP. The QD0 cryostat moves with the detector during switchover, whereas the QF1 cryostat remains fixed on the beamline. The QD0 magnet is inside the detector solenoidal and therefore cannot have magnetic-flux-return yokes. At the closest coil spacing, the

magnetic cross-talk between the two beamlines is controlled via actively shielded coil configurations and through the use of local correction coils, dipole, skew-dipole and skew-quadrupole, skew-sextupole, octupole or skew-octupole as appropriate. The QD0 coils can be split into two half-length coils, where both coils are powered for the 500 GeV CM operation. However for the 250 GeV operation, only the first half is powered to reduce the higher order aberrations of beam optics by moving the effective magnetic center of QD0 closer to the IP.

The superconducting coil winding technology has advanced since the TDR was finalized, and later projects have proposed and/or implemented new IR design options. The “sweet spot” coil concept was developed for the BNL Electron Ion Collider (EIC) IR. The sweet spot concept uses a combination of dipole and quadrupole coils that are adjusted to leave a zero net field at the main QD0 beam axis but then provide a tailored field profile to compensate for the main QD0 coil external field at the extraction line. The sweet spot configuration is magnetically more efficient than the baseline active shielding option. Furthermore, the BNL Direct-Wind coil production scheme was demonstrated recently. The BNL Direct-Wind technology is used to produce closely spaced coil layers of superconducting multi-strand cables. The design is extremely compact, and the coils practically touch inside shared cold-mass volumes. Cooling is provided by the superfluid helium at 1.9 K to avoid the risk of exciting vibration in the magnet cryostat and the formation of a long transfer line from the helium heat exchanger in the Service Cryostat. The above options represent a sample of the new magnet winding schemes and coil geometries that should be investigated before we finalized the ILC EDR FD design. The budget proposed for this work represents an investment to ensure that we reach a final mature design for the EDR, yielding the best possible FF optics performance in the most cost-effective manner.

The fluctuation of the vertical beam position at the QD0 magnet must be stable in the order of 50 nm, to stay within the capture range of the intra-train collision feedback. This requirement is well beyond the experience with existing accelerators and is considered in the choice of the 1.9 K superfluid He-II cooling for QD0 cryostat. More specially, the column of He-II maintains the QD0 magnet coils at the same temperature as the heat exchanger in the Service Cryostat without the necessary for mass flow, which carries the risk of becoming a strong vibration source (He-II effectively provides rapid and efficient “conduction cooling”). The effectiveness of this design strategy was partially demonstrated for the TDR during the dedicated R&D for constructing and measuring a full QD0 prototype. However, there was no follow-up to complete this work after the TDR was published (final R&D status: 90% complete). It is important to complete the technical work for this vibration stability measurement using the existing QD0 prototype hardware while also taking advantage of the later experience that has been gained during the SuperKEKB IR magnet vibration measurement development work. When the prototype QD0 cryostat is finally connected via the He-II cryogenic connection line (line parts are yet to be fabricated) to the Service Cryostat, we will perform the actual vibration stability measurements using the setup. In the laboratory, we can stabilize a 2000 turn pickup coil inside the QD0 bore from both sides and directly measure the magnetic center motion with a sensitivity of a few nanometers. Previous work has established that it is considerably easier to stabilize a pickup coil from two ends than from a single side support to proceed with in. situ measurement. Note that because the pickup coils are sensitive to the relative motion of the probe with respect to the magnet, it is important to stabilize these pickup coils to ensure that the probe’s

signal corresponds to the true magnetic center motion. Note that we also have sets of geophones and a contactless laser doppler vibrometer measurement system for comparison with the pickup coil readings. We will first use these other devices to perform baseline room temperature measurements and subsequently acquire pickup coil data when the QD0 magnet is cold and may be powered to its 140 T/m operation gradient.



QD0 active shielding coils layout

QD0 Coil Layout

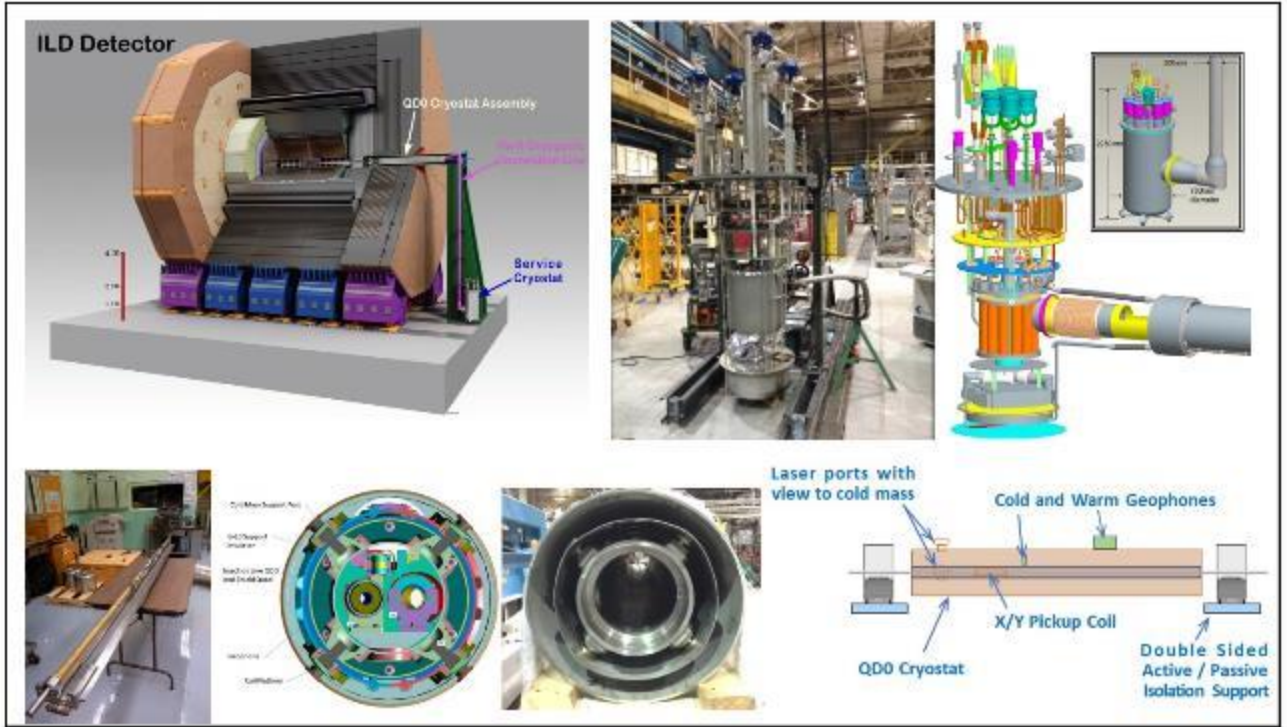
Example of ILC 250 QD0 cryostat using shorter QD0 SC coils ($L^*=4.1$ m)

Baseline half-length QD0 Direct Wind R&D coil layer production

QD0 Coil Winding (250 GeV Update)

Main coils & correctors are wound on a common coil support tube.

BNL Direct Wind constant gradient tapered double helical coil winding



Area System 6: Beam dump

(Ver.1,2020-Dec-29)

Overview:

Beam dumps are distributed along the ILC accelerator and operate continuously during commissioning, regular operation, or they receive an abort beam in the event of a malfunction to prevent damage.

Tune-up dumps are used for commissioning and system tuning, where the beam energy is given by the maximum operating parameters of each accelerator section, but other parameters, such as the bunch charge, number of bunches per pulse, and pulse repetition frequency may be reduced compared to the nominal operating parameters. The maximum beam power for tune-up dumps is optimized for 60 kW and 400 kW, distributed before and after the ML, respectively. These beam dumps are designed with experiences of solid material dumps such as the aluminum dump of SLAC (120 kW) and the graphite dump of XFEL (300 kW); thus, no prioritized preparation is expected in the Pre-Lab period.

The main beam dump absorbs the electron or positron beam after collision at the end of each beamline. Because the beam power of full power operation after the 1-TeV upgrade will be rated at 14 MW, a pressurized water dump that is capable of 17 MW, including a 20% safety margin, was designed based on the 2.2-MW water dump at SLAC. In addition, a water dump rated at 8 MW will be prepared for 5 + 5 Hz positron production in the undulator scheme. During the Pre-Lab period, the engineering design of the water dump system, prototype test of the beam window, and its remote exchange will be carried out to improve the reliability of the system.

The photon dump is a special dump for undulator photons, which are used for positron production and pass through the target. The maximum power, including a 20% safety margin, is rated at 300 kW. Owing to the high concentration of photons by the undulator, the photon absorber should be well designed taking into account the effect caused by heavy local energy deposition. Two types of photon dumps have been proposed: water curtain and graphite on cooled copper 2 km downstream of the target. The engineering design of these systems should be done in the Pre-Lab period. The contents of this area system mentioned above need to be described in the EDR (Engineering Design Report).

| Dump | Max. Power | No. of units | examples |
|--------------------|---------------|--------------|--|
| Tune-up | 60 kW | 9 | Aluminum; SLAC, graphite; XFEL |
| Tune-up ML | 400 kW | 2 | Graphite; XFEL (300 kW) |
| Undulator photon | 300 kW | 1 | Conceptual designs (water curtain, graphite) |
| Main beam dump | 17 MW (1 TeV) | 2 | SLAC (2.2 MW), JLAB (1 MW) |
| Undulator 5 + 5 Hz | 8 MW | 1 | Same as main dump |

Area System Beam Dump: WPs:

| | |
|--|---|
| WP- 17: System design of the main beam dump | Engineering design of water flow system |
| | Engineering design and prototyping of components; vortex flow in the dump vessel, heat exchanger, hydrogen recombiner |
| | Engineering design and prototyping of window sealing and remote exchange |
| | Design of the countermeasure for failures / safety system |
| WP- 18: System design of the photon dump for undulator positron source | System design and component test of water curtain dump |
| | System design and component test of graphite dump |

WP-17: System design of the main beam dump

(Ver.2,2021-Jan-26)

Technical Preparations Plan:

The SCJ and MEXT's ILC Advisory Panel stated technical concerns regarding the reliability, earthquake protection, and stability of the window of the main beam dump, reaction between the high-energy beam and water, and containment of activated water. This plan is proposed to proceed with the design of the main beam dump and to demonstrate the stability of the window and its handling procedure.

The design work will be carried out with the collaboration of experts from the field of high-power targets and dumps worldwide. CERN operates beam dumps for large accelerators and high-power beam dumps, and SLAC and JLAB have experience with water-circulated beam dumps. KEK will lead the system design of the beam dump facilities, ensuring environmental and radiation safety in collaboration with the government, industry, and the scientific community. The engineering design of the vortex flow system in the water dump vessel and the overall water circulation system will be done following the experiences at SLAC and JLAB. The stability of the window will be confirmed from the perspective of radiation damage and mechanical robustness. The Ti alloy, Ti6Al4V, was selected as a window material following the experiences involving high-power targets and dumps globally, which was mostly conducted by proton beams. Further studies that increase the robustness will continue through collaboration. The mechanical robustness of the window is confirmed through the prototyping of the sealing and demonstration of the remote exchange. A scheme for monitoring the integrity of the window will also be studied. The design for safety, that is, earthquake protection, containment of activated water, including the countermeasure for failures, is a major engineering issue to be addressed. These will be conducted through collaboration with industries.

Goals of technical preparation:

Establish the engineering design of the whole dump system.

List of items:

| <i>Items</i> |
|---|
| Engineering design of water flow system |
| Engineering design and prototyping of components; vortex flow in the dump vessel, heat exchanger, hydrogen recombiner |
| Engineering design and prototyping of window sealing and remote exchange |
| Design of the countermeasure for failures / safety system |

Status and Prospects:

The design of the ILC main beam dump was developed in the mid-2000s by experts in Europe and the US. In 2012, the basic design was established as an 18-MW water dump and compiled into the TDR.

This design was based on the 2.2-MW water dump designed at SLAC, which was operated at 0.75 MW. JLAB has another water dump, which is a 1-MW design that is currently used for CEBAF operations.

At this point, the design is a conceptual one that meets the basic parameters, and must proceed with its embodied design.

The water that serves as an absorber for the beam is supposed to rotate in the tank as a vortex flow to sweep out the heated portion. Although there is a conceptual design of the inlet and outlet, to date, there is no operational design.

Tritium accumulates in the water owing to activation by the beam. Although the radiation of tritium is weak, a solid water leakage countermeasure is desired. There remains the need for a detailed design of the beam window and water circulation system considering these factors.

The radiation dose in the dump room will increase owing to severe activation of the dump vessel and its surrounding shielding over the years of operation. Therefore, the periodic replacement of the beam window will be performed remotely. This mechanism, including the structure for mounting the window, has not yet been designed.

The maximum power based on the latest beam parameters is 14 MW for a 500-GeV beam and 2.6 MW for a 125-GeV beam. The beam dump is designed to be up to 17 MW, assuming a 20% margin.

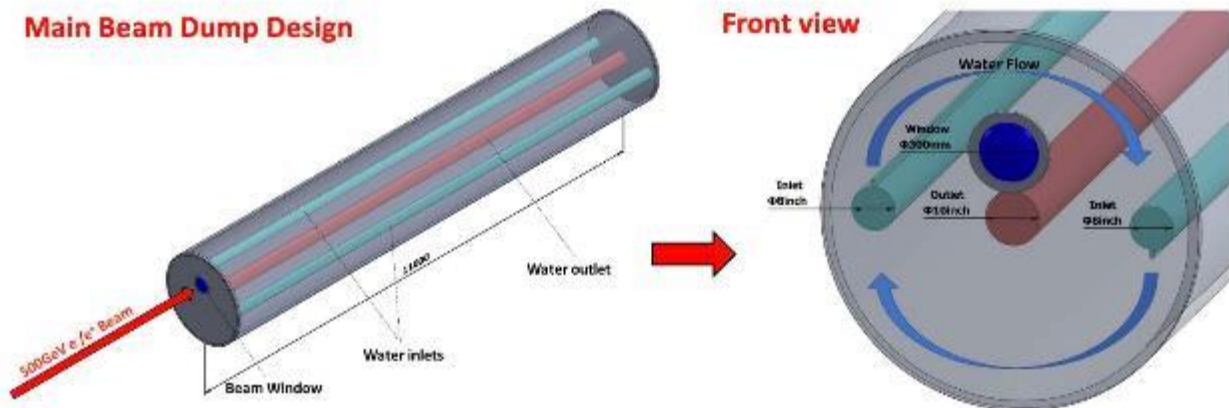
In 2017, a group was set up at KEK to advance the design of the ILC beam dump, and this group exchanges information and consults with beam dump experts at CERN, SLAC, and JLAB.

In addition, the design of the dump system for radiation safety management at the candidate site and the design of a large underground cavern for the main dump and its utilities are currently being carried out in collaboration with industry and academia.



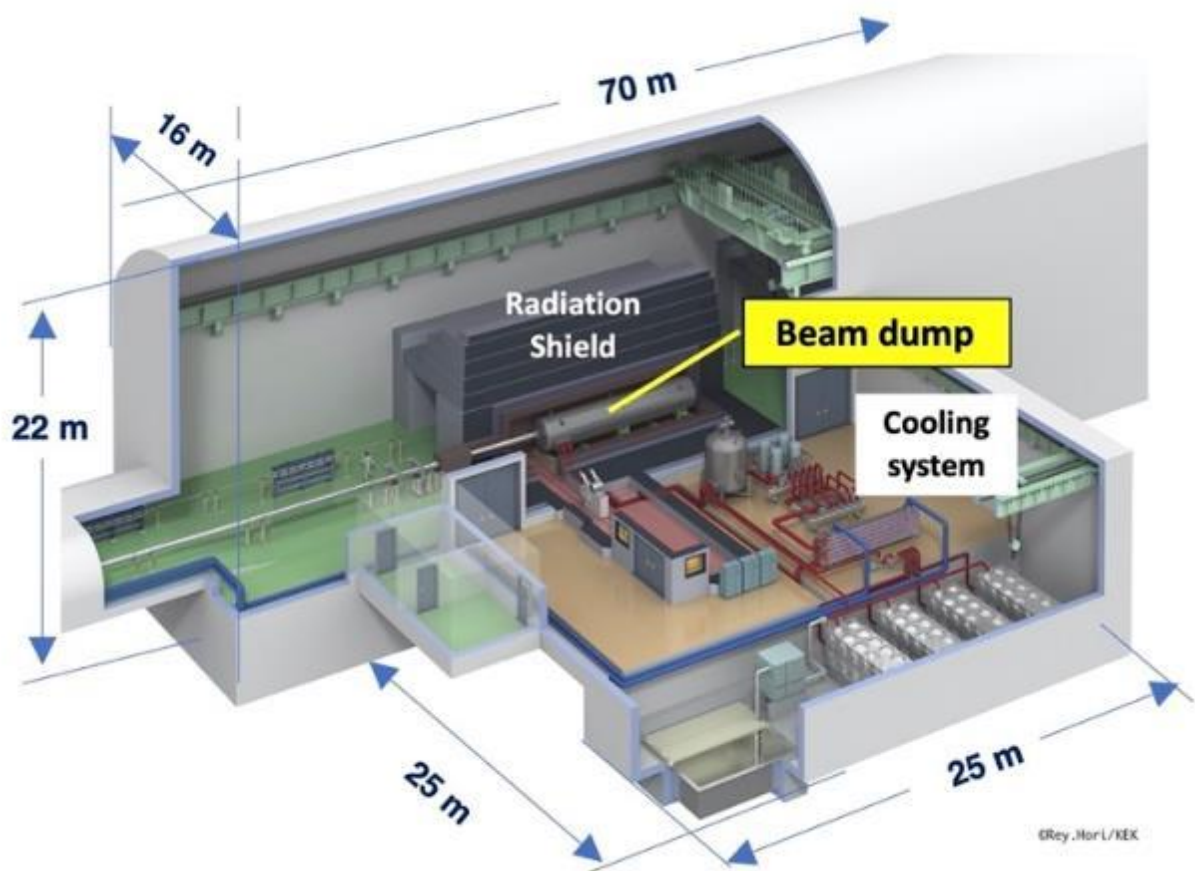
Base design of ILC Main Beam Dump

Main Beam Dump Design



【Base Design】

- **Water power absorber** and **forced convection** to extract the heat.
 - * Water is compressed **1 MPa** \Rightarrow **boiling temp 180°C**
 - * Vortex water flow \Rightarrow Mass flow rate : **104.5kg/s** each inlet, Ave flow velocity **2.17m/s**
- Beam Window made of **Ti-6Al-4V**.
 - Beam sweep : 1kHz sweep, sweep radius : **6cm**



WP-18: System design of the photon dump for undulator positron source

(Ver.2,2021-Jan-26)

Technical Preparation Plan:

The photon dump for the undulator positron source, which should absorb an average power of 120 kW for the 250-GeV high-luminosity case, needs to be changed from TDR, where a water dump similar to the main beam dump was assumed. For the possible future option of a 10-Hz collision, it is rated at 300 kW, including a 20% safety margin. Owing to the high concentration of photons by the undulator, the local energy deposition in water is high and the water should be pressurized to about 12 atm to prevent temporary boiling during or at the end of each pulse. The window should be Ti alloy more than 1-mm thick to resist water pressure, and such a thick window will suffer from fatigue through the high thermal cycles during each pulse and severe radiation damage. Two alternative designs are currently proposed. One is a water curtain dump and the other is a graphite dump to be installed 2 km downstream. These designs are based on heat and radiation damage analysis, and need to move forward by incorporating technical issues, especially pertaining to power absorption structures and the maintenance of activated equipment.

These design works will be carried out in collaboration with experts from the field of high-power targets and dumps throughout the world. Prototyping of the key structure is expected.

Goals of technical preparation:

The system design of the photon dump is established at an engineering level, including the photon absorption structure, infrastructures for cooling, and the maintenance of the activated equipment.

List of items:

| <i>Items</i> |
|---|
| System design and component test of water curtain dump: water flow and window cooling |
| System design and component test of graphite dump; cooling of graphite absorber on copper |

Status and Prospects:

The photon dump for the undulator positron source (Figure 1) should absorb an average power of 120 kW for the 250-GeV high-luminosity case and 108 kW for the 500-GeV high-luminosity case. For the possible future option of a 10-Hz collision, it is rated at 300 kW, including a 20% safety margin. A water dump similar to the main beam dump was assumed in the TDR. In contrast to the main water dump for electron and positron beams, the photon beam cannot be swept magnetically. Owing to the high concentration of photons, a cross section of below 2 mm, the local energy deposition in water is high, and the water should be pressurized to about 12 atm to prevent temporary boiling during or at the end of each pulse. A 1-mm-thick Ti-window is required to resist water pressure, and such a thick window will suffer from fatigue through the high thermal cycles during each pulse and severe radiation damage. To solve these difficulties, two different types of dumps have been proposed.

The water curtain dump is an idea related to a photon dump (Figure 2). In contrast to the main beam dump filled with water, a free-falling water curtain relaxes the issues in water caused by a high-density heat deposition by a photon pulse. The water falls vertically and is not pressurized, that is, 1 atm. The double-walled beam window is located approximately 10 m upstream of the dump to separate the water section and beamline. Each window will be made of Ti alloy, Ti6Al4V, approximately 15 cm in diameter, and will be 0.2~0.4-mm thick. Double windows will be cooled by He gas, which flows between them at a flow rate of 100 m/s, and mechanically tumbled, for example, has a 3-cm radius and velocity of 2.5 cm/s, to reduce the heat density by the pulse-like sweeping of an electron beam. The location of the water curtain dump was evaluated approximately 40 m from the target (near) and 2 km from the target (far). The latter case is very relaxed.

Another idea is a dump based on graphite, which tolerates high temperatures (Figure 3). Locating a graphite dump 2 km from the target and receiving photons at a shallow angle of 10 mrad will make the thermal distribution acceptable. The entire graphite part will be 1-cm thick, 50-cm wide, and 4-m long, and it will consist of several short units. Each graphite plate needs to be attached or brazed on water-cooled copper. All graphite units with a copper base will be in vacuum, and the window between the dump and beamline will then be removed.

In both designs, basic studies on heat, stress, and radiation damage have been studied using the simulation code of ANSYS and FLUKA. Further studies should be conducted to establish an engineering design that includes infrastructure, maintenance, and failure scenarios.

The polarized e+ source scheme

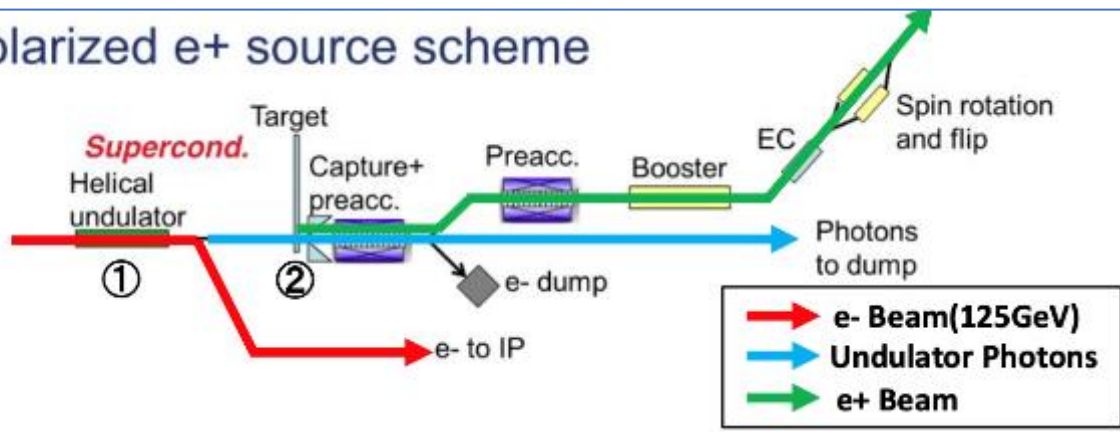
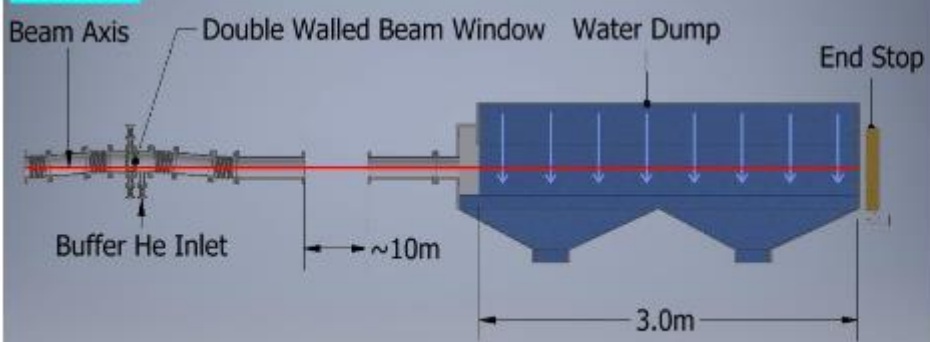


Figure 1: Configuration of undulator positron source

- ① Beam incidents to falling water (**Water Curtain**)
This system can accept water boiling.
Pressure wave don't attack the window.
- ② **Double Walled Beam Window** cooled by Helium gas.
This window is tumbled to reduce the radiation damage.

Overview



Window

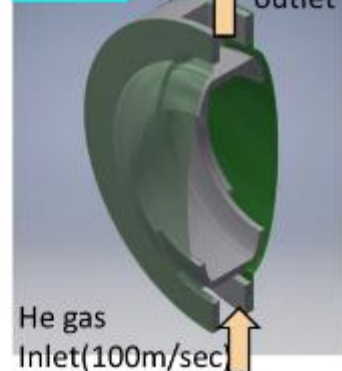


Figure 2: Configuration of water curtain photon dump.

② Angle

Absorber 10mrad

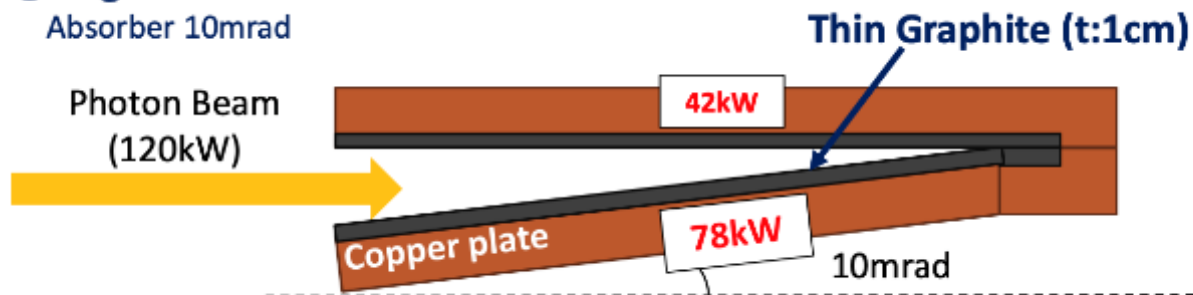


Figure 3: Concept of graphite-based photon dump.

Appendix

List of WPs

Following work packages are listed in this technical proposal.

| | Work package | Items |
|------|---|---|
| 1. | ML&SRF | |
| WP-1 | Cavity Industrial- Production Readiness # production: 3 x 40 (16 of 40 go to CM assembly) | Cavity production readiness, incl. cavities w/ He tank + magnetic shield for cavity, high-pressure-gas regulation, surface-preparation/heat treatment (HT)/Clean-room work, partly including the 2nd pass, vertical test (VT) |
| | | Plug compatibility, Nb material, and recipe for surface treatment to be reconfirmed/decided |
| | | Cavity Production Success yield to be confirmed (before He tank jacketing) |
| | | Tuner baseline design to be established |
| | | <u>Note:</u> Infrastructure for surface treatment, HT, VT, pre-tuning, etc. (with each regional responsibility) |
| WP-2 | Cryomodule (CM) Global Transfer and Performance Assurance # production: 3 x 2 | Coupler production readiness, including preparation/RF processing (# Couplers, 3 × 20) |
| | | <u>Note:</u> Infrastructure for coupler conditioning: klystron, baking furnace, and associated environment (with each regional responsibility) |
| | | Tuner production readiness, including reliability verification (# Tuners, 3 × 20) |
| | | Superconducting Magnet (SCM: Q+D combined) production readiness (# SCMs, 3 × 3 (1 prototype + 2)) |
| | | CM production readiness incl. high-pressure-gas, vacuum vessel (VV), cold-mass, and assembly (cavity-string, coupler, tuner, SCM etc.) |
| | | CM test including degradation mitigation (in 2-CM joint work, etc.) at assembly site before ready for CM transportation |
| | | CM Transportation cage and shock damper to be established |
| | | Ground transportation practice, using mockup-CM |
| | | Ground transportation test, using production-CM longer than Eu-XFEL |
| | | Global transport of CM by sea shipment (requiring longer container) |
| | | Performance assurance test after CM global transport (at KEK) |
| | | Returning transport of CM back to home country (by sea shipment) |
| | | <u>Note:</u> Hub-lab Infrastructure for the CM production, assembly, and test (with each regional responsibility) |
| WP-3 | Crab Cavity (CC) for BDS #CC production: 4 # CC-CM production: 1 | Decision of installation location with cryogenics/RF location accelerator tunnel |
| | | Design and development of prototype cavity/coupler/tune/CM including beam extraction line |
| | | Cavity production, including cavities w/ He tank + mag. shield for CM, high-pressure gas regulation, EP/HT/Clean work, including VT |
| | | Coupler production including preparation/RF processing readiness (excluding klystron, baking furnace, clean room) |
| | | Tuner production readiness |
| | | CM production including High-pressure-gas formality, vacuum vessel, cold-mass, and assembly (cavity-string, coupler/tuner, SCM, etc.) |
| | | CM test including harmonized operation with two cavities |
| | | CC-CM transport cage and shock damper |
| | | CC-CM transport tests |
| | | Infrastructure for CC and CM development and test (with each regional responsibility.) |

| | | |
|-------------------------|---|--|
| Sources | | |
| 2. e- source | | |
| WP-4 | Electron Source | Drive laser system |
| | | HV Photogun |
| | | GaAs/GaAsP Photocathodes |
| 3. e+ source | | |
| 3.1 e+ undulator scheme | | |
| WP-5 | Undulator | Simulation (field,errors, alignment) |
| WP-6 | Rotating target | Design finalization, partial laboratory test, mock-up design |
| | | Magnetic bearings: performance, specification, test |
| | | Full wheel validation, mock-up |
| WP-7 | Magnetic focusing system | Design selection (FC, QWT, pulsed solenoid, plasma lens), with yield calculation |
| | | OMD with fully assembled wheel |
| 3.2 e+ e-driven scheme | | |
| WP-8 | Rotating target | Target stress calculation with FEM |
| | | Vacuum seal |
| | | Target module prototyping |
| WP-9 | Magnetic focusing system | Flux concentrator conductor |
| | | Transmission line |
| | | Flux concentrator system prototyping |
| WP-10 | Capture cavity, linac | APS cavity for the capture linac |
| | | Capture linac beam loading compensation and tuning method. |
| | | Capture linac operation and commissioning |
| | | Power unit prototyping |
| | | Solenoid prototyping |
| WP-11 | Target Maintenance | Capture linac prototyping |
| 4. Damping Ring | | |
| WP-12 | System design of ILC damping ring | Optics optimization, simulation of the dynamic aperture with magnet model |
| | | Magnet design : Normal conducting magnet |
| | | Magnet design : Permanent magnet |
| | | Prototyping of permanent magnet |
| WP-13 | Evaluation of the collective effect in the ILC damping ring | Simulation : Electron cloud instability |
| | | Simulation : Ion-trapping instability |
| | | Simulation : Fast ion instability (FII) |
| | | System design : Fast FB for FII |
| | | Beam test : Fast FB for FII |
| WP-14 | System design of ILC DR injection/extraction kickers | Fast kicker: System design of DR and LTR/RTL optics optimization |
| | | Fast kicker: Hardware preparation of FID pulsar |
| | | Fast kicker: System design & prototyping of induction kicker |
| | | Fast kicker: Long-term stability test at ATF |
| | | E-driven kicker: System design,including induction kicker development |
| 5. BDS | | |
| WP-15 | System design of ILC final focus beamline | ILC-FFS system design: Hardware optimization |
| | | ILC-FFS system design: Realistic beam line driven / IP design |
| | | ILC-FFS beam tests: Long-Term stability |
| | | ILC-FFS beam tests: High-order aberrations |
| | | ILC-FFS beam tests: R&D complementary studies |
| WP-16 | Final doublet design optimization | Re-optimization of TDR FF design considering new coil winding technology and IR design advances. |
| | | Assemble QD0 prototype, connect to Service Cryostat and undertake warm/cold vibration stability measurements with a sensitivity of a few nanometers. |
| 6. Beam Dump | | |

| | | |
|-------|--|---|
| WP-17 | System design of the main beam dump | Engineering design of water flow system |
| | | Engineering design and prototyping of components; vortex flow in the dump vessel, heat exchanger, hydrogen recombiner |
| | | Engineering design and prototyping of window sealing and remote exchange |
| | | Design of the countermeasure for failures / safety system |
| WP-18 | System design of the photon dump for undulator positron source | System design and component test of water curtain dump System design and component test of graphite dump |

ILC parameters:

| Parameter | Unit | Design | Achieved | Comments |
|--|---------------|------------------------------------|----------|--|
| 1. ML&SCRF | | | | |
| Module gradient | MV/m | 31.5 (+/- 20%) | ~31.5 | DESY, FNAL, JLab, Cornell, KEK, |
| Cavity gradient | MV/m | 35 (\pm 20%) | 33.4 | |
| Cavity Q value (Q0) | | 0.8E10@35MV/m, 1E10@31.5 MV/m | ~1E10 | |
| Cavity gradient (@cost reduction R&D) | MV/m | 38.5 (\pm 20%) | | |
| Cavity Q value (Q0) (@cost reduction R&D) | | 1.6E10@38.5MV/m , 2E10@35 MV/m | | |
| Cavity production yield | % | 90 | | |
| Beam current | mA | 5.8 | > 5.8 | DESY, KEK |
| Number of bunches | | 1312 | 1312 | DESY |
| Bunch charge | nC | 3.2 | 3 | |
| Bunch interval | ns | 554 | 333 | |
| Beam pulse width | μ s | 730 | 800 | DESY, KEK |
| RF pulse width | ms | 1.65 | 1.65 | DESY, KEK, FNAL |
| Repetition | Hz | 5 | 10 | DESY |
| Crab kick voltage | MV | 0.615 @ 3.9 GHz 1.845 @ 1.3 GHz | | |
| Uncorrelated phase jitter (crab cavity) | fs | 61 | | |
| 2. Electron Source | | | | |
| Electrons per bunch (at gun exit) | | 3×10^{10} | | |
| Electrons per bunch (at DR injection) | | 2×10^{10} | | |
| Number of bunches | | 1312 | | |
| Bunch repetition rate | MHz | 1.8 | | |
| Bunch train repetition rate | Hz | 5 (10) | | |
| FW Bunch length at source | ns | 1 | | |
| Peak current in bunch at source | A | 3.2 | | |
| Energy stability | % (rms) | < 5 | | |
| Polarization | % | > 80 | | |
| Photocathode quantum efficiency | % | 0.5 | | |
| Drive laser wavelength (tunable) | nm | 790 ± 20 | | |
| Single bunch laser energy | μ J | 5 | | |
| 3. Positron Source | | | | |
| Bunch Charge | nC | 4.8 | 8 | SLAC SLC (E-Driven) |
| 3.1 Undulator scheme | | | | |
| Undulator pitch | mm | 11.5 | 2.5 | SLAC E166 |
| Positron Polarization (optional) | % | 30 | 80 | SLAC E166 |
| Ti alloy Target Heat Load (PEDD) | J/g | 61 | 160 | Estimated from physics constant table KEK |
| QWT peak field | T | 1 | 2.3 | |
| Target radius | mm | 500 | | |
| Target weight | kg | 50 | | |
| Target tangential velocity | m/s | 100 | | |
| Target rotation | rpm | 2000 | | |
| Beam heat load | kw | 2 | | |
| Vacuum pressure | Pa | 10^{-6} | | |
| 3.2 E-driven scheme | | | | |
| W-Re Target Heat Load (PEDD*) | J/g | 34 | 70 | SLAC SLC (E-Driven) |
| Flux Concentrator Peak field | T | 5 | 10 | BINP |
| Target radius | mm | 250 | | |
| Target weight | kg | 65 | | |
| Target tangential velocity | m/s | 5 | | |
| Target rotation | rpm | 200 | | |
| Beam heat load | kw | 20 | | |
| Vacuum pressure | Pa | 10^{-6} | | |
| 4. DR | | | | |
| Normalized Emittance ($\gamma \epsilon_x / \gamma \epsilon_y$) | μ m/nm | 4/20 | 4/15 | ATF |
| Dynamic aperture ($\gamma (A_x + A_y)$) | M | 0.07 (action variable) | | |
| Longitudinal acceptance ($\Delta \delta \times \Delta z$) | % \times mm | $\pm 0.75 \times \pm 33$ | | |
| Bunch population | | 2.00×10^{10} | | |
| Number of bunches in DR | Bunches | 1312 / 2625 | | |
| Beam position fluctuation | | $\leq 0.2 \sigma_y$ | | |
| Repetition rate | Hz | 5 | | |
| 5. BDS | | | | |
| Bunch population | | 2.00×10^{10} | | |
| IP beam size (H/V) | mm / nm | 0.515 / 7.66 | | |
| IP position stabilization | | $\leq 0.2 \sigma_y^*$ | | |
| Crab kick voltage | MV | 0.615 @ 3.9 GHz 1.845 @ 1.3 GHz | | |
| Uncorrelated phase jitter (crab cavity) | fs | 61 | | |
| 6. Beam Dump | | | | |
| ILC 250GeV | MW | 17 | - | Designed for 500GeV beam |